



HAL
open science

Environmental performance in Construction : A case-study of 3D Concrete Printing Technology

Kateryna Kuzmenko

► **To cite this version:**

Kateryna Kuzmenko. Environmental performance in Construction : A case-study of 3D Concrete Printing Technology. Civil Engineering. École des Ponts ParisTech, 2021. English. NNT : 2021ENPC0009 . tel-03720006

HAL Id: tel-03720006

<https://pastel.hal.science/tel-03720006v1>

Submitted on 11 Jul 2022

HAL is a multi-disciplinary open access archive for the deposit and dissemination of scientific research documents, whether they are published or not. The documents may come from teaching and research institutions in France or abroad, or from public or private research centers.

L'archive ouverte pluridisciplinaire **HAL**, est destinée au dépôt et à la diffusion de documents scientifiques de niveau recherche, publiés ou non, émanant des établissements d'enseignement et de recherche français ou étrangers, des laboratoires publics ou privés.

***Performance Environnementale
dans la Construction : Cas d'Etude de
l'Impression 3D Béton.
Modélisation et Caractérisation des Impacts.
Application aux Structures Architecturées.***

École doctorale SIE (Sciences, Ingénierie et Environnement)

Thèse préparée au sein de laboratoire Navier, UMR8205,
équipe de recherche MSA (Matériaux et Structures Architecturées)

Thèse soutenue le 11 mai 2021, par
Kateryna KUZMENKO

Composition du jury :

Richard BUSWELL Professeur, Loughborough University	<i>Président</i>
Guillaume HABERT Professeur, ETH Zurich	<i>Rapporteur</i>
Corentin FIVET Professeur, EPFL	<i>Rapporteur</i>
Charlotte ROUX Chargée de recherche, Ecole des Ponts ParisTech	<i>Examineur</i>
Nicolas COCHARD Docteur, KARDHAM	<i>Examineur</i>
Adélaïde FERAILLE HDR, Ecole des Ponts ParisTech	<i>Directeur de thèse</i>
Nicolas ROUSSEL Directeur de recherche, Université Gustave Eiffel	<i>Co-Directeur de thèse</i>
Olivier BAVEREL Professeur, Ecole des Ponts ParisTech	<i>Co-Directeur de thèse</i>
David HABRIAS et Chantal AIRA CROUAN KARDHAM Architecture	<i>Jury Invités</i>

Résumé

Le développement actuel de la technologie d'impression 3D béton est principalement motivé par l'avènement de l'industrie de personnalisation de masse, ses promesses de productivité et de performance environnementale.

Cette perspective de construction durable, basée sur la capacité de dépôt de matière rationnel par fabrication additive, est étudiée dans ce travail avec la méthode d'analyse du cycle de vie (ACV) appliquée à une technologie d'impression par extrusion.

Le manuscrit débute par un point détaillé sur l'impact environnemental de la construction béton, en introduisant le cadre théorique de la méthode ACV et en présentant la problématique de l'étude. Ensuite, l'analyse environnementale de la technologie d'impression 3D béton est réalisée avec un focus particulier sur l'impact lié au procédé. Deux cas d'études, représentatifs de deux échelles constructives, sont évalués : la brique élémentaire du procédé de construction et le système constructif complet. Enfin, certains aspects de déploiement de la pratique à l'échelle de l'industrie sont examinés à la lumière du phénomène de l'effet rebond au titre de perspectives de ce travail.

L'apport principal de cette étude est un modèle d'impact environnemental du procédé d'impression 3D béton, permettant de calculer le bilan environnemental de tout objet imprimé. De plus, ce modèle peut être intégré dans les études de conception et d'optimisation des éléments de construction. Les résultats des cas d'études soulignent l'importance de l'impact lié au procédé, qui, malgré les économies de matériaux, entraîne d'importants transferts d'impact et de pollution dans l'équilibre du cycle de vie d'un élément.

En effet, à l'échelle de base du procédé constructif, l'impact de 1m^3 de béton imprimé est presque deux fois plus grand que celui de 1m^3 de béton coulé. L'impact lié au procédé représente environ 13% dans la catégorie d'impact du Changement Climatique et peut varier considérablement en fonction de la résolution de l'impression.

Les gains environnementaux à l'échelle d'une structure se sont avérés insignifiants dans le cadre des structures maçonnées, pour autant ils peuvent représenter presque 50% dans le cadre du béton armé. L'impact lié au procédé reste important mais peut être compensé par les économies de matière. Néanmoins, la quantité de matériau s'est montré être une métrique inappropriée pour l'optimisation environnementale des structures imprimées.

Des études complémentaires à l'échelle de l'industrie, quantifiant l'ampleur de l'effet rebond, s'avèrent nécessaires afin de comprendre le profil environnemental de la pratique ainsi que des conséquences environnementales de son déploiement global.

Abstract

The ongoing development of 3D Concrete Printing technology is broadly associated with the boons of mass-customization industry, with the potential of productivity, time and cost optimization, as well as with the sustainable potential of the practice, leaning on a largely discussed capacity of smart and rational material deposition offered by additive manufacturing. This latter is investigated in the present work by means of the Life-Cycle Assessment (LCA) method applied to an extrusion-based printing technology built upon the 6-axis robotic arm.

The manuscript begins with a review of environmental impact of concrete construction, introducing the theoretical framework of the LCA discipline and presenting the question of the study. Then, the environmental analysis of 3D Concrete Printing technology is carried out with a particular focus on its process-related impact. Finally, two case studies, on different constructive scales, are evaluated: from the elementary brick of a construction procedure to the full-bodied building system. In closing, some aspects of the industry-wide deployment of the practice are outlooked in light of the rebound effect phenomenon.

The main contribution of this work is a model of environmental impact of 3D Concrete Printing technology, allowing to calculate the environmental impact of any printed object. Furtherly, the model can be integrated into design and optimization studies of building elements. The outcomes of the case studies point out a fair significance of the process-related impact that prompts some important impact transfers and pollution shifts into the life-cycle balance of a concrete element.

Precisely, on the basic scale of the construction procedure, the impact of the 1m^3 of printed concrete is almost twice bigger than the impact of 1m^3 of casted concrete. The process-related impact represents around 13% in Climate Change category and can vary significantly in function of the printing resolution.

The environmental gains of the 3D Concrete Printed structures were shown to be insignificant in the masonry framework but go up to 50% in the reinforced concrete perspective. The process-related impact remains significant but can be compensated by the material savings if properly taken into account during the design phase. It is worth noting that the material quantity was shown to be an inappropriate metric for environmental optimization of the printed structures.

In future, the industry-wide studies quantifying the magnitude of the rebound effect are needed in order to understand the global environmental profile of the practice as well as the environmental consequences of the industrial deployment of construction automation.

Remerciement

Tout d'abord, je souhaite remercier David Habrias et Chantal Aïra Crouan pour leur support et leur confiance qui m'ont accompagné tout au long de cette thèse. Je remercie également Mathieu Viollet et toute l'équipe toulousaine de Kardham Architecture au sein de laquelle ce projet est né, ainsi que toute l'équipe parisienne où il s'est déroulé.

Merci à Nicolas Roussel de m'avoir appris à faire la science et à mes collègues du laboratoire Navier pour les échanges qui ont tant enrichi ma réflexion. Je pense particulièrement à Koliann Mam – le vrai *bro* de thèse, et à Julian Cravero – le preux chevalier ACV.

Enfin, je remercie Romain Duballet d'être toujours à mes côtés et Nicolas Ducoulombier d'avoir redonné espoir à ce travail avec un litre de l'eau bouillie.

Je remercie Adélaïde Ferraille, l'encadrement ainsi que le jury pour leur travail.

Preface to *The Meaning of Life: A Very Short Introduction*
by Terry Eagleton

“Anyone rash enough to write a book with a title like this had better brace themselves for a postbag crammed with letters in erratic handwriting enclosing complex symbolic diagrams. The meaning of life is a subject fit for either the crazed or the comic, and I hope I have fallen more into the latter camp than the former. I have tried to treat a high-minded topic as lightly and lucidly as possible, while at the same time taking it seriously. But there is something absurdly overreaching about the whole subject, in contrast to the more miniature scale of academic scholarship.

Years ago, when I was a student in Cambridge, my eye was caught by the title of a doctoral thesis which read “Some aspects of the vaginal system of the flea”. It was not, one would guess, the most suitable work for those with poor eyesight; but it revealed an appealing modesty that I have apparently failed to learn from.

I can at least claim to have written on of the very few meaning-of-life books which does not recount the story of Bertrand Russel and the taxi driver. I am very grateful to Joseph Dune, who read the book in manuscript and made some invaluable criticisms and suggestions”.

Oxford University Press

Table of content

INTRODUCTION	1
<hr/>	
<u>PART I</u>	
<u>CONCRETE, ROBOTS AND ENVIRONMENT</u>	<u>5</u>
1.1. CONTEXT	6
1.1.1. CASE OF CONCRETE	8
1.1.2. 3D CONCRETE PRINTING TECHNOLOGY	9
1.2. RESEARCH METHODOLOGY	12
1.2.1. IMPACT TRANSFER AND POLLUTION SHIFT	14
1.2.2. FUNCTIONAL UNIT	14
1.2.3. METHODOLOGY OF THE PRESENT STUDY	17
1.3. ENVIRONMENTAL PROFILE OF CONCRETE MATERIAL	17
1.4. ENVIRONMENTAL PROFILE OF CONCRETE CONSTRUCTION PROCESSES	19
1.4.1. CONVENTIONAL CONSTRUCTION PROCESSES	19
1.4.2. AUTOMATED CONSTRUCTION PROCESSES	22
1.5. PROBLEM STATEMENT	25
BIBLIOGRAPHY OF PART I	27
<u>PART II</u>	
<u>MODELING & CHARACTERIZATION OF ENVIRONMENTAL IMPACT OF 3D CONCRETE PRINTING TECHNOLOGY</u>	<u>33</u>
2.1. CASE-STUDY OF 3D CONCRETE PRINTING TECHNOLOGY FOR ENVIRONMENTAL ANALYSIS	34
2.2. MODEL OF ENVIRONMENTAL IMPACT	36
2.3. ENVIRONMENTAL IMPACT OF PRINTABLE CONCRETE : M_{FP} COEFFICIENT	38
2.4. ENVIRONMENTAL IMPACT OF ROBOTIC CONSTRUCTION	41

2.4.1. EMBODIED IMPACT OF ROBOTIC CONSTRUCTION PROCESSES: RFP COEFFICIENT	42
2.4.1.1. RESULTS	43
2.4.1.2. AMORTIZATION TO THE PRINTING PROCESS	43
2.4.1.3. SENSITIVITY STUDY ON THE LIFE-SPAN	46
2.4.1.4. SENSITIVITY STUDY ON THE SIZE OF THE ROBOTIC ARM	47
2.4.2. OPERATIONAL IMPACT OF ROBOTIC CONSTRUCTION PROCESS OFP COEFFICIENT	50
2.5. ENVIRONMENTAL IMPACT OF 3D CONCRETE PRINTING : M_{FP} , R_{FP} & O_{FP} COEFFICIENTS	57
BIBLIOGRAPHY OF PART II	59
<u>PART III</u> <u>APPLICATION</u>	61
3.1. ENVIRONMENTAL IMPACT OF 3D CONCRETE PRINTING PROCESS	63
3.1.1. RESULTS	64
3.1.2. SENSITIVITY STUDY ON THE PRINTING RESOLUTION	67
3.1.2. CONCLUSIONS & PERSPECTIVES 3.1	69
3.2. ENVIRONMENTAL IMPACT OF 3D CONCRETE PRINTED STRUCTURE & BUILDING SYSTEM	71
3.2.1. SPACE-TRUSS WALL SYSTEM	71
3.2.2. NORMATIVE FRAMEWORK	74
3.2.3. ENVIRONMENTAL LIFE-CYCLE ASSESSMENT OF SPACE-TRUSS WALL	75
3.2.3.1. RESULTS	78
3.2.3.2. SENSITIVITY STUDY ON THE PRINTING PROCESS-RELATED PARAMETERS	78
3.2.3.3. FRENCH INDUSTRIAL CONTEXT	81
3.2.4. COMPARISON WITH CONVENTIONAL STRUCTURAL SYSTEMS	83
3.2.4.1. MASONRY	83
3.2.4.2. REINFORCED CONCRETE	85
3.2.5. APPROACH TO THE END-OF-LIFE	89
3.2.6. CONCLUSIONS & PERSPECTIVES 3.2	90

BIBLIOGRAPHY OF PART III	93
<u>PART IV</u>	
<u>CONCLUSIONS & PERSPECTIVES</u>	<u>95</u>
4.1. CONCLUSION	96
4.2. PERSPECTIVES	98
4.2.1. TOWARDS AN INDUSTRIAL DEPLOYMENT OF 3D CONCRETE PRINTING TECHNOLOGY	98
4.2.2. JEVONS PARADOX	100
4.2.3. REBOUND EFFECT OF 3D CONCRETE PRINTING TECHNOLOGY	102
4.2.4. SUSTAINABLE POTENTIAL OF CONSTRUCTION AUTOMATION	105
BIBLIOGRAPHY OF CONCLUSION & PERSPECTIVES	107
<u>ANNEX 1</u>	
<u>LIFE-CYCLE INVENTORY OF THE ROBOTIC PRINTING CELL</u>	<u>109</u>
<u>ANNEX 2</u>	
<u>POWER MEASUREMENTS</u>	
<u>EXPERIMENTAL PROTOCOL & TECHNICAL DETAILS</u>	<u>115</u>
1. ELECTRIC POWER	116
2. POWER MEASUREMENT DEVICES	120
3. DATA PROCESSING	123

Introduction

Progressivist historians tend to claim that the architecture is systematically late to embrace technical progress.¹ Indeed, at the end of the nineteenth century when most of the industries had already switched to mechanical production, the building sector had largely ignored or even argued against the new technologies.² The situation has radically changed with the rise of an after-war housing crisis that triggered the global urbanization in the second part of the twentieth century. Hereby, *l'Esprit Nouveau*³ of Le Corbusier and his fellow modernists got to an apex of its conceptual relevance and placed *la maison en serie*⁴ in the heart of the philosophical system framing the mass construction. What happened next was broadly set out by the chroniclers: the architects have re-designed the buildings in order to fit the industrial mass production, the urbanists have re-designed the cities in order to fit the metropolitan mass circulation and housing; both establishing the point of no return in a way the architecture is thought, designed and produced.

Before the industrial revolutions, back to the antique times, the technical progress seems to similarly go unheeded amongst the architects. Notably, the ten volumes of Vitruvius' *De Architectura*, mention barely its coeval construction techniques and structural innovations, e.g. stereotomy, arches and vaults.⁵ Instead, the seminal text of the discipline presents some extensive detailing on antique war machines and only describes some obsolete Hellenistic construction technologies based on clay and sun-dry brick masonry, very much outdated for Augustus' Rome.

Nowadays, when most of the industries have already integrated the digital technologies, anew the same inertial delay confronts the construction automation.

As a conceptual entity the construction automation stands for the technical change from mechanical mass-production towards the industry of mass-customization. In practice, it refers basically to numerical control manufacturing and algorithmic modeling of building elements, both unrolling within the same digital design-to-fabrication continuum. As follows, the variability within the object's shape can be directly transmitted from the digital model to the fabrication sequence, providing in that way a possibility of the differentiated series, i.e. the serial production of the non-standard elements.⁶

Thus, the inertia facing the advent of construction automation may be of manifold reasons connected with the technological transition. However, besides the natural delay related to the general infrastructure shift, hardware replacement etc., the systematic resistance to the technological innovations demonstrated by the construction sector (literally from the beginning of time) may be of some philosophical order.

In philosophy of science, the inertia associated with the new tool has originally been described by an instrument law, epigrammatically put forward as follows:

¹ M. Carpo, *The Second Digital Turn: Design Beyond Intelligence*, 1 edition. Cambridge, Massachusetts: The MIT Press, 2017;

² *Ibid.*

³ L. Corbusier, *Vers une architecture*, Paris: Editions Flammarion, 2008.

⁴ *Ibid.*

⁵ M. Carpo, *The Second Digital Turn: Design Beyond Intelligence, Op.cit*

⁶ Bernard Cache, "Towards the non-standard production" in *Architecture Words 6: Projectiles*. Architectural Association, 2014.

*“When all you’ve got is a hammer - everything looks like a nail”*⁷

The expression thus illustrates a cognitive bias of the problem solving, pushing to systematically adapt a given task to an available tool rather than to reinvent the proceeding method according to an inquired problem. In other words, independently from the nature or structure of a task, one will naturally opt for the familiar media. Reversing the inference from this former, in a similar way the new tool itself may be a vector of the profound procedural changing within a given discipline.

Modernism may be the most outstanding example of the morphological transformations the architectural discipline has to pass through in order to fit the novel production system. For the automated construction, a similar idea has appeared in the middle eighties within the principle of “robot-oriented design”⁸, that later evolved into the full-bodied theoretical system⁹, formulating the guidelines, design and re-design orientations for the building systems in order them to fit the robotic fabrication and assembly.

In the field of architectural avant-garde, the novel formal framework emerging from the retooling of the discipline has been a long-lasting theoretical quest since the early seventies. It has initiated with the movement of Folding¹⁰, progressively evolved into the Non-Standard Architecture¹¹ and succeeded by Parametricism - *the great new style after Modernism, that was supposed to articulate in terms of architecture the growing complexity of the post-fordist society*.¹² Notwithstanding, in barely ten years, Parametricism has also got denoted as archaic and inaccurate and followed with the movement of Discrete,¹³ re-defining *again* the way the discipline might appear and proceed in the era of automation.

In the end, it’s barely possible to say with certainty in which theoretical framework the ongoing development of construction automation unrolls. Yet, a particularly strong point of Parametricism was to insist on the profoundly old-fashioned term of *style*, that with the words of the same progressivist historian can be understood as follows. All the objects of the same non-standard series will not share the same form, but rather the same style, in the original sense of the term referring to the *stylus* of a writer and therefore to his tool and not to his aesthetic creed.¹⁴

Therefore, in a way, all the objects produced within the same design-to-fabrication continuum and even generally within the framework of construction automation may pertain to Parametricism. Yet, if Parametricism is indeed “*the great new style*”, or simply the good old modernist doctrine acting within the digital environment, remains to be debated.

⁷ Abraham Maslow, 1966

⁸ Thomas-Alexander Bock, “Robot-oriented Design”, The 5th International Symposium on Robotics in Construction June 6-8, 1988 Tokyo, Japan

⁹ <http://rod.de/>

¹⁰ G. Lynn, « Folding in Architecture (1993) », in *The Digital Turn in Architecture 1992–2012*, Wiley-Blackwell, 2015, p. 28-47.

¹¹ Centre Georges Pompidou, *Architectures non standard*. Paris, France: Centre Georges Pompidou Service Commercial, 2003.

¹² P. Schumacher, « Parametricism: A New Global Style for Architecture and Urban Design », *Architectural Design*, vol. 79, n° 4, p. 14-23, 2009, doi: 10.1002/ad.912.

¹³ G. Retsin, « Discrete Architecture in the Age of Automation », *Architectural Design*, vol. 89, n° 2, p. 6-13, 2019, doi: 10.1002/ad.2406.

¹⁴ M. Carpo, *The Alphabet and the Algorithm*, 1 edition. Cambridge, Massachusetts: The MIT Press, 2011.

Putting aside the epistemological seek for the formal relevance, the current development of construction automation got closely bound up with the argument of productivity increase, time and cost optimization, affordable housing worldwide and furthermore sustainability. In fact, progressively, the formal complexity originally proper to the algorithmic modeling got more and more associated with the efficiency; the efficiency - with the global optimization of production and with the productivity increase; finally combined together, a sustainable vision of the practice was set as a general framework in which the re-design of building elements nowadays unfolds. In other words, the pursuit of the cogent design agenda got superseded by the growing environmental concern in the sector and today almost universally got adopted as the central argument for the practice development.

The present work addresses the sustainable potential of construction automation and performs an environmental evaluation of 3D Concrete Printing technology, focusing on the impact coming from the robotic construction process. The analysis is placed into a specific framework of 3D Concrete Printing practice, addressing the re-design and optimization of building elements by the means of more rational material deposition enabled by additive manufacturing. The process-related impact is thus compared to the material-related one on different constructive scales, in order to identify an eventual trade-off between those two. In a larger outline, this study aims to bring some novel insights into the sustainable potential of 3D Concrete Printing, endeavoring to understand whether the efficiency of the 3D Concrete Printed elements will perform an expected environmental efficiency.

The manuscript is organized as follows. Part I introduces the current environmental context of construction sector, putting forward the role played by concrete construction and pointing out the potential improvements the 3D Concrete Printing technology could bring. Then, the research methodology is described, introducing the environmental Life-Cycle Assessment method and reviewing the existing works in the field. The problem statement of the study concludes this part.

Part II describes the environmental Life-Cycle Assessment study carried out on the 3D Concrete Printing technology. The model of environmental impact is proposed and the impact coming from the robotic construction process is characterized.

Finally, in Part III, three case-studies evolving in scale are evaluated, using the developed method. The manuscript concludes with the general discussion on the sustainable development of the practice and the perspectives for the further studies.

Part I
Concrete, Robots and Environment

1.1. Context

The construction sector faces great challenges regarding its modernization and its role in the growing environmental emergency.

Indeed, taking into account the current population growth, the need for new construction by 2060 has been estimated to be around 230 billion square meters [1] (which represents roughly building a surface equivalent to the city of Paris every week for the next forty years [1]). Figure 1.1 depicts the magnitude as well as the partitioning of those surfaces worldwide. At the same time, the construction sector remains the first consumer of raw materials (for which scarcity problem has already raised [2]) while its industrial productivity has barely evolved since the 1990s [3]. Indeed, in contrast to other manufacturing industries, as well as the world economy in general, both continuously increasing their productivity, the annual growth rate of the construction sector has been stagnating for the last 30 years (see Figure 1.2). Finally, the construction sector is currently responsible for 36% of final energy use and for almost 40% of global carbon dioxide (CO₂) emissions, 11% of which result from manufacturing building materials and products, e.g. cement, steel, and glass [4].

In order to face those challenges, many strategies have been developed in industry and academia. They can be regrouped in three categories. The first category addresses the renovation, refurbishment, and the normative update of the existing building stock. Its necessity can be exemplified with the case of the french housing stock. As a matter of fact, in France, 79% of housing that will be available in 2030 exists already, almost 50% of which has been built before the first thermal regulation (RT), appeared in 1974 (after the first petroleum shock) [5].

The second category addresses the end-of-life issue in the construction sector, i.e. reuse and recycling practice. In fact, only in 2014 in France, the construction sector has produced 227,5 million tonnes of waste, 80% of which was inert¹⁵, and thus ready for reuse.

The third category addresses the development of sustainable design and construction techniques for the new construction. In fact, since 2017, more than half of the world's population resides in cities, i.e. the industrially built urban areas, and by 2050, the urban population is expected to reach 68%. That growth suggests that the future framework of the sector pertains to industrial construction, which has to rapidly become more efficient and more sustainable. Thus, despite the importance of developing the refurbishment and reuse strategies (first and second categories), they will not be able to cover the pressing need for new construction. Therefore, there is an urgent need to develop sustainable and efficient design and construction techniques.

The present work focuses on this third category and addresses the ongoing development of construction automation, in particular 3D Concrete Printing. The following section describes the current context of concrete construction and the potential improvements associated with an advent of 3D Concrete Printing.

¹⁵ Source : enquête « Déchets et déblais produits par l'activité de construction en 2014 », SOeS

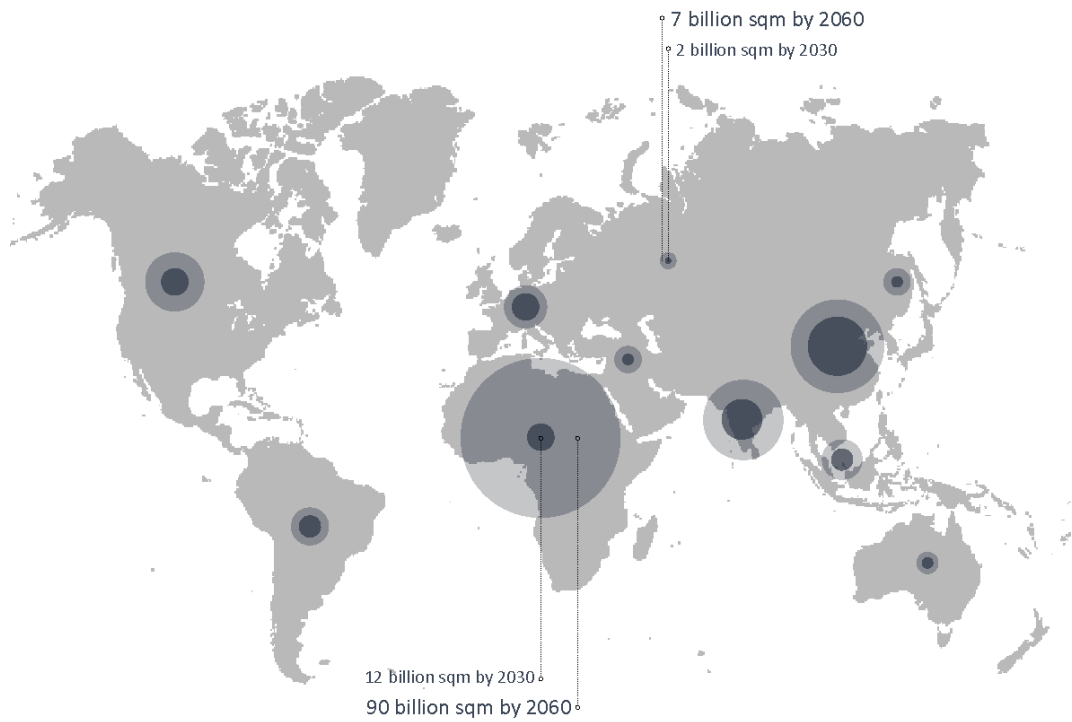


Figure 1.1. Partition and magnitude of surfaces to be built worldwide in the following 40 years
Source: IEA (2017), Energy Technology Perspectives 2017, IEA/OECD, Paris; www.iea.org/etp

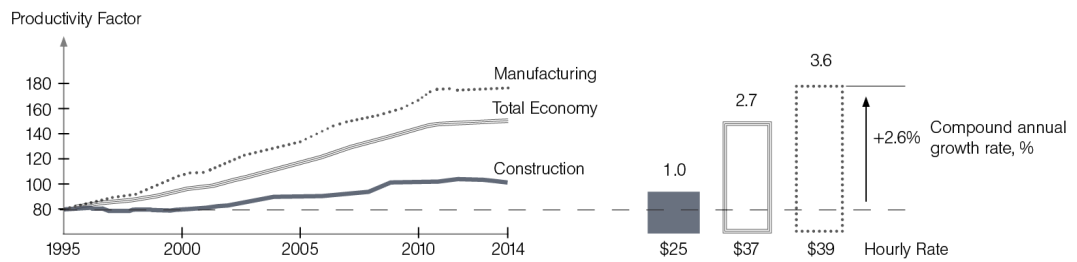


Figure 1.2. Based on a sample of 41 countries that generate 96% of global GDP.
Source: OECD; WIOD; GGCD-10, World Bank; BEA; BLS; national statistical agencies of Turkey, Malaysia, and Singapore; Rosstat;
Reproduced from: McKinsey Global Institute “Reinventing construction: A route to higher productivity” 2017

1.1.1. Case of Concrete

Within this previously exposed context, the case of concrete construction is particularly interesting. In fact, concrete is the most used construction material in the world ([6], [7], [8]), and more concrete is consumed by the construction sector than all other building materials combined [7]. The yearly consumption of concrete represents roughly 35 billion tonnes ([7], [9]).

From a historical perspective, a local increase of concrete consumption is directly related to an economical and industrial development of a territory and thus to its urban expansion. As an example, China consumed between 2011-2013 as much concrete as the United States of America during the twentieth century¹⁶ [10], and those numbers will increase considering the ongoing urban development in the world. Figure 1.1 depicts the partitioning and the magnitude in square meters of new construction estimated to be built worldwide in the next forty years¹⁷, combining these estimations with the current popularity of concrete material in construction sector, this illustration can be interpreted as the partitioning and magnitude of the concrete use worldwide in the next forty years.

According to Flatt et al. [6] the popularity of concrete material in the construction sector is mainly related to the broad availability of its components, its relatively low cost, as well as the ease with which those components can be processed into a strong and durable, rock-like material. Indeed, *“there seems to be no other material that could replace concrete in the foreseeable future to meet our societies' legitimate needs for infrastructure, housing, shelter and protection, by the unique property of cement and water transforming a pile of aggregates into rock in a few hours at room temperature”* [7].

Concrete is a mix of water, sand and gravel bonded together by cement, the most used binder. Despite the fact that the production of Portland cement represents from 5% [11] to 8% [6] of all anthropogenic carbon dioxide emissions, the other raw constituents needed for concrete composition, e.g. sand and gravel, are usually local, broadly available and possess a very low carbon footprint (1 tonne of aggregates represents around 2,75 kg CO₂ Eq [12]). It is common in the field of environmental sciences to consider these other constituents as an unlimited resource at the planetary scale [13]. However, in the local context, the sand and gravel are subject to depletion and can be estimated through the cement consumption [14]. Thus, the production of cement is reported by 150 countries and reached 3.7 billion tonnes in 2012 [15], almost doubling since 2004 [11]. As follows, considering that for one tonne of cement the concrete mix will need six to seven tonnes of sand and gravel [16], the world's use of aggregates can be estimated from 25.9 to 29.6 billion tonnes in 2012.

Therefore, as it was outlined by Van Damme [7] and Flat et al. [6], it is not only and not exactly the impact of concrete material itself, but rather its gigantic amount consumed yearly (around 35 billion tonnes per year) that triggers its environmentally alarming status.

¹⁶ USGS Cement Statistics 1900–2012; USGS, Mineral industry of China 1990–2013.

¹⁷ IEA (2017), Energy Technology Perspectives 2017, IEA/OECD, Paris; www.iea.org/etp

As follows, at the scale of material and to address the volumic impact of concrete, the environmental improvement potential dwells mainly in cement substitution with alternative binders, e.g. sulfo-aluminate clinker and many others ([11], [6], [9], [17]).

At the industry-wide scale and to address the intensity of the concrete use, even greater optimization potential lies in a more rational material deposition using numerically controlled additive manufacturing, largely known as 3D Concrete Printing ([18], [19], [8], [20], [21]).

1.1.2. 3D Concrete Printing Technology

The development of additive manufacturing with cementitious materials, referred to as 3D Concrete Printing (3DCP), has initially started with the work of Pegna [22] and led to the development of a large variety of printing technologies. Amongst those, three can be mentioned as pioneering: the Contour Crafting [23] developed at the University of Southern California, extruding the permanent clay formwork to be backfilled then with conventional concrete; the Loughborough systems [24] referred to as the 3D Printing, as directly extrudes the fresh mortar into the fully dense elements; and the D-Shape system, built upon on a large-scale 3-axis jetted binder system relying on the particle sand-bed [25]. Besides those, there exist a multitude of other digital fabrication processes with cement-based materials currently under development in academia and industry, a detailed taxonomy of which was proposed by Buswell et al. [26] and depicted on Figure 1.4. The classification of building systems produced with 3D Concrete Printing has been proposed by Duballet et al.[18].

The present work is focused on the extrusion-based additive manufacturing with cement-based materials, referred to as 3D Concrete Printing, which basically consists of a successive layer-by-layer stacking of concrete filaments contouring an object, with no formwork, i.e. by the direct material placement. It is thus usually associated with a vision of a so-called “*free-form construction*” [22], which in the following years got combined with smart and rational material deposition strategy, entailing a sustainable vision of this technology [27], [28]. A 3D Printing technology used for the environmental evaluation of the present study will be detailed in the next part. Figure 1.3 depicts four different building and infrastructure elements produced with 3D Concrete Printing technology enabling the material savings through topological optimization. Concretely, the surfacic weight is reduced to almost 80% compared to its conventional analogues in the case of the space-truss wall system [10], and to around 70% in the case of the funicular floor system [29].

From the epistemological standpoint, 3D Concrete Printing technology perfectly outlines the precept of the Non-Standard Architecture, which was supposed to bring some spectacular changes to the discipline by releasing its form from the constraints of standardization [30]. Firstly theorized in Deleuze’s book *The Fold: Leibniz and the Baroque* [31] within the definition of the *objectile*, this principle of serial production of non-standard elements, largely known as mass-customization, was initially made possible with the advent of numerical control machines and algorithmic modeling in early 1970s. Ever since, multiple movements ([32], [33]) and even styles ([34], [35]) appeared, longing to inscribe the digital into the discipline in order to formulate an adequate design agenda within the new industrial paradigm.

Later in the early 2010s, the computation went public and merged with the development made in the field of optimization algorithms and finite elements. Combined together, the fully-integrated software platforms for building design and analysis appeared and spread, initiating hereby a phenomenon that Carpo would later call *The Second Digital Turn* [36], i.e. a systematic recourse to optimization strategies while choosing the design parameters. Thus, the advent of 3D Concrete Printing technology coincides with both: the optimum trend, as well as the fundamental need of formal re-design of objects in order to fit the novel fabrication process by additive manufacturing. Here, the concrete blocks became continuous and hollow, and despite original Pegna's vision for "*solid free-form construction*" [22], evolved into largely optimized and rational building systems (see Figure 1.3), that rapidly got labeled as more sustainable, drawing upon a one principal argument of material quantity reduction ([37], [29]), which seems to be a wrong metric for the environmental question.

The present work addresses the issue of lowering the impact of the construction sector and evaluates the capacity of the ongoing development of the 3D Concrete Printing technology to face that issue. The part is organized as follows. In the first place, the research methodology of environmental analysis is described. Then, the environmental profile of the concrete construction is reviewed, including the previous study on the automated concrete construction with 3D Printing. The research question of the present work will conclude this part.

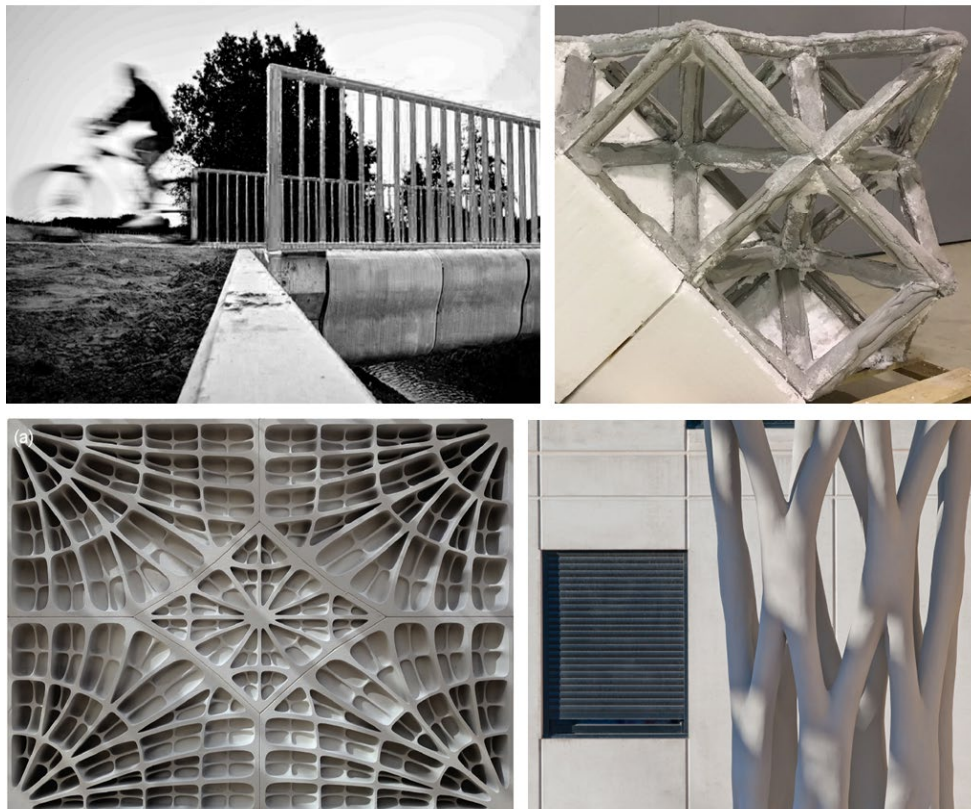


Figure 1.3. Building Systems re-designed with 3D Concrete Printing Technology:
(top, left) Pre-stressed topology-optimized bicycle bridge [38]; (top, right) Space-truss Wall System [10];
(bottom, left) Funicular Floor System [39]; (bottom, right) Krypton column [40].

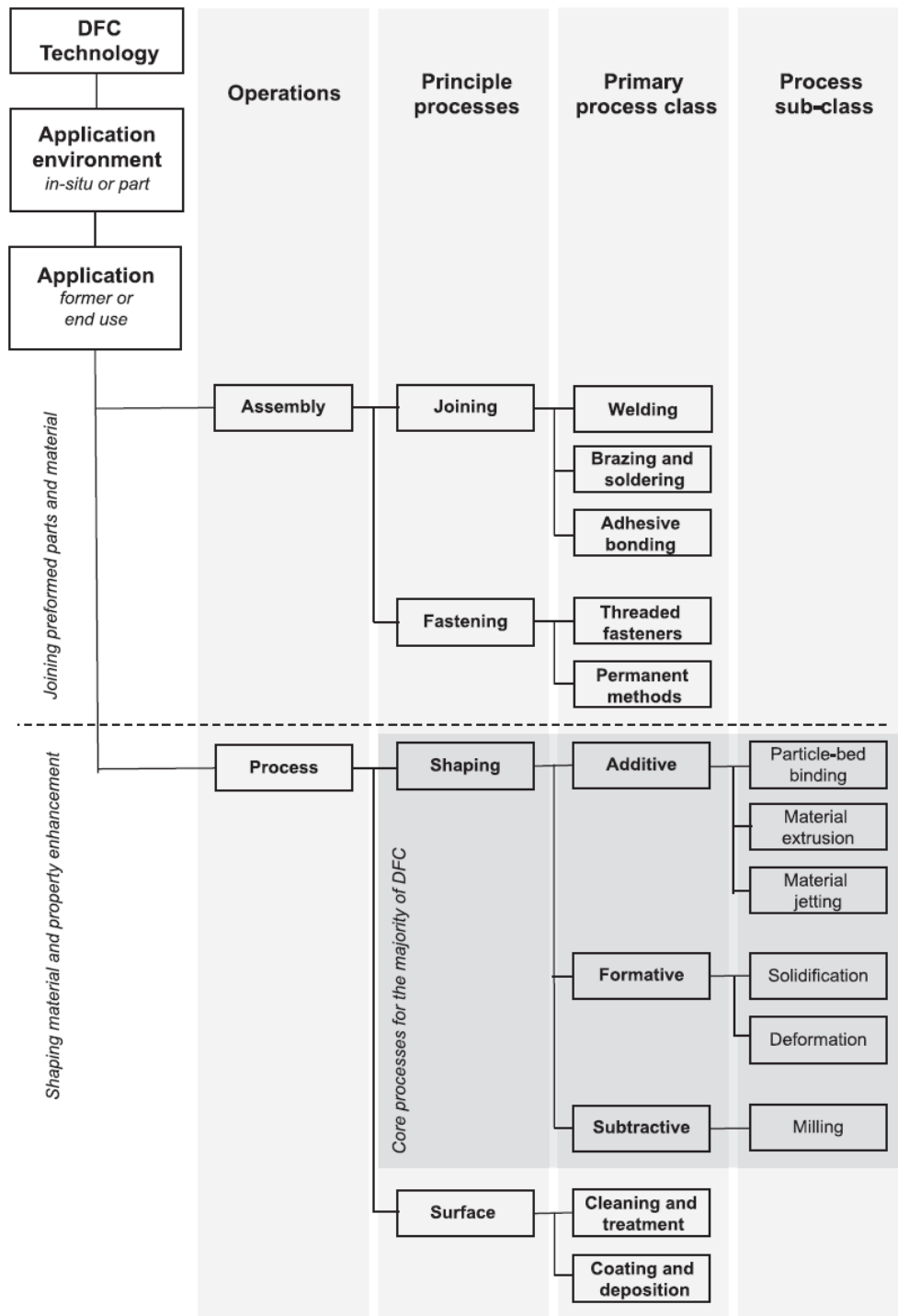


Figure 1.4. The RILEM process classification framework for DFC technologies. Reproduced from [26]

1.2. Research methodology

The methodology of the present research is based on the environmental Life Cycle Assessment method framed by the international standards ISO 14040 [41], ISO 14044 [42] and the European norm EN 15804 [43]. Beyond the normative references, the methodology applied in this work is based on the theoretical framework described by Jolliet et al. [44] and Simonin [45]. The specificities of the method application to the construction sector were extensively described by Peuportier et al [46].

The environmental Life-Cycle Assessment method consists in tracing all the energy and resource flows needed for a system to function, from raw materials extraction to end-of-life. In the building sector, we particularly distinguish the operational impact of a system, related to the operational life-cycle phase of a building (e.g. heating, cooling, water use, etc.); and the embodied impact, related to the prior phases: raw material extraction, transportation, production, construction processes and end-of-life. Figure 1.5 depicts the main phases of the building life-cycle, pointing out that the operational impact stands for one phase of the total life-cycle, while the embodied impact represents the remaining five.

The present work addresses the construction phase of the embodied impact of the building life-cycle.

According to ISO 14040, the methodological framework of the LCA method is composed of three iterative steps. First, the goal and scope definition of the study are stated, including the definition of objectives and boundaries of the studied system, the definition of its function and functional unit. Then, the inventory analysis is performed, usually with the help of a database gathering the inventory data for products and services with the quantitative information on their associated emissions (inflows, outflows). Finally, an impact assessment is carried out to evaluate the environmental impact of the inventoried emissions.

The evaluation of the environmental impact can, in turn, be divided into several steps, described by Jolliet et al. [44]. To perform this evaluation, impact categories and their associated characterization models are selected in order to classify the emissions according to their associated environmental impact category (e.g. climate change, toxicity, eutrophication, resource depletion, etc.). First, the Midpoint characterization step aims to weight and aggregate the emissions into midpoint impact categories. Then, the Endpoint characterization step aims to aggregate the impacts into damage categories. Figure 1.6. shows the midpoint categories of impact and the endpoint categories of damage and depicts the relation as well as the transition between those two. An optional normalization step can be carried out to inscribe the results into a global industrial/geographic/national context, to show the fraction of the global impact that the studied system represents into a specific environmental impact category.

To sum up, the LCA method allows to quantify the environmental performances of a system at every stage of its life-cycle and in different environmental categories, permitting in that way to assess the occurrence of impact transfers and/or pollution shifts.

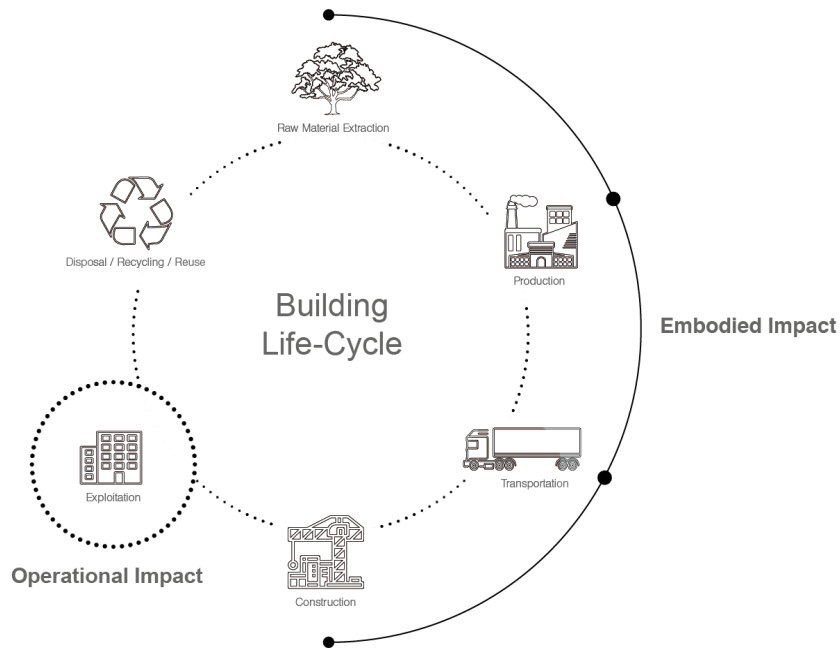


Figure 1.5. Life-cycle diagram of a building

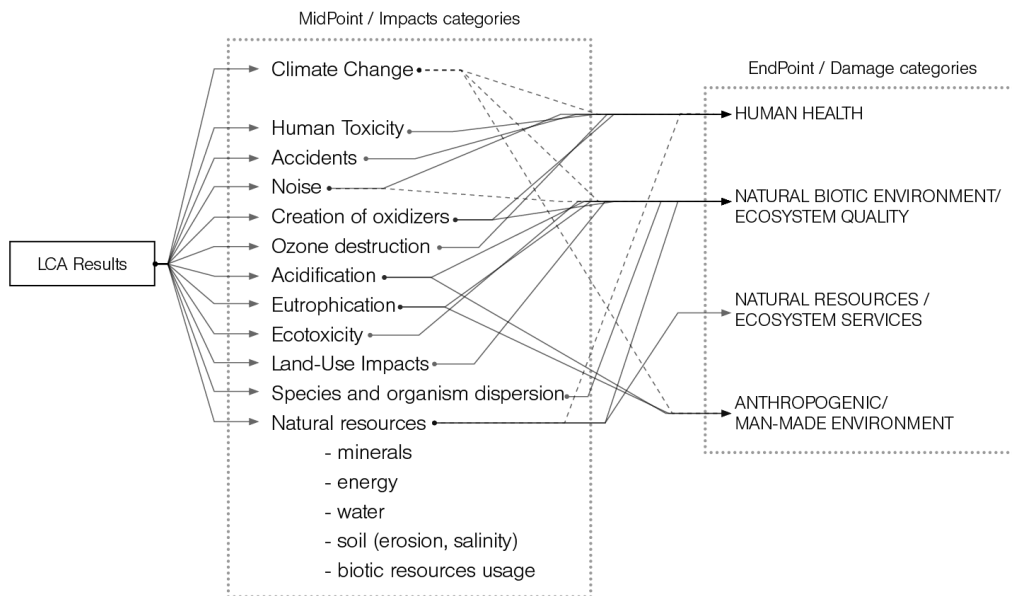


Figure 1.6. General structure of the UNEP-SETAC impact assessment framework. The dotted arrows represent conversions from midpoint to damage categories that are particularly uncertain. Adapted from O. Jolliet et al., International Journal of LCA, 9, 394-404, 2004; Source: O. Jolliet et al., Environmental Life Cycle Assessment, 1st Edition. CRC Press, 2016

1.2.1. Impact Transfer and Pollution Shift

The impact transfer phenomenon stands for the transposition of pollution from one phase of life-cycle to another and usually occurs after technological modifications in a given system. A typical example of impact transfer is the replacement of combustion engines by electric motors in the car industry. While the latter are emission free during the operational phase, their production necessitates a more important and diverse set of materials that need to be extracted, processed, and taken care of at the end-of-life. Therefore, this technological modification transfers the impact from the operational phase to other phases of the life-cycle: raw material extraction and disposal.

The pollution shift phenomenon stands for the transposition of environmental burden from one environment to another. Using the same example of the car industry, the evolution from combustion engines to electric motors transfers pollution from oil-related categories to those related to electricity generation, extraction and treatment of metals and rare-earth elements. Furthermore, the shift can be seen from a geographic standpoint, where pollution is transferred from oil pumping countries to metal mining ones.

Within the construction sector, the occurrence of impact transfer and pollution shift phenomena are numerous [47]. The over-insulation of building envelopes offers a paradigmatic example of both phenomena: when the reduction of operational energy of a building for heating, cooling etc. is addressed through the massive envelope insulation, in some figures, the embodied impact of insulation material turns out to be greater than the savings of the operational impact it is supposed to bring ([48], [49]). In terms of impact transfer, the impact is transposed from the operational phase to the material extraction, production and construction phases. In terms of pollution shift, the reduction of the energy-related pollution on the operational phase is counterbalanced by the impact increase on the phases of raw material extraction, transportation and construction due to the supplementary material needed for insulation.

1.2.2. Functional Unit

The functional unit is a crucial methodological element of the LCA method. According to ISO 14044 (2006), the functional unit is the “*quantified performance of a product system for use as a reference unit*”. For example, different transportation methods are often compared based on the functional unit of transporting one person over a distance of 1 km, i.e. 1 person-km [44].

The functional unit is a measure that quantifies the function of a system in terms of the service offered. It must be quantifiable and additive, in other words, the impact of two functional units must be the double of that of one. Table 1.1 shows examples of functional units with their associated reference flows and key parameters.

To sum up, an integral part of the Life-Cycle Assessment method is to compare the environmental performance of different systems or products. The comparison is therefore guided on the basis of functional reference, not inventories. As an example, the comparison of the wall paint shown in Table 1.1, considers equivalent surfaces painted by different paints (function), rather than cans of paint (inventory).

Table 1.1. Examples of FU definition and their associated flows and key parameters

Source: O. Jolliet et al., Environmental Life Cycle Assessment, 1st Edition. CRC Press, 2016.

System	Functional Unit (Service Offered)	Reference Flows	Key Parameters linking reference flows to FY
Hand-dryer	1 pair of dried hands	1,5 Paper towels / Towel dispenser	N° towels per usage
		30s of working / Electric dryer	Power of dryer & duration use
Wall paint	100m ² of wall painted for 20 years	30 kg of long-lasting paint (20 years)	Amount of paint applied per m ²
		2 x 25 kg of less durable paint (10 years)	Life-time of paint

Within the construction sector, the importance of the definition of a proper functional unit can be illustrated with a case of the concrete mix. Indeed, the volumic impact of high-performance concrete is much higher than the one of conventional C25/30 concrete. However, along with the higher impact it also performs a much higher compressive strength. Therefore, when normalizing that impact per the unit of volume, the high-performance concrete performs much higher environmental impact. However, taking into account the much higher mechanical resistance of the high-performance concrete, its distribution into the building element is much lower, see Figure 1.8. As follows, the comparison of two material mixes must rather be normalized to the mechanical resistance unit, rather than to the volume unit.

Figure 1.7 depicts a comparison between conventional C25/30 and high-performance concrete (ETHZ IFB) per unit of volume (cubic meter) and then per unit of compressive strength (MPa), pointing out a substantial shift of performance. Concretely, when normalizing the Climate Change impact per 1 cubic meter (Figure 1.7. Left) the high-performance (ETHZ IFB) concrete is 40% more impacting. However, when normalizing the Climate Change impact of each material mix to 1 MPa (Figure 1.7. Right), the high-performance (ETHZ IFB) concrete is 20% less impacting. Figure 1.9 depicts a historical evolution of the mechanical performances of the concrete material and its associated carbon footprint due to advancements made in the concrete science.

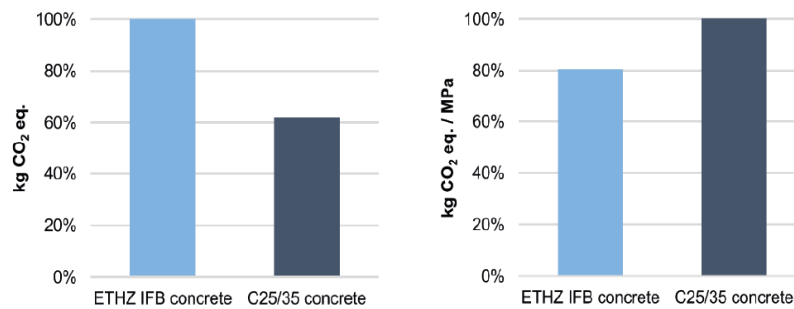


Figure 1.7. Left: Comparison of the Climate Change impact of 1 cubic meter between conventional C25/30 and Ultra-High Performance (ETHZ IFB) concrete, normalized by the highest value

Right: Comparison of the Climate Change impact expressed in kg CO₂/MPa between conventional C25/30 and Ultra-High Performance (ETHZ IFB) concrete, normalized by the highest value

Reproduced from [50].

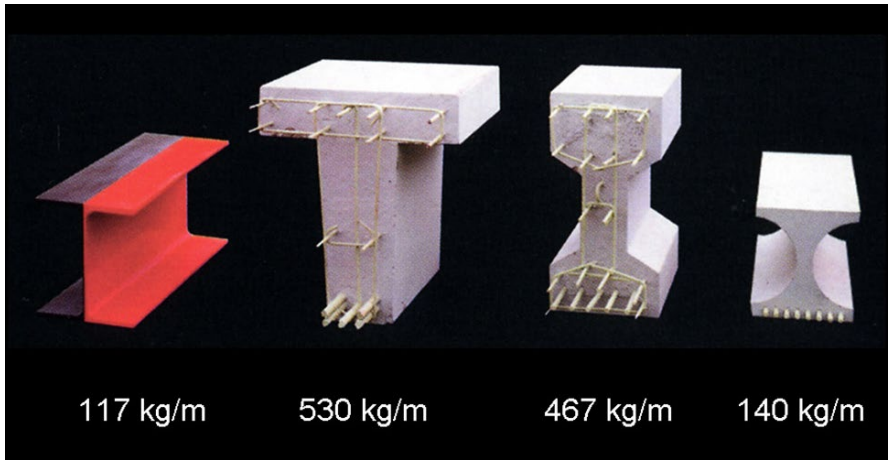


Figure 1.8. The four beams have the same load bearing capacity. The first (left) is made of mild steel. The second is made of classical reinforced (C25/30) concrete with iron rebars, as it was used in the 1930s. The third is made of prestressed high-performance concrete, with both rebars and prestress cables. The last one is a fiber-reinforced Ultra-High-Performance Concrete (UHPC), without any rebar, but with prestressing cables. It is only slightly heavier per unit length than the steel beam (+20%), whereas the classical concretes are much heavier (+450% and +400%, respectively) (courtesy: Ph. Gégout, Bouygues). Reproduced from [7].

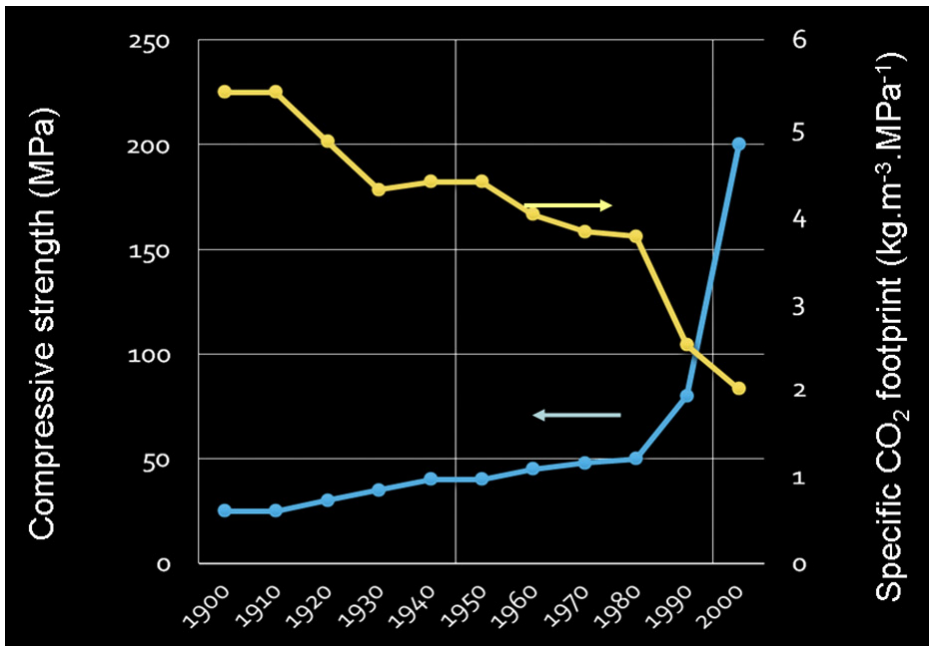


Figure 1.9. Evolution of the compressive strength and average specific carbon dioxide footprint of concrete during the 20th and early 21st century. Source: (F.-J. Ulm, Concrete Innovation Potential, Beton- und Stahlbetonbau 107 (2012) 504–509; Reproduced from [7].

1.2.3. Methodology of the present study

The present research studies the environmental performance of the 3D Concrete Printing technology using the environmental Life-Cycle Assessment method. This study is carried out within the cradle-to-gate boundaries, as the problematic addresses mainly the construction phase.

The modeling and calculation are made within the OpenLCA Software using EcoInvent 3.2. Cut-off database [51] for the inventory collection and analysis. The Recipe MidPoint (H) calculation method is used for impact evaluation. It is a well-known and comprehensive LCIA method, created in 2008 [52], updated in 2016 [53], that was largely used in previous studies ([50], [54], [55]). Moreover, several indicators of this methodology have been recommended by the ILCD initiative [56]. For the comparative studies the calculation method of EN 15804¹⁸ was used in order to have comparable results with that of EPD files from the INIES database [57]. Specific methodological precisions will be provided at the beginning of every case-study.

1.3. Environmental profile of concrete material

While concrete material is a mix of several components, its environmental profile is mostly defined by cement. Indeed, cement preparation involves chemical reactions (limestone decarbonation) that occur at high temperature (around 1450°C). Carbon dioxide emissions related to this process are equally distributed between the decarbonation of limestone, where CO₂ is chemically produced, and the energy used to maintain the conditions of decarbonation in a broadly fossil-based energy context¹⁹. As a result, the equivalent mass of CO₂ emitted during this process is approximately equal to the mass of cement produced (1 tonne of cement represents 1 tonne CO₂ Eq [17], [11]).

The other raw components needed for concrete preparation, e.g. sand and gravel, are usually local, broadly available and possess a very low Climate Change impact as mentioned previously (1 tonne of aggregates represents 2,75 kg CO₂ Eq [12]). As follows, the Climate Change impact of the concrete mix can be considered roughly proportional to the quantity of cement contained in the material mix.

In order to illustrate that previous statement, Table 1.2 depicts the material composition of one cubic meter of conventional C25/30 concrete for residential buildings, with references to the EcoInvent process. Table 1.3 depicts the results of the environmental impact calculation accomplished with the Recipe MidPoint (H) calculation method for one cubic meter of concrete C25/30 for residential buildings. The Climate Change impact of one cubic meter of concrete represents 299 kg CO₂ Eq, which corresponds roughly to the cement mass into the material mix.

¹⁸ Tiffany Desbois "Méthode d'évaluation environnementale sous OpenLCA Selon la norme NF EN 15804+A1 et la norme complémentaire NF EN 15804/CN", Cerema / DTerOuest / Laboratoire de Saint-Brieuc

¹⁹ In 2012, the world average electricity mix is on 40% consiste of the coal-fired power and equals to 0,75 kg CO₂-Eq per kWh [51]

Table 1.2. Composition of one cubic meter of C25/30 concrete for Residential Buildings

Component	Quantity / m3	Reference to Ecoinvent Process
Cement	300 kg	cement, Portland market for cement, Portland - RoW
Aggregates, Gravel	1200 kg	gravel, round market for gravel, round - GLO
Aggregates, Sand	600 kg	sand market for sand - GLO
Water	180 L	tap water market group for tap water - GLO

Table 1.3. Environmental Impact of one cubic meter of C25/30 concrete for Residential Buildings

Impact Category	Unit	Impact / m ³
agricultural land occupation	m ² *a	2,46E+00
climate change	kg CO2-Eq	2,99E+02
fossil depletion	kg oil-Eq	3,45E+01
freshwater ecotoxicity	kg 1,4-DCB-Eq	9,73E-01
freshwater eutrophication	kg P-Eq	3,17E-02
human toxicity	kg 1,4-DCB-Eq	3,63E+01
ionising radiation	kg U235-Eq	8,48E+00
marine ecotoxicity	kg 1,4-DCB-Eq	9,58E-01
marine eutrophication	kg N-Eq	2,28E-01
metal depletion	kg Fe-Eq	3,89E+00
natural land transformation	m ²	3,70E-02
ozone depletion	kg CFC-11-Eq	1,12E-05
particulate matter formation	kg PM10-Eq	3,32E-01
photochemical oxidant formation	kg NMVOC	6,73E-01
terrestrial acidification	kg SO2-Eq	6,92E-01
terrestrial ecotoxicity	kg 1,4-DCB-Eq	1,22E-02
urban land occupation	m ² *a	2,64E+00
water depletion	m ³	5,94E-01

1.4.

Environmental profile of concrete construction processes

“...whether reinforced with rebars, tendons, fibers, or a combination of those, or even not reinforced at all, concrete is first of all a construction system, in which the material itself is intimately coupled to an implementation and a construction method.” [7]

If we consider a concrete building element as an assembly between the material and its associated construction process, then the environmental impact of that element can also be considered as an assembly of its material- and process-related impact.

Thus, after having reviewed in the previous section the environmental profile of concrete material, the present will review the environmental impact of concrete construction processes.

1.4.1. Conventional Construction Processes

At the scale of the building element, the EPD files from Inies Database provide precise data for the processing and installation of the concrete elements: 0,0216 kWh of french electricity for the installation of one square meter of concrete wall containing 255 kg of concrete and 6,84 kg of steel rebars [58]; 0,065 L of diesel for pumping of 225 kg of concrete [59]; 10,6 Wh of french electricity for mixing and 32,6 Wh of french electricity for lifting and installation of the concrete facade element of 394,5 kg [60].

Based on these data, it is possible to deduce the energy quantity needed to process one cubic meter of concrete. Concretely, knowing that the average volumetric mass density of concrete material is around 2300 kg/m³, the values declared by the EPD files can be scaled for one cubic meter, see table below.

Table 1.4. Energy consumption for processing and installation of 1m³ of concrete

Process	Energy / 1m ³ of concrete	Reference
Installation	0,22 kWh	[58] and [60]
Pumping	0,663 L	[59]
Mixing	0,06 kWh	[60]

Those values are however lower than those coming from the french National R&D project RECYBETON ([61], [62]), where only the mixing energy for one cubic meter of concrete was estimated to represent 14,4 MJ (or 4 kWh). Additionally, the Betie software precise transport distances estimated for the french industrial context, see Table1.5. Figure 1.10 depicts the partitioning of the Climate Change impact between the components and processes, including the transport-related data (cf. Table1.5.) as well as the mixing energy (4kWh, cf. RECYBETON) for one cubic meter of concrete for the french industrial scenario. Again, 93% of the Climate Change impact pertains to cement.

Table 1.5. Average transport distances for the concrete components
 Source: Betie²⁰

Component	Transport type	Distance
Aggregates	Road	22 km
	Waterway	22,25 km
Cement	Road	123,8 km
	Waterway	26 km
	Rail	18,2 km

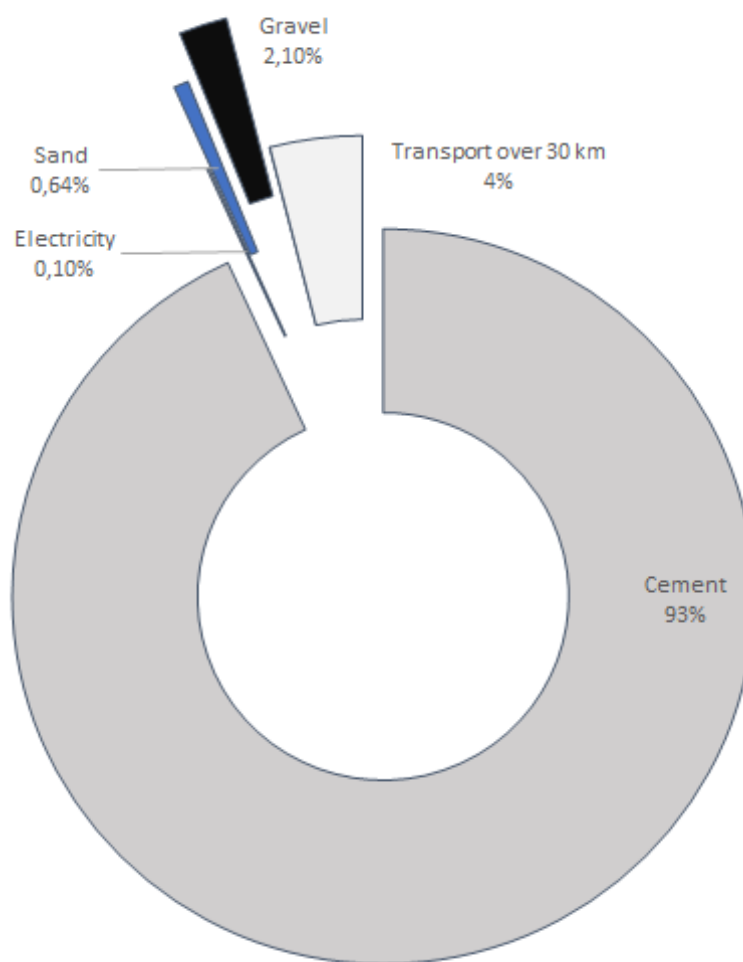


Figure 1.10. Climate Change impact partitioning between the components of 1m³ of concrete

²⁰ https://www.snbpe.org/developpement_durable/calcullette.

At the scale of the whole building, the on-site construction processes are usually reduced to the energy consumption on the construction site within the LCA studies. Thus, the study of Hong et al. [63] estimating the greenhouse gas emissions during the construction phase of buildings based on reinforced concrete shows that the construction processes represent 2,42% of the overall Climate Change impact.

The study of Li et al. [64], assessing the life-cycle CO₂ emissions of reinforced concrete structures on four case-studies from China, have demonstrated that the construction processes of reinforced concrete structures represent less than 1% of the Climate Change impact for school, hospital, commercial and residential buildings.

Within the pre-fabrication context, the processing of concrete and construction processes for concrete elements are not considered when assessing the building elements produced off-site, focusing on the impact coming from material production ([65], [66]).

The EPD files for the concrete building products declare to take into account “*Energy for concrete preparation and steelworking / Self-baking and demoulding / On-site Storage*”²¹ ([58], [59], [60]), the details of which do not appear in the reports. Furthermore, their impact does not appear either in the final results, dominated by the impact coming from material production (cement in particular as it was demonstrated on Figure 1.10).

Finally, a series of academic works assess and compare the environmental impact of structural systems including the concrete ones, without taking into account any of their associated construction processes, considering them as insignificant, see Figure 1.11 and Figure 1.12. Here again, the analysis considers only the impact coming from construction materials ([67], [37], [29]), even when comparing the construction elements issued from very different construction techniques.

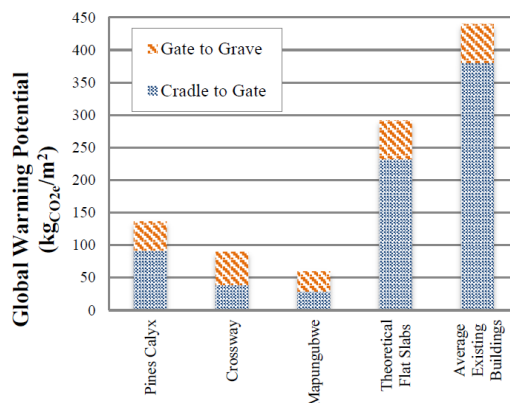


Figure 1.11. GWP of the case studies, compared to theoretical concrete slabs and existing building structures.

Reproduced from [67];

Where *Pines Calyx* is a vaulted tiled-stone building; *Crossway* is a brick masonry house, *Mapungubwe* is an earth brick masonry shell built with guastavino tiling; *Theoretical Flat Slabs* stand for multistorey reinforced concrete building slabs.

²¹ Translated from french by the author “*Énergie pour préparation du béton et façonnage des aciers / Auto-étuvage et démoulage / Stockage sur parc*” [58], [59], [60].

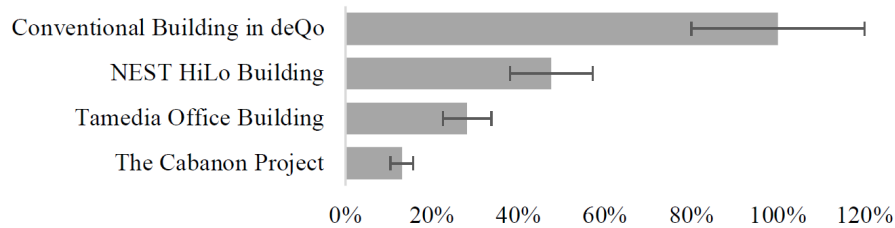


Figure 1.12. GWP of Swiss case studies relative to conventional buildings in deQo, including uncertainty
Reproduced from [29];

Where *NEST HiLo Building* is an experimental for research and demonstration of innovative building technologies developed at ETH Zurich, including 3D Printed slabs and digitally fabricated concrete walls; *Tamedia Office Building* is a seven-story high building in spruce wood; *The Cabanon Project* an art pavilion made of reused structural elements from the dismantling of the International Olympic Committee (IOC) headquarters.

1.4.2. Automated Construction Processes

Few academic studies have been previously conducted in the field of environmental performance of construction automation. Agusti-Huan et al. have performed a seminal work in the field, comparing digitally fabricated elements with the conventional ones [54], pointing out a strong potential of the first in terms of material reduction. The study has additionally provided a detailed life-cycle inventory for the robotic construction process. This latter will be analyzed in detail in Part 2. A specific study has been carried out by the same researchers for the Mesh Mould wall system [68], a digitally fabricated concrete wall, similarly interrogating its environmental viability over a conventionally fabricated concrete wall [50]. The results have demonstrated a fair environmental advantage of digital fabrication processes when complex, in particular curvilinear geometries are concerned. However, the mobile robotic technology ([69], [70]) assessed in the studies remains experimental equipment which hardly represents today's industrial set-ups for robotic printing cells. In addition, the mesh-mould wall system as such does not embody any material saving approach and utilizes even more metal armature than any traditional reinforced concrete wall.

Some environmental studies have been performed in the field of additive manufacturing on particle-bed fusion technology, outlining the importance of the process-related impact due to its energy consumption ([71], [72], [73]). Thus, based on the experimental measurements of the power consumption of the fabrication process, strategies were formulated in order to control and to decrease the process-related impact.

A study by Yao et al. [74] has performed a life-cycle assessment of the building elements produced with 3D Printing with geo-polymer concrete. The results similarly show the importance of the impact coming from the energy-consumption of the printing process. The author declares to operate with the “manufacturer's data”, without providing detail. Again, the analysis is focused on the material-related impact of geopolymers.

Comparative LCA studies between conventional construction elements and the one produced with large-scale additive manufacturing and 3D Printing were accomplished by Alhumayani et al. [55] and Mohammad et al. [75]. Both studies outline a potential for reduction of

environmental impact of concrete structure due to the material savings enabled by additive manufacturing.

However, both analyses have only considered the operational impact of the printing process, without considering its embodied impact.

Furthermore, Alhumayani et al. use a theoretical power consumption value of 8 kW for the robot's motor, that is then divided by two for the calculation. A total power consumption of 10.78 kW has been used by Mohammad et al. that includes the robot (3.4 kW) and the concrete mixer (7.38 kW), both based on theoretical values taken from equipment datasheets.

The operational power consumption of the robotic printing process will be discussed in detail in the next part.

A review of the latest development of the 3D Printing in construction sector analyzing its potential to reduce the carbon footprint of buildings points out a *“wide range of benefits of 3D Printing in construction to reduce material use, time and cost as well as to maximize quality, design performance, efficiency and productivity”* [27]. In the end, stating the lack of environmental studies and as a consequence a lack of knowledge in the field of the environmental performance of 3D Printing and additive manufacturing in construction sector, the author outlines that *“so far, most efforts are grappling with material design, printing hardware and software issues, and are not informed by scientific data generated using LCA”* [27].

Regarding the other industries, the study of Saade et al. [76] provides an extensive review on how the LCA has been applied to the 3D Printing technology within all industries combined. The paper outlines a general shift between material- and process-related impacts in the Climate Change category, that in some industries can go up to 80%. Figure 1.13 regroups the results of the comparative environmental studies between additive and conventional manufacturing within all industries combined, depicting the advantages of additive manufacturing over conventional manufacturing (and vice-versa) in Climate Change category.

Regarding the methodology of taking into account the additive manufacturing processes in other industries, in most of LCA studies it is resumed to an amount of the operational energy used for the production (as in the case of on-site construction processes and of some previous studies on 3D Concrete Printing in construction). Considering the substantial technological differences, no data from environmental studies accomplished in other industries can be reused in the present research addressing the additive manufacturing with concrete.

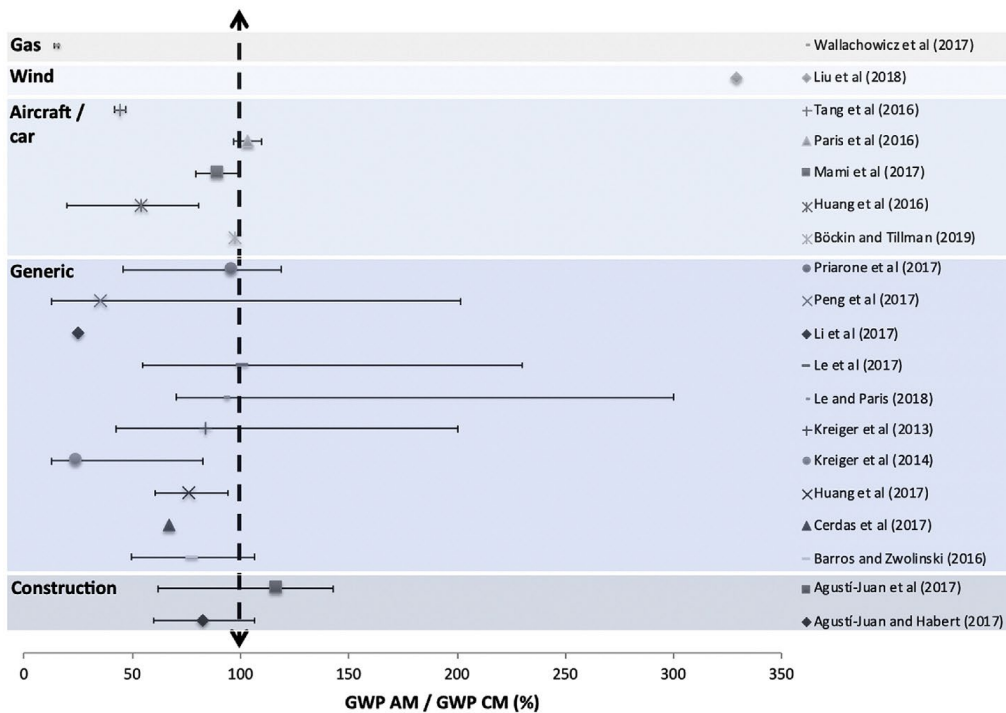


Figure 1.13.

Additive manufacturing GWP (Global Warming Potential²²) loads in relation to Conventional Manufacturing GWP loads. Geometric shapes represent the medians of values published in each paper, while horizontal error bars represent the total value range published.

The black dashed line refers to 100%, i.e. where AM's GWP (Additive Manufacturing Global Warming Potential) is equal to CM's GWP (Conventional Manufacturing Global Warming Potential).

Therefore, values to the left of that line represent those in which AM is more attractive than CM.

Reproduced from [76]

²² It is very common to see in publications the term GWP (Global Warming Potential) meaning the Climate Change category of environmental impact, see Figure 1.11, Figure 1.12 and Figure 1.13.

In fact, the Climate Change category measures the environmental impact of GHG (greenhouse gas) with the unit of CO₂-Eq. In order to obtain the CO₂-Eq of a given GHG emission, the characterization factor called Global Warming Potential is applied. Therefore, the GWP is a characterization factor of the Climate Change impact and not the impact itself.

For example, the GWP of carbon dioxide is 1 and thus 1 kg of CO₂ = 1 kg CO₂ Eq.

The GWP of methane is 26 and thus 1 kg of CH₄ = 26 kg CO₂ Eq.

For more details, see Jolliet et al. [44]

Flow	Category	Unit	Amount
Steel, low-alloyed, at plant	Material	kg	570.6
Steel, electric, un- and low-alloyed, at plant	Material	kg	120.6
Cast iron, at plant	Material	kg	119.5
Copper, primary, at refinery	Material	kg	35.55
Aluminium, production mix, at plant	Material	kg	37.70
Alkyd paint, white, 60% in H ₂ O, at plant	Material	kg	1.65
Epoxy resin, liquid, at plant	Material	kg	4.35
Polyvinylchloride, suspension polymerized, at plant	Material	kg	16.41
Polyurethane, flexible foam, at plant	Material	kg	0.31
Tin, at regional storage	Material	kg	0.14
Lead, primary, at plant	Material	kg	0.08
Nickel, 99.5%, at plant	Material	kg	0.05
Silver, at regional storage	Material	kg	0.004
Gold, primary, at refinery	Material	kg	0.001
Synthetic rubber, at plant	Material	kg	40.0
Lubricating oil	Material	kg	40.0
Battery, Lito, rechargeable, prismatic, at plant	Material	kg	50.0

Figure 1.14. Material composition and corresponding Ecoinvent processes used for the construction robot (kg/unit);
Reproduced from [54]

Thus, focusing on this last and on the construction sector in general, the environmental impact of elements fabricated with additive manufacturing still seems to be dominated by the burden coming from construction materials. This latter conclusion, as well as those of two previously cited reviews, are drawn upon the work of Agusti-Huan and Habert, cited in the beginning of this section, which currently remains the principal reference in the field.

Additionally, it is the only work providing the information on the life-cycle inventory used in the environmental study as considers both the operational and embodied impacts of robotic construction processes. This latter is modeled upon the in-situ fabricator - a mobile robotic construction technology developed in ETH Zurich, mainly for the purposes of concrete projection and on-site welding [70]; its life-cycle inventory is depicted on Figure 1.14.

The modeling strategy adopted for the inventory formalization consists of the decomposition of all components till the primal materials, available in the database. Hence, the proposed inventory set-up does not depict any specific part of robotic hardware, e.g. servo-motor or controller, which can be perceived as a limit of the developed approach, as disables the possible reconfigurations or scaling of the life-cycle model. Typically, with the given inventory one cannot model or configure his/her robotic platform, i.e. set multiple robots, add/remove a controller or change the size of the robot or any other element.

The modeling strategy of the life-cycle inventory developed in the present work will be discussed in detail in the next part.

1.5. Problem Statement

Summing up the previous developments, the environmental profile of concrete material is mainly defined by the cement quota in the material mix. Furthermore, conventional concrete construction techniques seem to have almost negligible Climate change contribution, i.e. less than 1-2 %, which means that the Climate Change impact of a building element is also defined by the amount of cement.

Past studies on the environmental assessment of the automated concrete construction processes do not share enough information and operate with theoretical values that lack consistency. The

sole model of embodied impact of the robotic construction process existing in the field is too generic and does not allow any generalization/reconfiguration in function of the specific composition of the robotic printing cell. Furthermore, no measured value of the operational power consumption for the printing process currently exists. Thus, the environmental characterization of concrete automated construction processes remains an open research question.

As follows, if the ongoing development of construction automation gets more and more associated with the sustainable vision it has acquired by enabling the fabrication of more optimal and lightweight structures, then from the life-cycle perspective, this technological change may inevitably bring a certain performance trade to the global balance. In other words, it is doubtful that by addressing the material reduction of a building element using an automated construction process, no impact transfer and/or pollution shift will occur.

Therefore, when the concrete is deposited by robotic printing, i.e. by the means of 6-axis robotic arm, along with the continuous mixing, pumping and admixturing, will this fabrication process remain insignificant within the environmental profile of concrete element from the Climate Change perspective (impact transfer) ?

Furthermore, will it bring some new pollutants into the system not previously existing (pollution shift) ?

To address those questions, the present work performs an environmental Life-Cycle Assessment of the 3D Concrete Printing technology and proposes a model of its environmental impact of the process-related impact. The model is then applied to two case-studies on the scale of the material and building system. Then, a comparison of environmental performances between 3D Concrete Printed building system and their conventional analogues is carried out in order to evaluate the eventual impact transfers and pollution shifts. Furthermore, the results of this comparison will give insights into potential environmental improvements of the building elements designed for and produced with 3D Concrete Printing technology. In closing, a general discussion on the sustainable development of the practice is carried out, concluding on the contribution of this work to the field and drawing the research perspectives.

Bibliography of Part I

- [1] United Nations, « World Urbanization Prospects : The 2018 Revision », Key Facts. Consulté le: oct. 17, 2018. [En ligne]. Disponible sur: <https://population.un.org/wup/Publications/Files/WUP2018-KeyFacts.pdf>
- [2] World Economic Forum et BCG, « The critical challenge for engineering, construction, and infrastructure companies is to increase productivity. » Consulté le: déc. 13, 2018. [En ligne]. Disponible sur: <https://www.bcg.com/industries/engineered-products-infrastructure/engineering-construction-infrastructure.aspx>
- [3] McKinsey & Company, « Reinventing Construction: A Route To Higher Productivity », McKinsey Global Institute, Executive Summary, févr. 2017.
- [4] « 2019 Global Status Report for Buildings and Construction Sector | UNEP - UN Environment Programme ». <https://www.unep.org/resources/publication/2019-global-status-report-buildings-and-construction-sector> (consulté le juin 02, 2021).
- [5] N. Kotelnikova-Weiler, « Optimisation mécanique et énergétique d’enveloppes en matériaux composites pour les bâtiments », These de doctorat, Paris Est, 2012. Consulté le: juin 02, 2021. [En ligne]. Disponible sur: <https://www.theses.fr/2012PEST1141>
- [6] R. J. Flatt, N. Roussel, et C. R. Cheeseman, « Concrete: An eco material that needs to be improved », *Journal of the European Ceramic Society*, vol. 32, n° 11, p. 2787-2798, août 2012, doi: 10.1016/j.jeurceramsoc.2011.11.012.
- [7] H. Van Damme, « Concrete material science: Past, present, and future innovations », *Cement and Concrete Research*, vol. 112, p. 5-24, oct. 2018, doi: 10.1016/j.cemconres.2018.05.002.
- [8] T. Wangler, N. Roussel, F. P. Bos, T. A. M. Salet, et R. J. Flatt, « Digital Concrete: A Review », *Cement and Concrete Research*, vol. 123, p. 105780, sept. 2019, doi: 10.1016/j.cemconres.2019.105780.
- [9] K. L. Scrivener, V. M. John, et E. M. Gartner, « Eco-efficient cements: Potential economically viable solutions for a low-CO2 cement-based materials industry », *Cement and Concrete Research*, vol. 114, p. 2-26, déc. 2018, doi: 10.1016/j.cemconres.2018.03.015.
- [10] R. Duballet, O. Baverel, et J. Dirrenberger, « Space Truss Masonry Walls With Robotic Mortar Extrusion », *Structures*, vol. 18, p. 41-47, avr. 2019, doi: 10.1016/j.istruc.2018.11.003.
- [11] E. Gartner, « Industrially interesting approaches to “low-CO2” cements », *Cement and Concrete Research*, vol. 34, n° 9, p. 1489-1498, sept. 2004, doi: 10.1016/j.cemconres.2004.01.021.
- [12] Union Nationale des Producteurs de Granulats, « Module d’information environnementale de la production de granulats à partir de roches meubles », Conforme aux normes NF EN 15804+A1 et NF EN 15804/CN, sept. 2017.
- [13] J. B. Guinée *et al.*, « Life cycle assessment and operational guide to the ISO standard — final report may 2001 ». Centre of Environmental Science - Leiden University (CML). Consulté le: juin 07, 2021. [En ligne]. Disponible sur: https://www.universitleiden.nl/binaries/content/assets/science/cml/publicaties_pdf/new-dutch-lea-guide/part1.pdf
- [14] UNEP Global Environmental Alert Service (GEAS), « Sand, rarer than one thinks ». mars 2014.
- [15] USGS, « Cement, statistics and information ». U.S. Geological Survey, Reston., 2013.
- [16] USGS, « Sand and gravel (construction) statistics, in: Kelly, T.D., Matos, G.R., (Eds.), Historical statistics for mineral and material commodities in the United States. » U.S. Geological Survey Data Series 140, Reston., 2013.
- [17] A. Feraille, « Du matériau à l’ouvrage : quelques apports méthodologiques relatifs à l’Analyse de Cycle de Vie », Laboratoire Navier, Ecole des Pont ParisTech, août 03, 2016.

- [18] R. Duballet, O. Baverel, et J. Dirrenberger, « Classification of building systems for concrete 3D printing », *Automation in Construction*, vol. 83, p. 247-258, nov. 2017, doi: 10.1016/j.autcon.2017.08.018.
- [19] T. Wangler *et al.*, « Digital Concrete: Opportunities and Challenges », *RILEM Tech Lett*, vol. 1, p. 67, oct. 2016, doi: 10.21809/rilemtechlett.2016.16.
- [20] R. A. Buswell, W. R. Leal de Silva, S. Z. Jones, et J. Dirrenberger, « 3D printing using concrete extrusion: A roadmap for research », *Cement and Concrete Research*, vol. 112, p. 37-49, oct. 2018, doi: 10.1016/j.cemconres.2018.05.006.
- [21] C. Gosselin, R. Duballet, Ph. Roux, N. Gaudillière, J. Dirrenberger, et Ph. Morel, « Large-scale 3D printing of ultra-high performance concrete – a new processing route for architects and builders », *Materials & Design*, vol. 100, p. 102-109, juin 2016, doi: 10.1016/j.matdes.2016.03.097.
- [22] J. Pegna, « Exploratory investigation of solid freeform construction », *Automation in Construction*, vol. 5, n° 5, p. 427-437, févr. 1997, doi: 10.1016/S0926-5805(96)00166-5.
- [23] B. Khoshnevis, « Automated construction by contour crafting—related robotics and information technologies », *Automation in Construction*, vol. 13, n° 1, p. 5-19, janv. 2004, doi: 10.1016/j.autcon.2003.08.012.
- [24] S. Lim, R. A. Buswell, T. T. Le, S. A. Austin, A. G. F. Gibb, et T. Thorpe, « Developments in construction-scale additive manufacturing processes », *Automation in Construction*, vol. 21, p. 262-268, janv. 2012, doi: 10.1016/j.autcon.2011.06.010.
- [25] G. Cesaretti, E. Dini, X. De Kestelier, V. Colla, et L. Pambaguian, « Building components for an outpost on the Lunar soil by means of a novel 3D printing technology », *Acta Astronautica*, vol. 93, p. 430-450, janv. 2014, doi: 10.1016/j.actaastro.2013.07.034.
- [26] R. A. Buswell *et al.*, « A process classification framework for defining and describing Digital Fabrication with Concrete », *Cement and Concrete Research*, vol. 134, p. 106068, août 2020, doi: 10.1016/j.cemconres.2020.106068.
- [27] M. Dixit, « 3-D Printing in Building Construction: A Literature Review of Opportunities and Challenges of Reducing Life Cycle Energy and Carbon of Buildings », *IOP Conference Series: Earth and Environmental Science*, vol. 290, p. 012012, juin 2019, doi: 10.1088/1755-1315/290/1/012012.
- [28] G. De Schutter, K. Lesage, V. Mechtcherine, V. N. Nerella, G. Habert, et I. Agusti-Juan, « Vision of 3D printing with concrete — Technical, economic and environmental potentials », *Cement and Concrete Research*, vol. 112, p. 25-36, oct. 2018, doi: 10.1016/j.cemconres.2018.06.001.
- [29] C. D. Wolf, « Low Carbon Pathways for Structural Design », présenté à IASS Symposium 2018, MIT, Boston, USA, 2018.
- [30] Centre Georges Pompidou, *Architectures non standard*. Paris, France: Centre Georges Pompidou Service Commercial, 2003.
- [31] G. Deleuze, *Le pli: Leibniz et le Baroque*, Critique edition. Paris: Editions de Minuit, 1988.
- [32] G. Lynn, « Folding in Architecture (1993) », in *The Digital Turn in Architecture 1992–2012*, Wiley-Blackwell, 2015, p. 28-47. doi: 10.1002/9781118795811.ch2.
- [33] G. Retsin, « Discrete Architecture in the Age of Automation », *Architectural Design*, vol. 89, n° 2, p. 6-13, 2019, doi: 10.1002/ad.2406.
- [34] P. Schumacher, « Parametricism: A New Global Style for Architecture and Urban Design », *Architectural Design*, vol. 79, n° 4, p. 14-23, 2009, doi: 10.1002/ad.912.
- [35] P. Schumacher, « Parametricism 2.0: Gearing Up to Impact the Global Built Environment », *Architectural Design*, vol. 86, n° 2, p. 8-17, 2016, doi: 10.1002/ad.2018.
- [36] M. Carpo, *The Second Digital Turn: Design Beyond Intelligence*, 1 edition. Cambridge, Massachusetts: The

MIT Press, 2017.

- [37] C. De Wolf, « Low Carbon Pathways for Structural Design: Embodied Life Cycle Impacts of Building Structures », MIT, Cambridge, USA, 2017.
- [38] T. A. M. Salet, Z. Y. Ahmed, F. P. Bos, et H. L. M. Laagland, « Design of a 3D printed concrete bridge by testing », *Virtual and Physical Prototyping*, vol. 13, n° 3, p. 222-236, juill. 2018, doi: 10.1080/17452759.2018.1476064.
- [39] M. Rippmann, A. Liew, T. Van Mele, et P. Block, « Design, fabrication and testing of discrete 3D sand-printed floor prototypes », *Materials Today Communications*, vol. 15, p. 254-259, juin 2018, doi: 10.1016/j.mtcomm.2018.03.005.
- [40] N. Gaudillière *et al.*, « Large-Scale Additive Manufacturing of Ultra-High-Performance Concrete of Integrated Formwork for Truss-Shaped Pillars », in *Robotic Fabrication in Architecture. Art and Design 2018*, 2019, p. 459-472. doi: 10.1007/978-3-319-92294-2_35.
- [41] International Organization for Standardization, *ISO 14040 : 2006 « Environmental management -- Life cycle assessment -- Principles and framework »*. Consulté le: févr. 28, 2019. [En ligne]. Disponible sur: <http://www.iso.org/cms/render/live/en/sites/isoorg/contents/data/standard/03/74/37456.html>
- [42] International Organization for Standardization, *ISO 14044 : 2006 « Environmental management -- Life cycle assessment -- Requirements and guidelines »*. [En ligne]. Disponible sur: <http://www.iso.org/cms/render/live/en/sites/isoorg/contents/data/standard/03/84/38498.html>
- [43] « EN 15804:2012 Sustainability of construction works - Environmental product declarations - Core rules for the product category of construction products ».
- [44] O. Jolliet, M. Saadé-Sbeih, S. Shaked, A. Jolliet, et P. Crettaz, *Environmental Life Cycle Assessment*, 1st Edition. CRC Press, 2016.
- [45] K. Simonen, *Life Cycle Assessment*, 1 edition. London ; New York: Routledge, 2014.
- [46] B. Peuportier (coordination), *Eco-conception des ensembles bâtis et des infrastructures*. Presses des Mines.
- [47] K. Kuzmenko, C. Roux, A. Feraille, et O. Baverel, « Assessing environmental impact of digital fabrication and reuse of constructive systems », *Structures*, juin 2020, doi: 10.1016/j.istruc.2020.05.035.
- [48] M. Rivallain, « Étude de l'aide à la décision par optimisation multicritère des programmes de réhabilitation énergétique séquentielle des bâtiments existants », Paris-Est, Paris, France, 2013.
- [49] S. Copiello, « Building energy efficiency: A research branch made of paradoxes », *Renewable and Sustainable Energy Reviews*, vol. 69, p. 1064-1076, mars 2017, doi: 10.1016/j.rser.2016.09.094.
- [50] I. Agustí-Juan, F. Müller, N. Hack, T. Wangler, et G. Habert, « Potential benefits of digital fabrication for complex structures: Environmental assessment of a robotically fabricated concrete wall », *Journal of Cleaner Production*, vol. 154, p. 330-340, juin 2017, doi: 10.1016/j.jclepro.2017.04.002.
- [51] « ecoinvent ». <https://www.ecoinvent.org/> (consulté le oct. 19, 2020).
- [52] M. Goedkoop, R. Heijungs, M. Huijbregts, A. Schryver, J. Struijs, et R. Zelm, « Recipe 2008 », *A life*, janv. 2009.
- [53] M. A. J. Huijbregts *et al.*, « ReCiPe2016: a harmonised life cycle impact assessment method at midpoint and endpoint level », *Int J Life Cycle Assess*, vol. 22, n° 2, p. 138-147, févr. 2017, doi: 10.1007/s11367-016-1246-y.
- [54] I. Agustí-Juan et G. Habert, « Environmental design guidelines for digital fabrication », *Journal of Cleaner Production*, vol. 142, p. 2780-2791, janv. 2017, doi: 10.1016/j.jclepro.2016.10.190.
- [55] H. Alhumayani, M. Gomaa, V. Soebarto, et W. Jabi, « Environmental assessment of large-scale 3D printing in construction: A comparative study between cob and concrete », *Journal of Cleaner Production*, vol. 270, p.

122463, oct. 2020, doi: 10.1016/j.jclepro.2020.122463.

- [56] European Commission, Joint Research Centre, et Institute for Environment and Sustainability, *International reference life cycle data system (ILCD) handbook general guide for life cycle assessment: provisions and action steps*. Luxembourg: Publications Office, 2011.
- [57] « Construction products (FDES) – INIES ». <https://www.inies.fr/construction-products/> (consulté le avr. 20, 2020).
- [58] CERIB, « FDES _ Mur à coffrage intégré (sans béton de remplissage) ». [En ligne]. Disponible sur: N°7-412:2019
- [59] CERIB, « FDES_Mur a coffrage et isolation intègres (avec béton de remplissage, CEM III/A et isolant PSE) ». nov. 2020. [En ligne]. Disponible sur: N°7-413:2019
- [60] CERIB, « FDES_Panneau architectural plein en béton ». mars 2020. [En ligne]. Disponible sur: N°1-70:2020
- [61] « National Project RECYBETON », *RECYBETON*. <https://www.pnrecybeton.fr/en/> (consulté le juin 02, 2021).
- [62] S. Braymand, A. Feraille, et N. Serres, « RECYBETON. Thème 3: Évaluation environnementale du béton de granulats recyclés – 2ème étape », Projet National de recherche et développement, févr. 2017. [En ligne]. Disponible sur: www.pnrecybeton.fr
- [63] J. Hong, G. Q. Shen, Y. Feng, W. S. Lau, et C. Mao, « Greenhouse gas emissions during the construction phase of a building: a case study in China », *Journal of Cleaner Production*, vol. 103, p. 249-259, sept. 2015, doi: 10.1016/j.jclepro.2014.11.023.
- [64] H. Li, Q. Deng, J. Zhang, B. Xia, et M. Skitmore, « Assessing the life cycle CO2 emissions of reinforced concrete structures: Four cases from China », *Journal of Cleaner Production*, vol. 210, p. 1496-1506, févr. 2019, doi: 10.1016/j.jclepro.2018.11.102.
- [65] P. Ryklová, Š. Mančík, et A. Lupíšek, « Environmental Benefits of Timber-Concrete Prefabricated Construction System for Apartment Buildings – a Simplified Comparative LCA Study », *IOP Conf. Ser.: Earth Environ. Sci.*, vol. 290, p. 012083, juin 2019, doi: 10.1088/1755-1315/290/1/012083.
- [66] G. Boscato, T. D. Mora, F. Peron, S. Russo, et P. Romagnoni, « A new concrete-glulam prefabricated composite wall system: Thermal behavior, life cycle assessment and structural response », *Journal of Building Engineering*, vol. 19, p. 384-401, sept. 2018, doi: 10.1016/j.jobbe.2018.05.027.
- [67] C. De Wolf, M. Ramage, et J. Ochsendorf, « Low Carbon Vaulted Masonry Structures », *Journal of the International Association for Shell and Spatial Structures*, vol. 57, n° 4, p. 275-284, déc. 2016, doi: 10.20898/j.iass.2016.190.854.
- [68] N. Hack et W. V. Lauer, « Mesh-Mould: Robotically Fabricated Spatial Meshes as Reinforced Concrete Formwork », *Architectural Design*, vol. 84, n° 3, p. 44-53, 2014, doi: 10.1002/ad.1753.
- [69] M. Gifthaler *et al.*, « Mobile robotic fabrication at 1:1 scale: the In situ Fabricator », *Constr Robot*, vol. 1, n° 1, p. 3-14, déc. 2017, doi: 10.1007/s41693-017-0003-5.
- [70] « Mesh Mould and In situ Fabricator », *Gramazio Kohler Research*, 2017 2017. <https://gramaziokohler.arch.ethz.ch/web/e/forschung/324.html> (consulté le avr. 27, 2020).
- [71] F. L. Bourhis, O. Kerbrat, J.-Y. Hascoët, et P. Mognol, « Sustainable manufacturing: evaluation and modeling of environmental impacts in additive manufacturing », *Int J Adv Manuf Technol*, vol. 69, n° 9, p. 1927-1939, déc. 2013, doi: 10.1007/s00170-013-5151-2.
- [72] O. Kerbrat, F. Le Bourhis, P. Mognol, et J.-Y. Hascoët, « Environmental Impact Assessment Studies in Additive Manufacturing », in *Handbook of Sustainability in Additive Manufacturing*, vol. 2, 2016, p. 31-63. doi: 10.1007/978-981-10-0606-7_2.
- [73] M. Yosofi, O. Kerbrat, et P. Mognol, « Additive manufacturing processes from an environmental point of view:

a new methodology for combining technical, economic, and environmental predictive models », *Int J Adv Manuf Technol*, vol. 102, n° 9, p. 4073-4085, juin 2019, doi: 10.1007/s00170-019-03446-2.

- [74] Y. Yao, M. Hu, F. Di Maio, et S. Cucurachi, « Life cycle assessment of 3D printing geo-polymer concrete: An ex-ante study », *Journal of Industrial Ecology*, p. jiec.12930, août 2019, doi: 10.1111/jiec.12930.
- [75] M. Mohammad, E. Masad, et S. G. Al-Ghamdi, « 3D Concrete Printing Sustainability: A Comparative Life Cycle Assessment of Four Construction Method Scenarios », *Buildings*, vol. 10, déc. 2020, doi: 10.3390/buildings10120245.
- [76] M. R. M. Saade, A. Yahia, et B. Amor, « How has LCA been applied to 3D printing? A systematic literature review and recommendations for future studies », *Journal of Cleaner Production*, vol. 244, p. 118803, janv. 2020, doi: 10.1016/j.jclepro.2019.118803.

Part II
Modeling & Characterization
of Environmental Impact of 3D Concrete
Printing Technology

In the present part, the environmental Life-Cycle Assessment study is performed on the 3D Concrete Printing technology and focuses on the impact coming from the robotic printing process, furtherly referred to as process-related impact. The impact coming from material production, furtherly referred to as material-related impact, is not a principal focus of the present study, however its approximate impact is necessary to estimate the relative impact of the robotic printing process. Thus, the material-related impact will be discussed in the beginning of this part.

The part is organized as follows. In the first place, the case-studied technology of 3D Concrete Printing is described, presenting the modelling approach of the study. Then, the model of environmental impact of 3D Concrete Printing is defined and the material- and process-related impacts are characterized.

2.1. Case-study of 3D Concrete Printing Technology for Environmental Analysis

As it was discussed in Section 1.1.2, currently there exist a multitude of additive manufacturing techniques, differentiated by the type of printing device, material formulation, fabrication environment and as a consequence by the size and type of an object they can produce. The present work is focused on the extrusion-based additive manufacturing with cement-based materials, referred to as 3D Concrete Printing, initially developed and described by Gosselin et al. [1] and is currently under industrialization by the french company XtreeE [2]. The technology is also used by Build'In Lab at Ecole des Ponts ParisTech, Loughborough University, Technical University of Denmark DTU, ETH Zurich, Sika Group etc.

Figure 2.1 depicts the layout of the studied robotic printing cell. In a large outline, the cell is built upon the 6-axis robotic arm (3) carrying the printing head (4), supplied from the concrete preparation unit (2); a command station (1) commands the system. Being based on the robotic arm with 6-axis degrees of freedom, the specificity of this printing technology is that it allows to go beyond the 2,5 axis vertical extrusion, providing in that way, more complex toolpaths feasibility, that can be used for more methodical material placement [3]. The high printing resolution of the set-up allows an elaborate detailing and formal control, which combined together with toolpath intricacy and the limited working area of the robot (about 25m² for ABB IRB 8700 and 9m² for ABB IRB 6620), naturally encircle the industrial applications of the technology to the prefabrication, e.g. modular and non-standard building elements and/or complex formworks.

Despite a singular case-study of the present work displaying the conduct of one particular printing technology, the environmental impact model is formulated within the universal approach to the printing process as a generalization of the following processes: concrete preparation (the primal mixing), concrete mixing & pumping during the printing process and the conduct the printing device itself (robotic arm in our case), to ease the future generalization of the model.

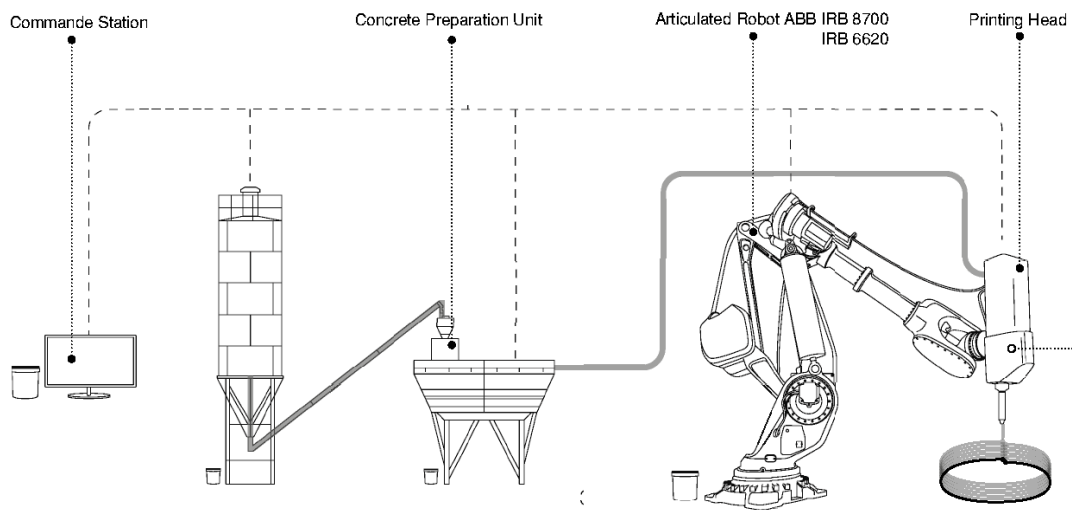


Figure 2.1. 3D Concrete Printing Cell based on 6-axis robotic arm
Image: Courtesy of XtreeE

In other terms, any extrusion-based 3D Concrete Printing cell is composed of a concrete preparation unit with a certain mixing & pumping capacity, a printing device with a certain weight and a printing head with a certain technicity.

Therefore, any printing cell can be considered as a certain assembly of those components performing their corresponding processes. Thus, again, despite being case-studied with a unique set-up, the outcomes of this study can be extrapolated to any extrusion-based printing techniques. The following section presents the modeling approach.

2.2. Model of Environmental Impact

In a universal way, i.e. independently from the technological set-up of the printing cell, the environmental impact of a 3D Concrete Printed element on the construction phase will be composed of material- and process-related impact. This latter comes from the embodied and the operational footprint of the robotic printing cell.

The printing process stands for the process of reference according to which all the energy and the resources flows of the system are traced. Figure 2.2 depicts the flowchart of the life-cycle model for the 3D Concrete Printing process, graphically describing the interactions between different flows and processes.

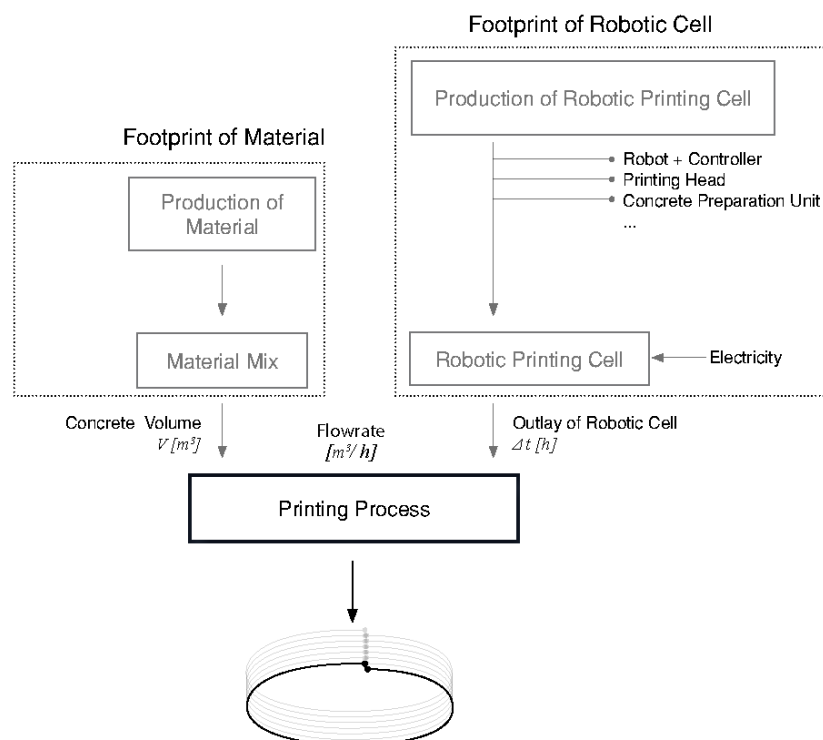


Figure 2.2. Flowchart of Life-Cycle Model Of 3D Concrete Printing

Concretely, two main flows enter the process of reference: the material quantity V and the printing time Δt . The printing time parameter defines the process-related impact and comprises the embodied and operational impacts of the robotic printing process, both described in Section 2.4. The parameter of the material volume V deposited during the printing time defines the material-related impact and will be described in Section 2.2.

Hence, the environmental impact of the 3D Concrete Printing I is the function of the material volume V and the printing time Δt and equals to the sum of their respective impacts, see formula below:

$$(1) \quad I = V M_{fp} + \Delta t (R_{fp} + O_{fp})$$

Where: V is the material volume; M_{fp} is the coefficient of material volumic footprint; Δt is the printing time; R_{fp} is the coefficient of hourly footprint of the embodied impact of the robotic printing process; O_{fp} is the coefficient of the operational footprint of the robotic printing process. The relation between the material volume V and of the printing time Δt would be defined by the *flowrate* of the printing procedure, precisely describing the volume of material processed by the system per the unit of time. Therefore, the flowrate of the printing procedure defines the relation between material and process-related footprints in the final result, which is one of the primal enquiries of the present study. It will be discussed in detail in Part III.

Figure 2.3 illustrates the model graph describing the relation between all the model's parameters and coefficients. The next section describes the characterization of the M_{fp} coefficient. Section 2.4 provides the characterizations of R_{fp} and O_{fp} coefficients.

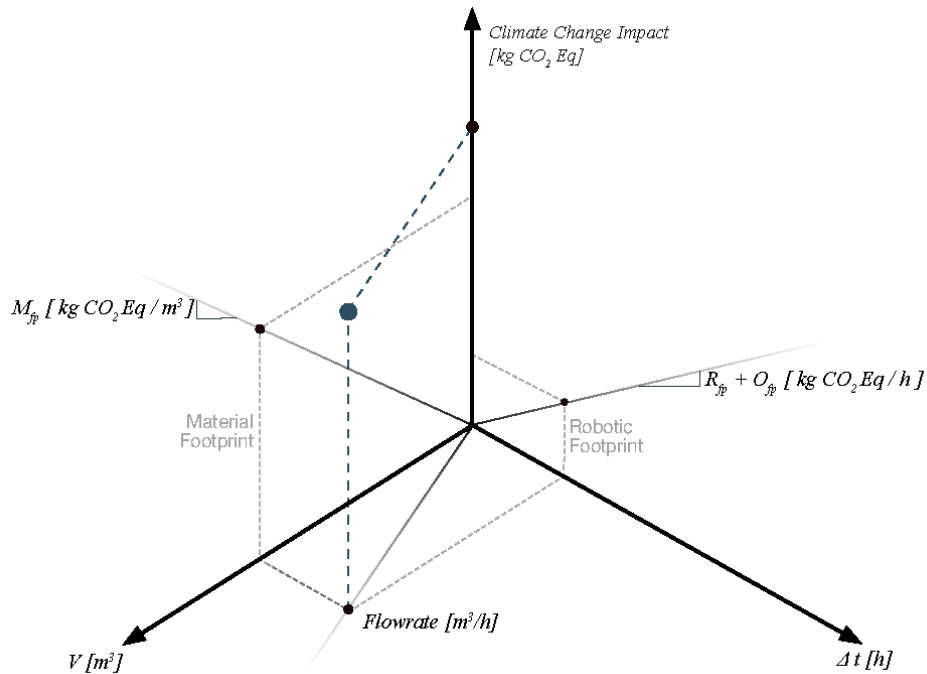


Figure 2.3. Model of Environmental Impact of 3D Concrete Printing Process

The setup of the Life-Cycle Assessment

The characterization of the environmental impact of 3D Concrete Printing technology is carried out using the Life-Cycle Assessment method. The impact characterization is split onto the material-related impact, characterized per cubic meter of material and on the process-related impact, characterized per one hour of printing. Therefore, the present part addresses the characterization of inventory for the environmental analysis rather than the environmental analysis itself. The environmental analysis will be carried out in Part III on material, structural and building scale.

The boundaries of the study are defined to be cradle-to-gate or A1-A3, A5 according to EN 15804 [4]. No end-of-life scenario is taken into account, as the problematic of the analysis addresses mainly the construction phase of the life-cycle.

For the robotic printing cell, no replacement or maintenance of equipment during the lifespan is considered in the present study. Being an under-development technology, the current industrial data of the replacement and general maintenance of equipment does not depict the industrially mature conditions. In general, the full-bodied mature industrial scenarios have been considered in the study, instead of the prototyping ones.

All the industrial hypotheses were developed with XtreeE [2].

The modeling and calculation are made within the OpenLCA software using EcoInvent 3.2. Cut-off database [5] for the inventory collection and analysis.

Recipe MidPoint (H) calculation method is used for the impact evaluation, cf. Section 1.2.3.

Table 2.1 sums up the settings for the Life-Cycle assessment study.

Table 2.1. Set-up of the Life-Cycle Assessment set-up

Functional Unit	1m ³ of Printable Concrete
	1 hour of printing for Robotic Printing Cell
Life-Cycle Boundaries	Cradle-to-Gate or A1-A3, A5
Calculation Method	Recipe MidPoint (H)
Inventory database	EcoInvent 3.2 Cut-off

2.3. Environmental Impact of Printable Concrete:

M_{fp} coefficient

The footprint of printable concretes is not the focus of the present study; however, its approximate impact is necessary in order to evaluate the relative contribution coming from the robotic construction process. Again, the majority of the environmental impact of concrete will mainly come from cement (cf. Section 1.3).

For reminder, focusing on Climate Change impact category, 1 kg of cement represents approximately 1 kg CO₂ Eq, which means that the volumic Climate Change impact of concrete material will mainly be conditioned by the cement quota in material mix (cf. Section 1.3).

Accordingly, as the material-mixes for the 3DCP do not usually contain any large aggregates nor reinforcement, their cement portion is usually much higher than the one of conventional C25/30 concrete. As follows, along with the higher cement concentration they also perform a much higher mechanical resistance. In a general way, the 3D Printing technology usually operated with high- and ultra-high-performance concretes [1], [6].

In practice, the printable concretes are not the sole to make use of an increased cement concentration in order to compensate the insufficient granulometry of the material-mix. Indeed, every time when the aggregates, both big and small, exhibit poor granularity, i.e. possess the jagged and sharp geometry the irregularity of which constrain the good structuration of the particles, the optimum of the global granular skeleton matrix is systematically back-upped by the supplementary cement addendum. In other terms, when instead of smoothly-round and fine-compacting river sand (which has recently become a broad subject to depletion [7]) one decides to use a rough and longish desert sand (so far considered as unlimited resource [8]), this last may necessitate the supplementary dose of cement in the material mix formulation, increasing in that way the volumic impact of concrete.

The phenomenon also occurs in the case of formulations utilizing recycled / second-handed aggregates, where again, the rough and irregular granulometry of aggregate coming from recycling is systematically counterbalanced by the supplementary cement addendum [9]. Thus, the environmental impact of the concrete produced with recycled aggregates is usually higher than the one with freshly extracted [9], [10].

To sum up, the practitioners are generally lucid about the impacting character of printable mixes of concrete materials, and the alternative more sustainable formulations are constantly under development ([11], [12] and [13]). The relevance of alternative printable materials, like clay or earth, will be discussed in Part III.

For the present study, a generic high-performance printable material-mix was formulated in Navier Laboratory, based on the high-class cement CEM I 52,5.

The formulation is depicted in Table 2.2. with the LC inventory reference. Table 2.3 depicts the impact of one cubic meter of high-performance printable concrete. As expected, the volumic Climate Change impact of printable concrete is about 60% higher than the one of C25/30 concrete used for casting (cf. Section 1.3) and represents 466 kg CO₂ Eq / m³

Table 2.2. Formulation for 1 m³ of Printable Concrete

Components	kg / m ³	Reference / EcolInvent Process
Cement CEM I	540 kg	[14]
Silica fume	480 kg	market for silica fume, densified cut-off, U
Sand	1033 kg	[15]
Water	212 kg	market group for tap water cut-off, U
Superplasticizer	8,8 kg	[16]
Accelerator	6 kg	Not taken into account

Table 2.3. M_{fp} coefficient: Environmental Impact of 1m³ of Printable Concrete

Impact Category	Unit	M_{fp} coefficient
Agricultural Land Occupation	m ² a / m ³	2,33E-01
Climate Change	kg CO ₂ -Eq / m ³	4,66E+02
Fossil Depletion	kg Oil-Eq / m ³	1,54E+02
Freshwater Ecotoxicity	kg 1,4-DCB-Eq / m ³	1,34E+01
Freshwater Eutrophication	kg P-Eq / m ³	9,88E-04
Human Toxicity	kg 1,4-DCB-Eq / m ³	1,27E+02
Ionizing Radiation	kg U ₂₃₅ - Eq / m ³	2,81E+00
Marine Ecotoxicity	kg 1,4-DCB-Eq / m ³	2,21E+00
Marine Eutrophication	kg N-Eq / m ³	4,05E-01
Metal Depletion	kg Fe-Eq / m ³	2,26E-01
Natural Land Transformation	m ² a	4,64E-03
Ozone Depletion	kg CFC-11-Eq / m ³	3,26E-07
Particulate Matter Formation	kg PM ₁₀ -Eq / m ³	2,37E-01
Photochemical Oxidant Formation	kg NMVOC / m ³	1,03E+00
Terrestrial Acidification	kg SO ₂ -Eq / m ³	6,55E-01
Terrestrial Ecotoxicity	kg 1,4-DCB-Eq / m ³	2,62E-01
Urban Land Occupation	m ² a	9,72E-01
Water Depletion	m ³	8,40E-02

2.4.

Environmental Impact of Robotic Construction

As it was stated previously, the impact of robotic construction processes is defined by the parameter of the printing time Δt and by the values of its impact coefficients R_{fp} and O_{fp} .

The first one R_{fp} stands for the *embodied impact of the robotic printing process* coming from the production of the robotic hardware, comprising all the burden of raw material extraction to manufacturing, assembly, and transport of all the robotic cell's components. It will be characterized using the Life-Cycle Assessment method and amortized to one hour of printing, see Section 2.4.1.

The second one O_{fp} represents the *operational impact of robotic printing processes*, defined by the amount as well as by the type of operational energy used during the printing process. It will be characterized with physical measurements and brought to one hour of printing, see Section 2.4.2.

Figure 2.5 depicts both the embodied and operational impacts of robotic printing cell. Again, both impacts (embodied and operational) will be characterized for one hour of printing, in order to have the coefficient-like values with units of [impact / hour]. The following section describes the characterization procedure.

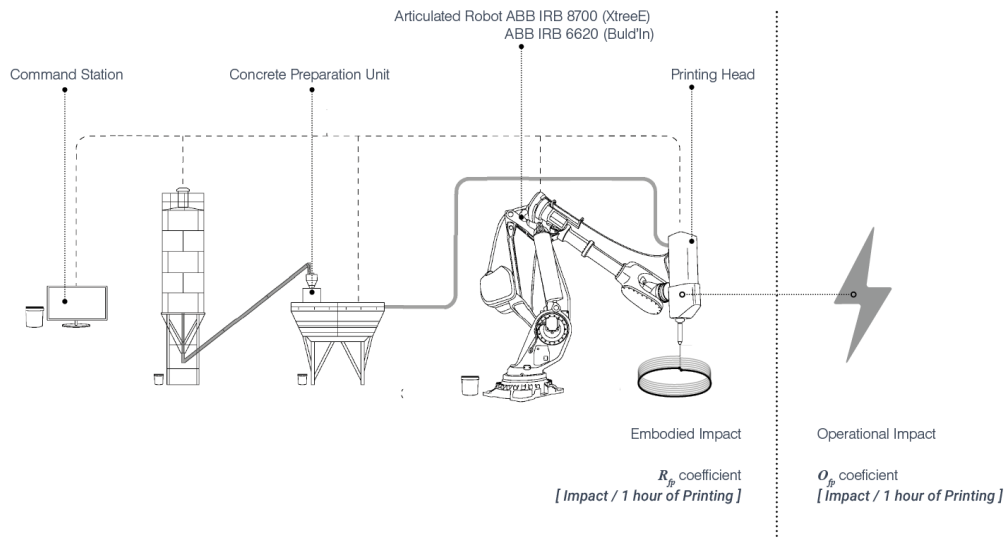


Figure 2.4. Embodied and Operational Impacts of 3D Concrete Printing Process

2.4.1. Embodied Impact of Robotic Construction Processes: R_{fp} coefficient

The embodied impact constituting of robotic construction processes will come from the raw material extraction, transportation, production and assembly of the robotic hardware and other cell's components. Thus, in order to evaluate this impact an environmental life-cycle model of the robotic printing cell was assembled and its outlay to the fabrication process is extensively studied.

As it was discussed in the previous part, of Section 1.4.2, the work of Agusti-Huan and Habert is currently the sole to provide the information on the life-cycle inventory. For reminder, the life-cycle inventory in question represents a generic life-cycle model of a construction robot based on the *in-situ fabricator* [18], and the modeling strategy adopted for the inventory formalization consists of the decomposition of all components till the primal materials, without depict any specific part of robotic hardware (e.g. servo-motor or controller), which limits importantly the further generalization of the proposed model. In other words, one can does not model or configure his/her robotic platform, i.e. set multiple robots, add/remove a controller or change the size of the robot or any other element.

As follows, for the present study, the modelling strategy does not decompose the robotic hardware till the primal materials, but rather till the basic functional entities available in the EcoInvent database to be approximated to, e.g. servo-motor, gear-boxed, integrated circuit etc. Generally, a lot of technical and informatic equipment is available in the EcoInvent database. Therefore, each component of the robotic construction cell, e.g. robotic arm, command cabinet, control station, concrete preparation unit, printing head etc. has been decomposed till these primal functional entities and approximated with an existing EcoInvent equivalent process. Some of the equipment, like servo-motors of robots, has been modeled independently based on the EPD documentation publicly available on the manufacturer's web-site (abb.com). The specific equipment of the robotic printing cell, e.g. the printing head or the elements of the concrete preparation unit, were modeled based on the industrial data provided by XtreeE.

A detailed list of inventories used for the life-cycle model including its source reference, quantity as well as the corresponding EcoInvent process can be found in Annex 1.

Figure 2.6 shows an extract of the life-cycle inventory for the robotic printing cell provided in Annex 1, zooming on the robot's servo-motor process. The table is organized from left to right in four columns. The first one indicated the name of the functional entity, here-below the servo-motor. The second column indicates the data source, product specification and the technical reference of the servo-motor defining the details and quantities of material and processes considered in the life-cycle model depicted in the third column. Finally, the fourth column depicts the corresponding EcoInvent process identified using the reports of the EcoInvent database [5].

Source / Reference	Details	Corresponding Process in EcolInvent 3.2 CutOff
// Product Specification	Weight_kg	
<p>https://new.abb.com/products/3HAC020536 024/irb 8700 https://library.e.abb.com/public</p> <p>Corresponding EcolInvent processes are identified based on Reports of EcolInvent Database</p>		
Motors (6 Servo-Motors)	EPD _ AC Low voltage cast iron motor, type M3BP 315 _cf.ABB	Servo-Motor
	Values per 1 kg of Servo-Motor	
	156,7	
	0,4191	steel, low-alloyed steel production, electric, low-alloyed - RER
	0,0609	steel, low-alloyed, hot rolled market for steel, low-alloyed, hot rolled - GLO
	0,4155	cast iron market for cast iron - GLO
	0,0147	aluminium, cast alloy market for aluminium, cast alloy - GLO
	0,0430	copper market for copper - GLO
	0,00001	metal working, average for copper product manufacturing market for metal working, average for copper product manufacturing - GLO
	0,0011	tube insulation, elastomere market for tube insulation, elastomere - GLO
	0,0358	Resin timber board
	0,0043	epoxy resin insulator, Al2O3 market for epoxy resin insulator, Al2O3 - GLO
	0,0057	electrostatic paint market for electrostatic paint - GLO
	156,7	
Axis 1,2,3,5 Rotating AC motor (including PINION)	3HAC058949-003	28,6 x 4
Axis 4 Rotating AC motor (including PINION)	3HAC058950-003	28,5
Axis 6 Rotating AC motor (including PINION)	3HAC058951-003	13,8
	Technical reference	Weight per unit and total

Figure 2.6. Zoom on the servo-motor process

The adopted modeling strategy based on the basic functional entities allows following things. In the first place, it permits to take advantage of already existing elements in the database; in the second place, it anticipates the analysis of impact partitioning between those entities. In other words, by running the life-cycle assessment of the 6-axis robotic arm and/or of robotic construction platform, one may wonder the redistribution of the burden between the platform's components, and at the scale of a robot itself, between robot's body, its servo-motors, controller etc. Furthermore, the sensitivity analysis on each component's properties can be easily set within the parametric study. The following section describes a sensitivity analysis accomplished on the size of the robotic arm.

2.4.1.1. Results

Table 2.4 depicts the total environmental impact of the production phase of the robotic printing cell. The following section will describe the interpretation of these results, normalizing them to the printing process.

2.4.1.2. Amortization to the printing process

As it was mentioned before, in the present study we are looking to quantify the impact coming from robotic construction processes in relation to the material's one, in order to understand the magnitude of the environmental impact coming from the smart and rational automated material deposition process.

Therefore, it is not exactly the absolute values (depicted in Table 2.4.) of the impact coming from the production of robotic cell components that we are interested in hereby, but rather the outlay/amortization of that impact to the construction/printing process.

Table 2.4. Embodied Impact of the Robotic Printing Cell

Impact category	Unit	Robotic Cell
agricultural land occupation	m ² *a	1,37E+04
climate change	kg CO ₂ -Eq	6,62E+04
fossil depletion	kg Oil-Eq	1,74E+04
freshwater ecotoxicity	kg 1,4-DCB-Eq	4,74E+03
freshwater eutrophication	kg P-Eq	8,93E+01
human toxicity	kg 1,4-DCB-Eq	1,47E+05
ionising radiation	kg U ₂₃₅ -Eq	4,31E+03
marine ecotoxicity	kg 1,4-DCB-Eq	4,35E+03
marine eutrophication	kg N-Eq	9,37E+01
metal depletion	kg Fe-Eq	4,28E+04
natural land transformation	m ²	1,03E+01
ozone depletion	kg CFC-11-Eq	4,31E-03
particulate matter formation	kg PM10-Eq	2,65E+02
photochemical oxidant formation	kg NMVOC	2,80E+02
terrestrial acidification	kg SO ₂ -Eq	5,97E+02
terrestrial ecotoxicity	kg 1,4-DCB-Eq	9,99E+00
urban land occupation	m ² *a	1,23E+03
water depletion	m ³	2,46E+02

Commonly, the LCA methodology estimates the outlay (amortization) of technical equipment as a percentage of their life-cycle labor dedicated to the production of the functional unit. Thus, the outlay of robotic hardware would be calculated as a quotient of the running time divided by the whole life-span of the equipment.

$$(2) \quad \text{Machine's Outlay} = (\text{Running Time} / \text{Life Span of Machine})$$

For example, if the life-span of the construction crane is 20 years and the crane has spent two years on the construction site of a given building, then that building would collect the tenth part of the overall life-cycle impact of the crane.

It goes the same way for the robotic construction platform. For reminder, in the present research the embodied and the operational impacts were separated and the burden due to the maintenance and to the end-of-life phase is not taken into account; thus, the outlay calculation concerns only the impact related to the production phase of the robotic equipment. And, as it can be concluded from the equation above, the parameter of the life-span in here will be crucial.

Typically, by increasing/decreasing this last, the value of the hourly outlay of the printing cell may increase/decrease accordingly in a significant way and so will do the value of the R_{fp} coefficient.

The life-span of the robotic cell is set in reference to the one of the robotic arm. In literature, the robot's life service is usually set to 8 or 10 years [19], [17]. According to ABB documentation "*the robot's life-cycle seldom exceeds 20 years*" [20]. In reality the life expectancy of a robot would depend on an exhaustion of its servo-motors, which is a function of bidding speed and torque as well as of the amplitude of its duty cycles. In similar industries the life expectancy of the technical equipment is usually simplified to a mere coefficient, e.g. a number of traveled kilometers for cars or number of on/off cycles for electronic devices. Industrial machines are usually guaranteed by the number of running hours.

Thus, based on the previous studies [19], [17], the technical documentation from the manufacturer [20] and conversations with robotic experts [21] and with industrial partners [9], the life-span of the robotic cell was set to 30000 hours, which corresponds to the 15-18 years of working with the XtreeE fabrication frequency²³, and to an average life-span value existing in literature. As follows, per one hour of working the fabricating piece/the printed material would collect 0,003% of impact related to the production of robotic cell components.

Table 2.5. depicts the hourly outlay of the embodied impact of robotic construction platforms within all environmental categories, presenting the R_{fp} coefficient.

The results in the Climate Change category are equal to 2,2 kg CO₂ Eq/hour. At the present stage, it is complicated to evaluate the magnitude of this value within the overall environmental impact of the 3D Concrete Printed piece. The synthesis of all the characterized impacts will be performed in Part III. The following section provides a sensitivity study on the life-span duration and the size of the robotic arm used within the printing cell, in order to quantify the amplitude of the R_{fp} coefficient variations.

²³ XtreeE printing runs 8-10 hours/day, 4-5 days a week

Table 2.5. R_{fp} coefficient: The Hourly OEmbodied Impact of Robotic Printing Cell

Impact category	Unit	R_{fp} coefficient
agricultural land occupation	m ² *a / hour	4,6E-01
climate change	kg CO ₂ -Eq / hour	2,2E+00
fossil depletion	kg Oil-Eq / hour	5,8E-01
freshwater ecotoxicity	kg 1,4-DCB-Eq / hour	1,6E-01
freshwater eutrophication	kg P-Eq / hour	3,0E-03
human toxicity	kg 1,4-DCB-Eq / hour	4,9E+00
ionising radiation	kg U ₂₃₅ -Eq / hour	1,4E-01
marine ecotoxicity	kg 1,4-DCB-Eq / hour	1,5E-01
marine eutrophication	kg N-Eq / hour	3,1E-03
metal depletion	kg Fe-Eq / hour	1,4E+00
natural land transformation	m ² / hour	3,4E-04
ozone depletion	kg CFC-11-Eq / hour	1,4E-07
particulate matter formation	kg PM10-Eq / hour	8,8E-03
photochemical oxidant formation	kg NMVOC / hour	9,3E-03
terrestrial acidification	kg SO ₂ -Eq / hour	2,0E-02
terrestrial ecotoxicity	kg 1,4-DCB-Eq / hour	3,3E-04
urban land occupation	m ² *a / hour	4,1E-02
water depletion	m ³ / hour	8,2E-03

2.4.1.3. Sensitivity study on the life-span

As it was described in the previous section, the parameter of the life-span will be critical for the hourly amortization of the robotic printing cell (R_{fp} coefficient). Again, the life-span of the robotic printing cell was set to a fixed value of 30000 hours (basing on the information collected from the literature and industry, cf. Section 2.4.1.2), in order to provide a fixed value for the R_{fp} coefficient.

In reality, the hourly amortization of the robotic printing cell will be a function of the life-span time and thus will decrease progressively as the duration of life-span increases. In absolute, if the robotic cell arrives broken and works for barely one hour, the R_{fp} coefficient will be equal to the entire production impact of the robotic printing cell, depicted in the Table 2.4.

In the opposite case, R_{fp} coefficient gets progressively close to zero as the life-span of the robotic printing cell expands. Figure 2.7 depicts the variation of the hourly amortization of the robotic printing cell in function of its life-span.

In reality, the life-span of the robotic printing cell will be conditioned by its economic service rather than by its physical obsolescence. In fact, technical equipment in industries is usually changed once amortized economically for the reasons of production modernization, systematically needed for economic competitiveness. Thus, it will be mainly equipment's economical rentability, identified to be 30000 hours, that will define its life-span.

The present study will use a fixed value of the R_{fp} coefficient, corresponding to the life-span defined to be 30000 hours.

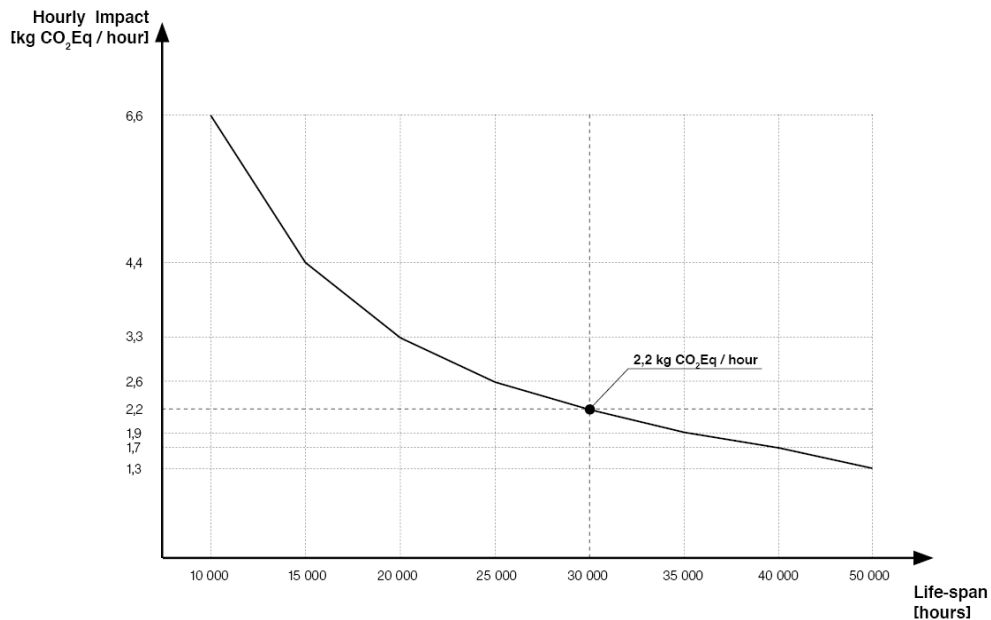


Figure 2.7. Variation of the hourly amortization of the robotic printing cell (R_{fp} coefficient) in function of its life-span.

2.4.1.4. Sensitivity study on the size of the robotic arm

Two robotic arms compared in the present section are differentiated by the size, weight and as a consequence by the printing area they provide. As a matter of fact, the robotic arm ABB IRB 8700 provides a printing area of around 25 m², while the printing area attainable with the robotic arm ABB IRB 6620 will be around 9 m². The size of the printing devices would thus contribute directly to the range of geometries attainable within the printing cell and consequently to the size and type of building elements those can produce. As follows, an obvious conclusion that smaller robot will constitute the less impacting printing cell is not entirely relevant, as two printing cells might have different functions in terms of industrial applications.

Thus, the present sensitivity study unfolds within the hypothesis that two robotic arms can be a part of an equivalent printing cell and are used for the production of equivalent objects. As follows, by addressing the size of the printing device, the present sensitivity study aims to quantify an amplitude of the impact variation coming from this parameter, for the further interpretation of the results.

Table 2.6 regroups the differences in the composition of two robotic arms.

Important to note, that the robot IRB 8700 is the biggest and the heaviest one of ABB catalog when the robot IRB 6620 is the medium one. Yet, it seems impossible to use smaller robot than that of IRB 6620 for construction purposes within a 3D Concrete Printing cell. Therefore, the present sensitivity study will basically show the range of impact variation between two printing cells with equivalent functions (i.e. set to produce equivalent objects) based on the smallest robot suitable for that function and the biggest robot existing in the manufacturer's catalog.

Table 2.6. The inventory data comparison of two robotic arms

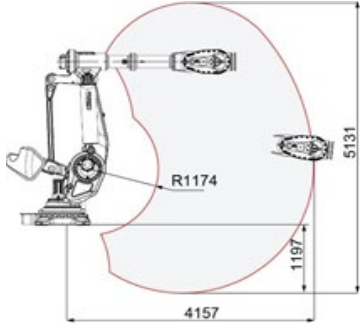
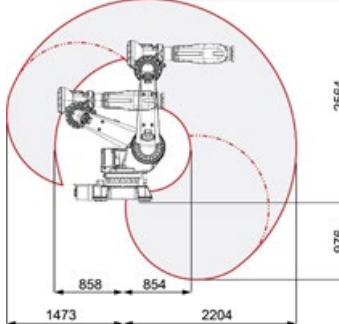
Model	<p style="text-align: center;">ABB IRB 8700</p>  <p style="text-align: center;"><i>Image source: abb.com</i></p>	<p style="text-align: center;">ABB IRB 6620</p>  <p style="text-align: center;"><i>Image source: abb.com</i></p>
Total Weight [kg] where:	4575	1030
Servo-Motors [kg]	156,7	119,3
Gear-Boxes [kg]	591	296
Body [kg]	3827,3	614,7
Power consumption at max load [kW]	4	2,8

Table 2.7 depicts the hourly outlays of the embodied impacts of two robotic printing cells. Figure 2.8 depicts the relative difference between those impacts in all environmental categories.

Table 2.7. Comparison of hourly embodied impact between two robotic printing cells, first based on 5-ton robotic arm ABB IRB 8700 and second one on 1-ton robotic arm ABB IRB 6620

Impact category	Unit	<i>R_{fp}</i> coef. of Printing Cell based on ABB IRB 8700	<i>R_{fp}</i> coef. of Printing Cell based on ABB IRB 6620
agricultural land occupation	m ² *a / hour	4,6E-01	4,5E-01
climate change	kg CO ₂ -Eq / hour	2,2E+00	2,0E+00
fossil depletion	kg Oil-Eq / hour	5,8E-01	5,2E-01
freshwater ecotoxicity	kg 1,4-DCB-Eq / hour	1,6E-01	1,5E-01
freshwater eutrophication	kg P-Eq / hour	3,0E-03	2,8E-03
human toxicity	kg 1,4-DCB-Eq / hour	4,9E+00	4,6E+00
ionizing radiation	kg U ₂₃₅ -Eq / hour	1,4E-01	1,3E-01
marine ecotoxicity	kg 1,4-DCB-Eq / hour	1,5E-01	1,3E-01
marine eutrophication	kg N-Eq / hour	3,1E-03	2,9E-03
metal depletion	kg Fe-Eq / hour	1,4E+00	1,1E+00
natural land transformation	m ² / hour	3,4E-04	3,1E-04
ozone depletion	kg CFC-11-Eq / hour	1,4E-07	1,3E-07
particulate matter formation	kg PM10-Eq / hour	8,8E-03	7,8E-03
photochemical oxidant formation	kg NMVOC / hour	9,3E-03	8,2E-03
terrestrial acidification	kg SO ₂ -Eq / hour	2,0E-02	1,9E-02
terrestrial ecotoxicity	kg 1,4-DCB-Eq / hour	3,3E-04	2,9E-04
urban land occupation	m ² *a / hour	4,1E-02	3,7E-02
water depletion	m ³ / hour	8,2E-03	7,6E-03

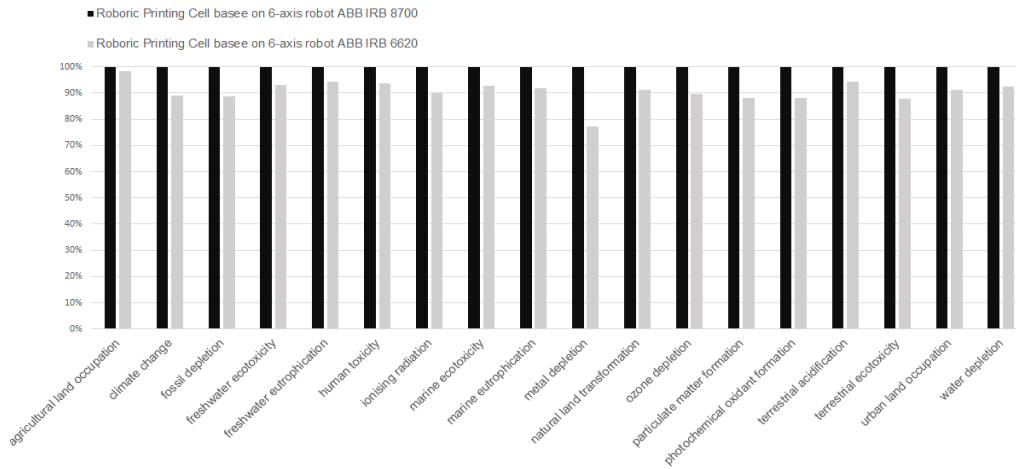


Figure 2.8. Comparison of embodied impact between two printing cells

Zooming specifically on the Climate Change category the variation of impact represents around 10%, which is mainly due to the difference of the metal containment in two robots. Thus, the impact difference in the category of Metal Depletion goes up to 20%. Regarding the other indicators the impact variation occurs between 5-10%. Finally, the impact categories affected in less than 5% are Agricultural Land Occupation and Terrestrial Acidification.

In general outline, considering the fact that the comparison was made with the biggest robot available in the ABB catalog (IRB 8700) and the one of medium size (IRB 6620), the mass difference between which is almost fivefold (see Table 2.6), no substantial difference has been observed in the Climate Change impact. Concretely, the Climate Change hourly embodied impact of the robotic printing cell based on the biggest robot (IRB 8700) represents 2,2 kg CO₂ Eq/hour, when the one of the medium size robot (IRB 6620) represents 2,0 kg CO₂ Eq/hour. As follows, a general conclusion can be drawn that the type/size and mass of the robot used within the printing cell has a minor influence on its hourly embodied impact. This topic will be discussed in detail in Section 3.1.

2.4.2. Operational Impact of Robotic Construction Process

O_{fp} coefficient

The impact related to the operational energy is entirely defined by the local type of electricity generation, which varies significantly from one country/region/city to another. For example, according to 2012 year statistics, the french electricity mix is on 70% composed of nuclear power, which despite its hazardous and radioactive character, remains nearly GHG-emissions free, in a difference to the coal-fired power is about 20% more emitting than the one based on the oil combustion, which basically means that in countries like Germany, England or China, where the coal-fired power is prevailing, an electric car would actually emit more of carbon dioxide than a similar car running on oil [5]. Figure 2.9 illustrates the impact variation of 1 kWh of electricity produced in different countries, normalized by the world average electricity mix.

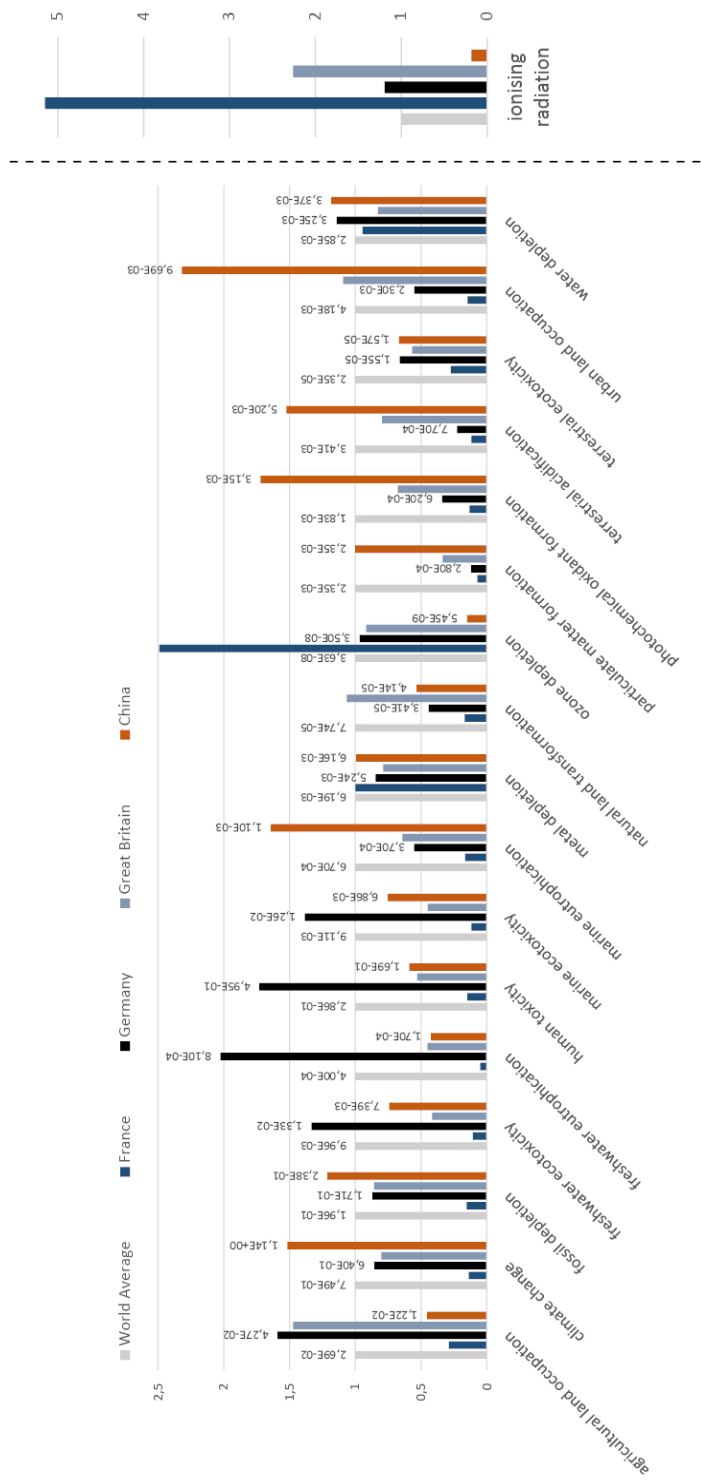


Figure 2.9. Environmental Impact per 1 kWh of medium voltage electricity produced in different countries, normalized by world average mix. Market data based on 2012 year statistics from EcoInvent database 3.2 Cut-Off

Hence, exactly like in the case of an electric car, the same robotic construction system would produce significantly different environmental impacts depending on the type of its running power.

Touching the factor of the quantity of operational energy needed to run the robotic construction process, it is highly expectable that the automation of the concrete deposition process will significantly increase its energy consumption in comparison to the casting process. In other terms, within the approach of smart and rational material deposition in very small amounts and exactly where it's needed, the mechanical work accomplished by the printing device will rise significantly compared to the conventional construction, considering the analytical assumption that goes as follows. With the printing section of 1 cm², a distance of 10 km has to be traveled by a printing device in order to deposit 1 m³ of material. Thus, considering a mass of a printing device, in our case varying from 1 to 5 tons (which corresponds to the weight of the robotic arm ABB IRB 6620 and IRB 8700 both studied in here), the mechanical work needed to deposit one cubic meter of material would therefore equal accordingly to 27 kWh or 124 kWh.²⁴

Therefore, considering the world average Climate Change impact per kWh of electricity (see Figure 2.8) the process-related impact may represent from 15 to 93 kg CO₂ Eq per cubic meter of material.²⁵ Thus, considering that the volumic impact of printable concretes in the Climate Change category is around 400-500 kg CO₂ Eq / m³ (which corresponds to the quota of the cement mass in formulation, cf. Section 1.3 and Section 2.3) this analytical assumption on the impact related to the operational phase of the printing process suggests that it may contribute significantly to the overall environmental impact of the 3DCP element.

The preliminary data collection on the energy consumption of the robotic construction platform was effectuated with industrial partners and resumed to the overall power consumption of 45kW, where 23 kW are attributed to the *concrete preparation unit*, 18 kW to the *printing head* and 4 kW to the *robot* itself.

Still the power consumption of 45 kW corresponds specifically to the sizing value for electric systems and thus represents a coarse theoretical maximum that includes additional safety margins. As follows, an everyday printing might consume twice or thrice less power, which will significantly decrease the global impact of the system.

Additionally, in the previous LCA studies of the robotic construction process the operational energy has been estimated based on the theoretical values coming from the technical documentations and the numbers are very different from one study to another (cf. Section 1.5).

²⁴ Mechanical work performed by robotic arm ABB IRB 6620 :
 $1000 \text{ [kg]} * 9,8 \text{ [m.s}^{-1}] * 10\,000 \text{ [m]} = 98\,000\,000 \text{ [J]} / 3.6e+6 = 27 \text{ [kWh]}$

Mechanical work performed by robotic arm ABB IRB 8700 :
 $4500 \text{ [kg]} * 9,8 \text{ [m.s}^{-1}] * 10\,000 \text{ [m]} = 448350000 \text{ J} / 3.6e+6 = 124 \text{ [kWh]}$

²⁵ $27 \text{ [kWh]} * 0,75 \text{ [kg CO}_2 \text{ Eq/kWh]} = 15 \text{ [kg CO}_2 \text{ Eq]}$
 $124 \text{ [kWh]} * 0,75 \text{ [kg CO}_2 \text{ Eq/kWh]} = 93 \text{ [kg CO}_2 \text{ Eq]}$

To sum up, no measured data currently available in the literature for the operational power consumption of the robotic printing process, while according to the analytical assumption previously described in this section, it may be the dominating parameter of the process-related impact. As follows, in the present study, an original experimental protocol was set up and the measurements of operational power consumption of the robotic 3D Concrete Printing Process have been carried out.

A detailed report on technical aspects of the experimental protocol of measurement procedure, including the power measurement devices and the processing of the measured data are detailed in Annex 2.

The following section describes the measurements of the power consumption and the analysis of the operational impact of the robotic printing process.

Power Consumption of Robotic Printing Process

Again, the operational impact of robotic printing processes comes from operational energy needed to run the process. Accordingly, it would be the quantity as well as the local production type of electricity that will define this value.

In the present study, the detailed measurements of electric power consumption of the printing process were carried out in order to determine the real apparent power consumption of the printing cell components. Concretely, the power measurement devices (representing basically an amperemeters) were installed on each component of the robotic printing cell and a series of measurement sessions has been carried out in order to determine an average power consumption for every process. Annex 2 regroups the technical details of the power measurements devices.

The measurements were carried out within two printing cells the one of Ecole des Ponts ParisTech²⁶, based on the robotic arm ABB IRB 6620 and the one of XtreeE, based on the ABB IRB 8700. Both printing cells are also slightly different in terms of industrial maturity of equipment. The cell of Ecole des Ponts ParisTech is a laboratory experimentation-oriented platform, while the cell of XtreeE is a more industrially mature one, containing more robust and efficient equipment dedicated to industrial functioning, in particular the elements of concrete preparation unit and the printing head.

Additionally, the measurements were conducted repeatedly on different objects and toolpaths of various complexity in order to understand an influence that those can have on the power consumption of the process. In the end, the mean values of power consumption for every process have been defined.

Figure 2.10 depicts the measured curves of the power consumption of every process. Table 2.1. regroups the mean power consumption value of every process of the robotic printing procedure.

²⁶ <https://www.buildin-enpc.fr/>

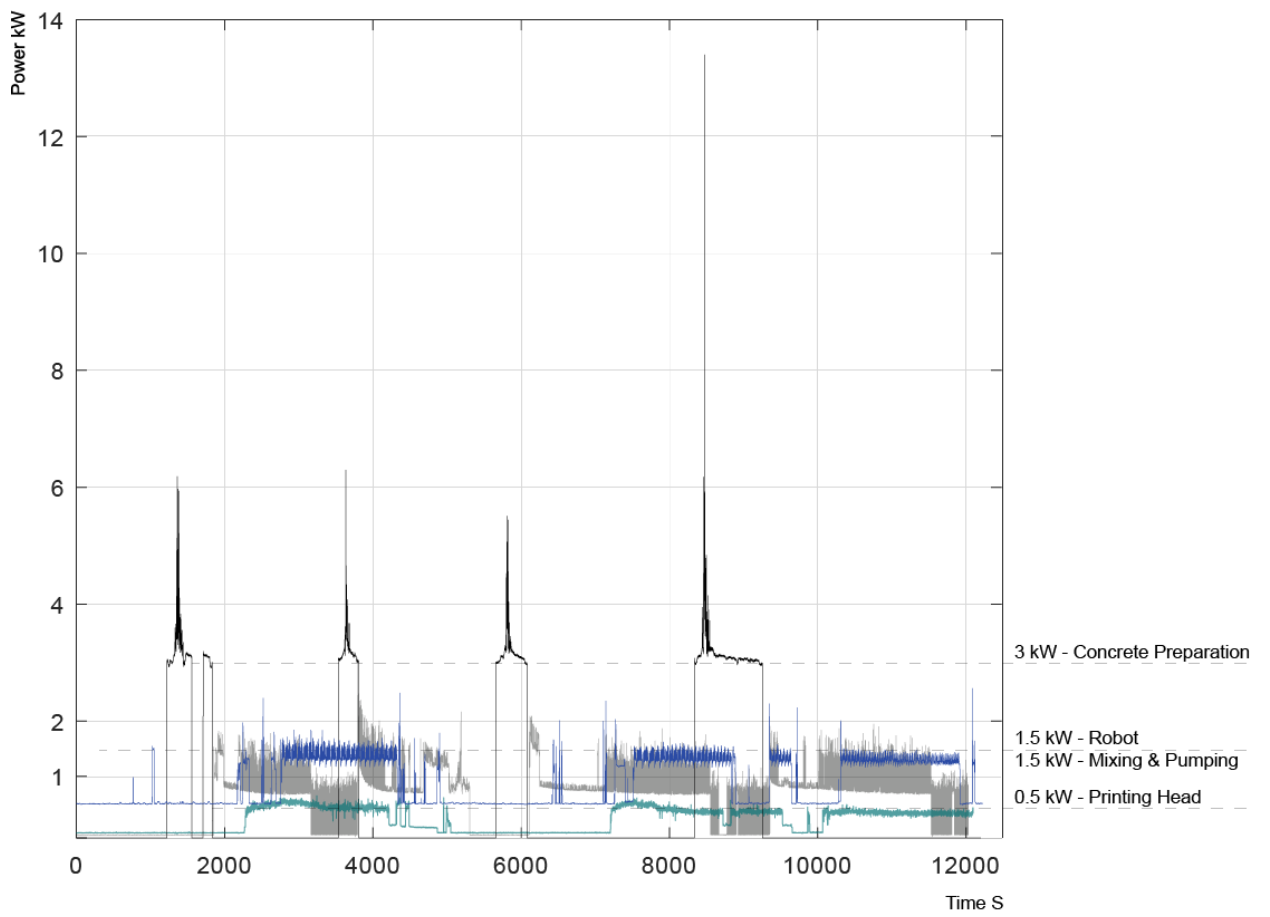


Figure 2.10. Experimentally Measured Curves of Power Consumption of the Printing Process

Table 2.8. Power consumption of Robotic Printing Cell

Process	Measured Power Consumption [kW]
Concrete Preparation	3
Concrete Mixing & Pumping	1,5
Robot ABB IRB 6620 / IRB 8700	1.5
Printing Head	0.5
Total Hourly Average	4 kW

Concretely, the *concrete preparation* process stands for the primal concrete mixing in the beginning of every batch that does not last for the whole printing session contrary to the other processes, i.e. *concrete mixing & pumping*, the functioning of *robot* and the functioning of the *printing head*, all continuous from the beginning to the end of printing session. As follows, the average hourly power consumption of the concrete preparation corresponds to roughly 15% (0.5kW) of the measured power consumption of this process (3kW).

As follows, the amount of energy needed to print a certain amount of material is equal to the power value multiplied by the time of printing. Thus again, for the printing section of 1 cm², the time needed to deposit 1 m³ of material would equal to 13,9 hours of a very fast printing (200 mm/s), consuming in that way 55,6 kWh of energy, which is approximately 14 times bigger than the amount of energy used during the casting processes of conventional concrete (4kWh / 1 m³, cf. Section 1.4).

For the present study, the world average electricity mix has been considered in order to maintain a generic character of the proposed coefficients. In fact, none of the national european mixes is representative of the european average. Furthermore, the european average electricity mix is different from the asian or the african one, and again not representative of the world average. Thus, by addressing the general question of the environmental performance of the 3D Concrete Printing technology it is more accurate to operate with world average electricity data. For specific case-studies, the electricity data can be adapted to the local contexts. Table 2.9 shows the hourly operational impact of the robotic printing process running on the world average electricity mix.

Beyond the precise numbers of the power consumption of the printing process, the present measurements explicitly show the origin of the operational impact of the 3D Concrete Printing process. In other terms, a relatively low consumption rate of the robotic arm signifies that the main power intake of the process does not come from the transportation of the robot's mass, as it was assumed with the initial hypothesis, but rather from the extension through the whole time of printing of the mixing & pumping process.

The power consumption of this last would thus be directly determined by the rheological properties of material, e.g. the viscosity and the yield stress. This hypothesis might explain the low power consumption of the measured pumping & mixing (~ 1.5 kW), as the concrete used in the studied process is particularly liquid, of low-viscosity and a with yield-stress around 100 Pa.

In consequence, the concretes with the higher yield stress and viscosity may cause a higher power consumption of the whole system, while the power consumption of the printing device

may only decrease, as the measured values correspond to the heaviest printing device possible in relation to the smallest printing section. Therefore, it is not only the type of the printing system that will define the operational impact of the printing process, but also and probably dominantly - the rheology of material used for that process. The topic will be discussed more detailedly in Part 3.

In the meantime, it is important to emphasize that the measured values of power consumption of every element of robotic construction platforms turn out to be impressively low, and in terms of magnitude are comparable to the power consumption of two hair dryers or a Hoover. The outcomes of this energy efficient industrial framework will be discussed at the conclusion.

Table 2.9. O_{fp} coefficient : Hourly Operational Impact of Robotic Printing Process

Impact category	Unit	Robotic Printing Cell
agricultural land occupation	m ² *a / hour	9,90E-02
climate change	kg CO ₂ -Eq / hour	3,03E+00
fossil depletion	kg Oil-Eq / hour	7,85E-01
freshwater ecotoxicity	kg 1,4-DCB-Eq / hour	4,10E-02
freshwater eutrophication	kg P-Eq / hour	1,68E-03
human toxicity	kg 1,4-DCB-Eq / hour	1,19E+00
ionising radiation	kg U ₂₃₅ -Eq / hour	4,72E-01
marine ecotoxicity	kg 1,4-DCB-Eq / hour	3,76E-02
marine eutrophication	kg N-Eq / hour	2,76E-03
metal depletion	kg Fe-Eq / hour	2,51E-02
natural land transformation	m ² / hour	2,93E-04
ozone depletion	kg CFC-11-Eq / hour	1,39E-07
particulate matter formation	kg PM10-Eq / hour	9,84E-03
photochemical oxidant formation	kg NMVOC / hour	7,44E-03
terrestrial acidification	kg SO ₂ -Eq / hour	1,38E-02
terrestrial ecotoxicity	kg 1,4-DCB-Eq / hour	8,90E-05
urban land occupation	m ² *a / hour	1,77E-02
water depletion	m ³ / hour	1,19E-02

2.5.

Environmental Impact of 3D Concrete Printing:

M_{fp} , R_{fp} & O_{fp} coefficients

Following the characterization procedures described in the previous sections, the coefficients of material- and process-related footprints can now be inserted into the previously defined formula of environmental impact of 3D Concrete Printing:

$$I = V M_{fp} + \Delta t (R_{fp} + O_{fp})$$

Table 2.10. regroups the values of each of three coefficients for all environmental categories of impact. As follows, an environmental impact in Climate Change category of any object fabricated with the extrusion-based printing technology based on 6-axis robotic arm will equal to:

$$I [kg CO_2 Eq] = 466 V + \Delta t (2,2 + 3,03)$$

Where V is the overall material volume and Δt is the overall printing time. Figure 2.11 depicts the model graph of environmental impact for 3D Concrete Printing featuring the values of the impact coefficients for the Climate Change category. A synthesis of all characterized coefficients and its associated parameters is carried out in Part 3 at the scale of material, structure and building envelope.

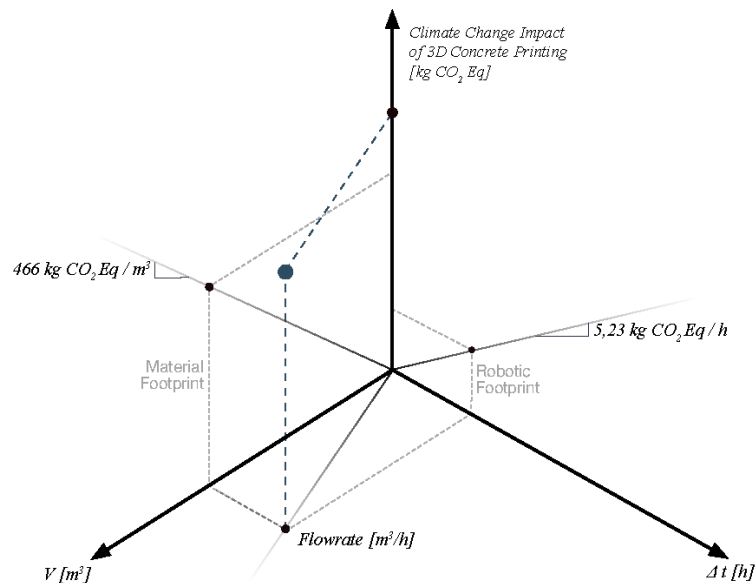


Figure 2.11. Model of Environmental Impact for 3D Concrete Printing featuring the values of the Impact Coefficients

Table 2.10. M_{fp} , R_{fp} & O_{fp} coefficients

<i>Impact Category</i>	M_{fp}	R_{fp}	O_{fp}
Agricultural Land Occupation	2,33E-01 m ² a / m ³	4,6E-01 m ² a / h	9,90E-02 m ² a / h
Climate Change	4,66E+02 kg CO ₂ -Eq / m ³	2,2E+00 kg CO ₂ -Eq / h	3,03E+00 kg CO ₂ -Eq / h
Fossil Depletion	1,54E+02 kg Oil-Eq / m ³	5,8E-01 kg Oil-Eq / h	7,85E-01 kg Oil-Eq / h
Freshwater Ecotoxicity	1,34E+01 kg 1,4-DCB-Eq / m ³	1,6E-01 kg 1,4-DCB-Eq / h	4,10E-02 kg 1,4-DCB-Eq / h
Freshwater Eutrophication	9,88E-04 kg P-Eq / m ³	3,0E-03 kg P-Eq / h	1,68E-03 kg P-Eq / h
Human Toxicity	1,27E+02 kg 1,4-DCB-Eq / m ³	4,9E+00 kg 1,4-DCB-Eq / h	1,19E+00 kg 1,4-DCB-Eq / h
Ionizing Radiation	2,81E+00 kg U ₂₃₅ -Eq / m ³	1,4E-01 kg U ₂₃₅ -Eq / h	4,72E-01 kg U ₂₃₅ -Eq / h
Marine Ecotoxicity	2,21E+00 kg 1,4-DCB-Eq / m ³	1,5E-01 kg 1,4-DCB-Eq / h	3,76E-02 kg 1,4-DCB-Eq / h
Marine Eutrophication	4,05E-01 kg N-Eq / m ³	3,1E-03 kg N-Eq / h	2,76E-03 kg N-Eq / h
Metal Depletion	2,26E-01 kg Fe-Eq / m ³	1,4E+00 kg Fe-Eq / h	2,51E-02 kg Fe-Eq / h
Natural Land Transformation	4,64E-03 m ² a / m ³	3,4E-04 m ² a / h	2,93E-04 m ² a / h
Ozone Depletion	3,26E-07 kg CFC-11-Eq / m ³	1,4E-07 kg CFC-11-Eq / h	1,39E-07 kg CFC-11-Eq / h
Particulate Matter Formation	2,37E-01 kg PM ₁₀ -Eq / m ³	8,8E-03 kg PM ₁₀ -Eq / h	9,84E-03 kg PM ₁₀ -Eq / h
Photochemical Oxidant Formation	1,03E+00 kg NMVOC / m ³	9,3E-03 kg NMVOC / h	7,44E-03 kg NMVOC / h
Terrestrial Acidification	6,55E-01 kg SO ₂ -Eq / m ³	2,0E-02 kg SO ₂ -Eq / h	1,38E-02 kg SO ₂ -Eq / h
Terrestrial Ecotoxicity	2,62E-01 kg 1,4-DCB-Eq / m ³	3,3E-04 kg 1,4-DCB-Eq / h	8,90E-05 kg 1,4-DCB-Eq / h
Urban Land Occupation	9,72E-01 m ² a / m ³	4,1E-02 m ² a / h	1,77E-02 m ² a / h
Water Depletion	8,40E-02 m ³ / m ³	8,2E-03 m ³ / h	1,19E-02 m ³ / h

Bibliography of Part II

- [1] C. Gosselin, R. Duballet, Ph. Roux, N. Gaudillière, J. Dirrenberger, et Ph. Morel, « Large-scale 3D printing of ultra-high performance concrete – a new processing route for architects and builders », *Materials & Design*, vol. 100, p. 102-109, juin 2016, doi: 10.1016/j.matdes.2016.03.097.
- [2] « XtreeE | The large-scale 3d ». <https://www.xtreee.eu/> (consulté le avr. 23, 2020).
- [3] P. Carneau, R. Mesnil, N. Roussel, et O. Baverel, « Additive manufacturing of cantilever - From masonry to concrete 3D printing », *Automation in Construction*, vol. 116, p. 103184, août 2020, doi: 10.1016/j.autcon.2020.103184.
- [4] « EN 15804:2012 Sustainability of construction works - Environmental product declarations - Core rules for the product category of construction products ».
- [5] « ecoinvent ». <https://www.ecoinvent.org/> (consulté le oct. 19, 2020).
- [6] R. Duballet, « Building systems in robotic extrusion of cementitious materials », Université Paris Est, Paris, France, 2019.
- [7] UNEP Global Environmental Alert Service (GEAS), « Sand, rarer than one thinks ». mars 2014.
- [8] J. B. Guinée *et al.*, « Life cycle assessment and operational guide to the ISO standard — final report may 2001 ». Centre of Environmental Science - Leiden University (CML). Consulté le: juin 07, 2021. [En ligne]. Disponible sur: https://www.universiteitleiden.nl/binaries/content/assets/science/cml/publicaties_pdf/new-dutch-lea-guide/part1.pdf
- [9] « National Project RECYBETON », *RECYBETON*. <https://www.pnrecybeton.fr/en/> (consulté le juin 02, 2021).
- [10] F. de Larrard et H. Colina, *Concrete Recycling: Research and Practice*, 1st Edition. CRC Press, 2019.
- [11] E. Gartner, « Industrially interesting approaches to “low-CO2” cements », *Cement and Concrete Research*, vol. 34, n° 9, p. 1489-1498, sept. 2004, doi: 10.1016/j.cemconres.2004.01.021.
- [12] R. J. Flatt, N. Roussel, et C. R. Cheeseman, « Concrete: An eco material that needs to be improved », *Journal of the European Ceramic Society*, vol. 32, n° 11, p. 2787-2798, août 2012, doi: 10.1016/j.jeurceramsoc.2011.11.012.
- [13] K. L. Scrivener, V. M. John, et E. M. Gartner, « Eco-efficient cements: Potential economically viable solutions for a low-CO2 cement-based materials industry », *Cement and Concrete Research*, vol. 114, p. 2-26, déc. 2018, doi: 10.1016/j.cemconres.2018.03.015.
- [14] ATILH, « Déclaration Environnementale de Produit Ciments courants français CEM I », En conformité avec la norme NF EN 15804+A1 et son complément national NF EN 15804/CN, mars 2017.
- [15] Union Nationale des Producteurs de Granulats, « Module d’information environnementale de la production de granulats à partir de roches meubles », Conforme aux normes NF EN 15804+A1 et NF EN 15804/CN, sept. 2017.
- [16] EFCA, « Declaration Environnementale des Plastifiants Normaux », mars 2006. [En ligne]. Disponible sur: www.admixtures.org.uk / www.efca.info
- [17] I. Agustí-Juan et G. Habert, « Environmental design guidelines for digital fabrication », *Journal of Cleaner Production*, vol. 142, p. 2780-2791, janv. 2017, doi: 10.1016/j.jclepro.2016.10.190.
- [18] « Mesh Mould and In situ Fabricator », *Gramazio Kohler Research*, 2017 2017. <https://gramaziokohler.arch.ethz.ch/web/e/forschung/324.html> (consulté le avr. 27, 2020).
- [19] H. Wyatt, A. Wu, R. Thomas, et Y. Yang, « Life Cycle Analysis of Double-Arm Type Robotic Tools for LCD Panel Handling », *Machines*, vol. 5, n° 1, p. 8, mars 2017, doi: 10.3390/machines5010008.

- [20] ABB Robotics, « Robotics Product Range: Improving productivity, quality and workplace safety ». 2015. Consulté le: août 12, 2019. [En ligne]. Disponible sur: https://library.e.abb.com/public/2bae3495c6be8548c1257e2000787b17/LR_ABB_Robotics_ROB0310EN.pdf
- [21] H. A. L. Robotics, « HAL Robotics | Versatile Robot Programming & Simulation Solutions », *HAL Robotics | Versatile Robot Programming & Simulation Solutions*. <https://hal-robotics.com/> (consulté le avr. 23, 2020).

Part III
Application

In the present part, the established model of environmental impact is applied to two case-studies on two scales.

In the first place, the analysis is carried out on the elementary brick of the printing process, i.e. one printed filament, in order to understand the material-process partitioning of impact at the basic scale of construction procedure.

Then, the analysis is scaled up to the building system, designed specifically for the 3D Concrete Printing technology. The material-process partitioning is similarly evaluated. Then the overall environmental impact of the 3D Concrete Printed building system is compared to its conventional analogues within two structural categories: masonry and reinforced concrete perspective.

The set-up of the Life-Cycle Assessment

The general set-up of the Life-Cycle Assessment is the following. Not the whole life-cycle is studied in here. The boundaries of the study are defined from cradle-to-gate or A1-A3,A5 according to EN 15804 [1], as the problematic of the analysis addresses mainly the construction phase of the life-cycle within the prefabrication industrial context.

No end-of-life scenario is taken into account but will be discussed in section 3.2.7.

The impact of the concrete material and robotic printing process is taken from Part II. For the other inventory used in this part the EcoInvent 3.2. Cut-off database [2] was used for the data collection. The modeling and calculation are accomplished using OpenLCA software.

Recipe MidPoint (H) calculation method is used for the impact evaluation.

For the comparative studies, the calculation method of EN 15804 was used in order to have comparable results with those of EPD files from the INIES database [3]. The detailed description of each functional unit will be provided at the beginning of every case-study.

Table 3.1 sums up the settings of the Life-Cycle Assessment study.

Table 3.1. Summary of the Life-Cycle Assessment study setup

Functional Unit	Case study N1: 1m ³ of Printable Concrete
	Case study N2: 1m ² of structural and insulating wall
Life-Cycle Boundaries	Cradle-to-Gate or A1-A3,A5
Calculation Method	Recipe MidPoint (H) and EN 15804
Inventory database	EcoInvent 3.2 Cut-off

3.1. Environmental Impact of 3D Concrete Printing process

The objectives of the process-scaled environmental analysis are the following. In the first place it allows a primal synthesis of all previously characterized impacts on the elementary level of the construction procedure, providing in that way a foremost information on the burden partition between material and process. In the second place, it allows to identify the process-related parameters influencing the global environmental character of the fabrication system.

In order to have the elementary level analysis, the functional unit of the studied system was set to an “elementary brick” of the construction procedure - the one printed filament. Continuing this analogy, the elementary brick of masonry construction for example, would be a brick itself or any other block of stone or concrete. As follows, understanding the impact of one brick or block, the environmental impact of any built object will be a mere sum of impacts of all blocks.

Thus, if the extrusion-based printing technique consists of the subsequent stacking of the concrete filaments, then any 3D printed object can be considered as an arrangement of those filaments. The elementary brick in here, as well as the functional unit, thus would be a one printed filament of length L , section A and of the total volume of one cubic meter. Figure 3.1. depicts a life-cycle diagram of the fabrication phase of the functional unit, based on one printed filament.

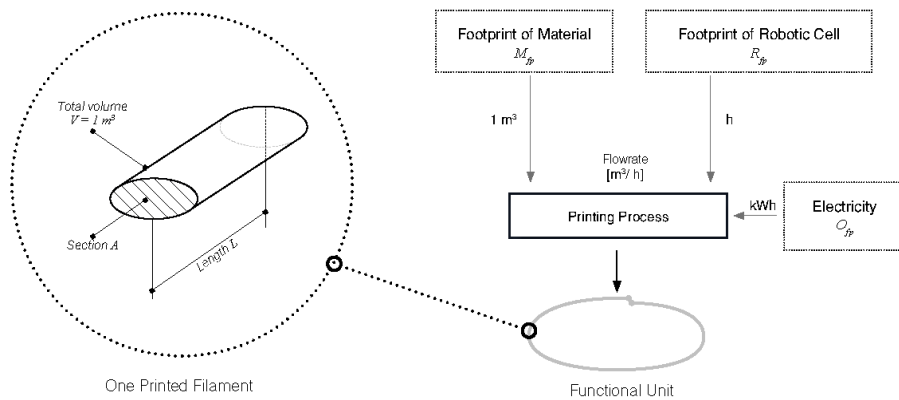


Figure 3.1. Life-Cycle Diagram for the Process-Based Analysis

Within the set-up of the studied printing cell a default section A of the filament would be equal to 1 cm^2 and the average printing speed would be close to 200 mm/s . Thus, based on the results of the characterization accomplished in the previous part the environmental impact of the present case-study for the Climate Change category can be calculated as follows:

$$(1a) \quad I = 1\text{m}^3 \times 466 + 13,9 \text{ h} (2,2 + 3,03) = 538,7 \text{ kg CO}_2 \text{ Eq/m}^3$$

The same calculation can be done for all environmental categories, using the corresponding coefficients regrouped in the Table 2.10. Figure 3.2. depicts the results and the process-concrete partitioning of environmental impact for one printed filament within all environmental categories of Recipe Midpoint (H) calculation method.

3.1.1. Results

Figure 3.2. depicts the results of the environmental evaluation of One Printed Filament of total volume $V=1 \text{ m}^3$ printed with the section $A=1\text{cm}^2$ featuring the process-concrete partitioning of impact within all environmental categories of Recipe Midpoint (H) calculation method.

Zooming specifically on the Climate Change indicator, the supplementary burden brought by the processing technology based on robotic printing, represents around 13% of the overall Climate Change impact per cubic meter. It should be considered as a very significant contribution, as the material-mix studied here is one of the most impacting ones available in the field of printable concretes (as strongly charged in cement, cf. Section 1.3). As follows, the overall impact of one printed cubic meter of concrete performs the impact of $538 \text{ kg CO}_2 \text{ Eq} / \text{m}^3$, which is almost twice bigger than the impact of one casted cubic meter of concrete (cf. Section 1.3 and Section 2.3.)

Regarding the rest of indicators, the impact coming from robotic printing process dominates (i.e. goes up to 50% of the overall impact) for the indicators of Agricultural Land Occupation, Freshwater Eutrophication, Ionizing Radiation, Marine Ecotoxicity, Metal Depletion, Natural Land Transformation, Ozone Depletion, Particulate Matter Formation and Water Depletion.

Furthermore, the contribution of the robotic printing process represents between 40% and 50% in categories of Human Toxicity, Particulate Matter Formation and Urban Land Occupation.

To sum up, the relative impact of the robotic construction processes prevails within half of indicators and almost equal to the concrete's impact in another three. However, in order to understand the absolute importance of that impact an additional normalization step has to be carried out. Concretely, as it was explained in Section 1.2, the normalization study allows to inscribe the results into a global industrial context, showing the fraction of the global impact that the studied system represents into a given impact category. In other words, despite the fact that the impact of the robotic construction process contributes importantly to the majority of impact categories, its fraction of the global impact may remain very low, especially in comparison to other industries. Typically, it is doubtful that the fraction of the global impact of the robotic construction process within the category of Agricultural Land Occupation is comparable to that of timber or textile industry. On the other hand, it may be comparable to the global impact of the automobile industry in categories of Metal Depletion and Climate Change. In order to answer those questions, the normalization study on the industry-wide scale should pertain to further research on the environmental impact of construction automation. The topic will be additionally discussed in the conclusion of the present manuscript.

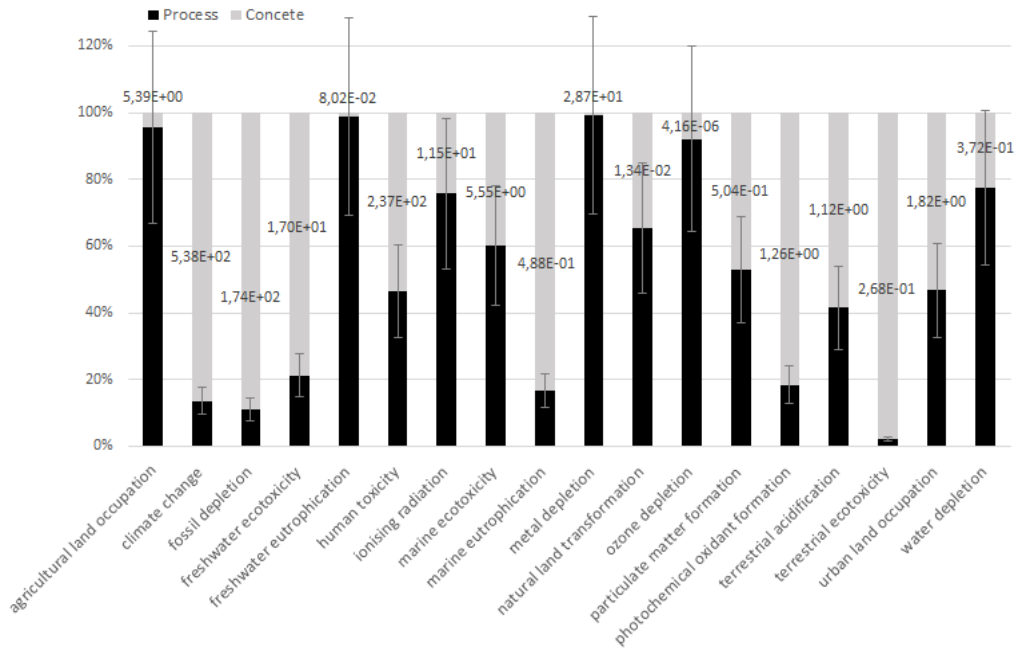


Figure 3.2. Environmental Impacts of One Printed Filament of total volume $V=1 m^3$ printed with the section $A=1 cm^2$ featuring the process-concrete partitioning of impact. The whiskers correspond to the lower and upper bounds of the embodied process-related impact related to the life-span of the robotic printing cell.

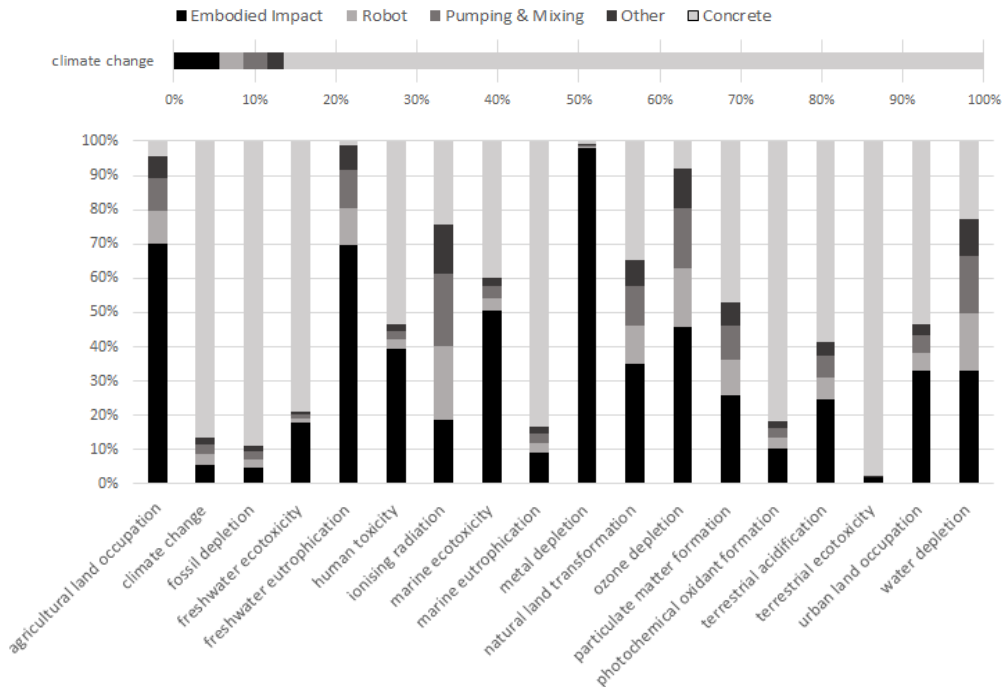


Figure 3.3. Environmental Impacts of One Printed Filament of total volume $V=1 m^3$ printed with the section $A=1 cm^2$ featuring the subdivision of the process-related partitioning of impact.

Figure 3.3. depicts the same results as Figure 3.2, showing the environmental impact of one printed filament with an additional sub-partitioning of the process-related impact. This sub-partitioning is based on the types of impact studied in the previous part, i.e. the *embodied impact* of robotic printing, coming from the production of the hardware (cf. Section 2.4.1), and the *operational impact* of robotic printing, related to the operational power consumption of the system (cf. Section 2.4.2).

In the present study the fixed values for each impact are considered. However, the embodied impact of the robotic printing cell may vary significantly in function of its life-span (cf. Section 2.4.1.3.); while the operational impact of robotic printing cell will vary significantly according to the geographical location, i.e. the local type of electricity generation. The total environmental impact and balance of the system may thus switch significantly by varying those two parameters. For reminder, in the present study a fixed life-span is considered (cf. Section 2.4.1) and the world average electricity mix is used in the simulation (cf. Section 2.4.2).

Thus, with the current set-up, the process-related impact is circa equally partitioned between the embodied and operational impacts. Focusing on the operational impact of the robotic printing process and considering that it is mainly controlled by the type of electricity used to run the construction process, the current partition of impact is determined by the fossil-based nature of the world average electricity mix used in the calculation.

Thus, the current 13% of supplementary process-related impact can be diminished twofold with an introduction of the decarbonized electricity mix, e.g. the nuclear-based one prevailing in France for example (cf. Figure 2.9), with an assumption of the pollution shift consequences towards the indicators of Ionizing Radiation, Ozone Layer Depletion, all water-related categories (cf. Figure 2.9) and a bunch of radioactive waste.

On the other hand, the process-related impact is expected to be higher than 13% in some geographic zones, where the local electricity production type is on the bigger part based on the coal-firing, e.g. Germany or China (cf. Figure 2.9).

In the meantime, apart from all the electricity-related pollution shifts, within the framework of one single electricity type, that importance of the process-related impact will also be defined by the printing set-ups.

The following section studies the influence of the printing resolution on the overall environmental impact of one printed cubic meter of concrete in the Climate Change category.

3.1.2. Sensitivity study on the printing resolution

The present section studies the influence of the printing resolution parameter on the Climate Change impact of one cubic meter of concrete processed with robotic printing. Concretely, the resolution parameter, stands for density of layers within a given object, usually defined according to the needed level of details. Thus, the area of the printing section A will define the level of the printing resolution parameter.

As it was mentioned at the end of Section 2.4.2.1 describing the power measurements of the printing process, this later is dominated by both: the power consumption of the robotic arm and the power consumption of material's mixing & pumping processes. As follows, the time of printing defines the total amount of energy consumed by the system in order to deposit a certain amount of material. In our case the amount of material is fixed to one cubic meter. The deposition time is thus equal to 13,9 hours²⁷ with the printing speed of $v = 200 \text{ mm/s}$ and the printing section of $A = 1 \text{ cm}^2$. As follows, given the fact that the speed during the single print is usually constant, when the area of the filament can be changed in function of the object's geometry and needed resolution, then for a fixed amount of material, e.g. 1 m^3 , the printing time and as a consequence the outlay of the whole system to the printing process, will be a function of the printing section A .

Table 3.1. depicts the variation of the part of the process-related Climate Change impact and as the consequence the overall Climate Change impact per cubic meter of the printed concrete in function of the printing section area A . Figure 3.4. illustrates the decrease of the process-related part of the impact and as a consequence of the global amount of kg CO₂ Eq per cubic meter in function of the printing section area A . Concretely, the area of the printing section is inversely proportional to the process-related impact and thus directly influences the material-process partitioning of impact.

Table 3.1. Influence of the Printing Section A on the Environmental Impact of the 3D Concrete Printing process

Printing Section [cm ²]	Printing Time [h]	[kg CO ₂ Eq / m ³]	Part of process-related impact
0,2	69,4	8,29E+02	44%
0,4	34,7	6,47E+02	28%
0,6	23,1	5,87E+02	21%
1	13,9	5,38E+02	13%
2	6,9	5,02E+02	7%
6	2,3	4,78E+02	3%
10	1,4	4,73E+02	2%

²⁷ The total length of the tootpath for 1 m^3 printed with the section of 1 cm^2 is equal to 10km. The speed of the printing is equal to 200 mm/s , thus $10 \text{ km} / 200 \text{ mm/s} = 13,9 \text{ h}$

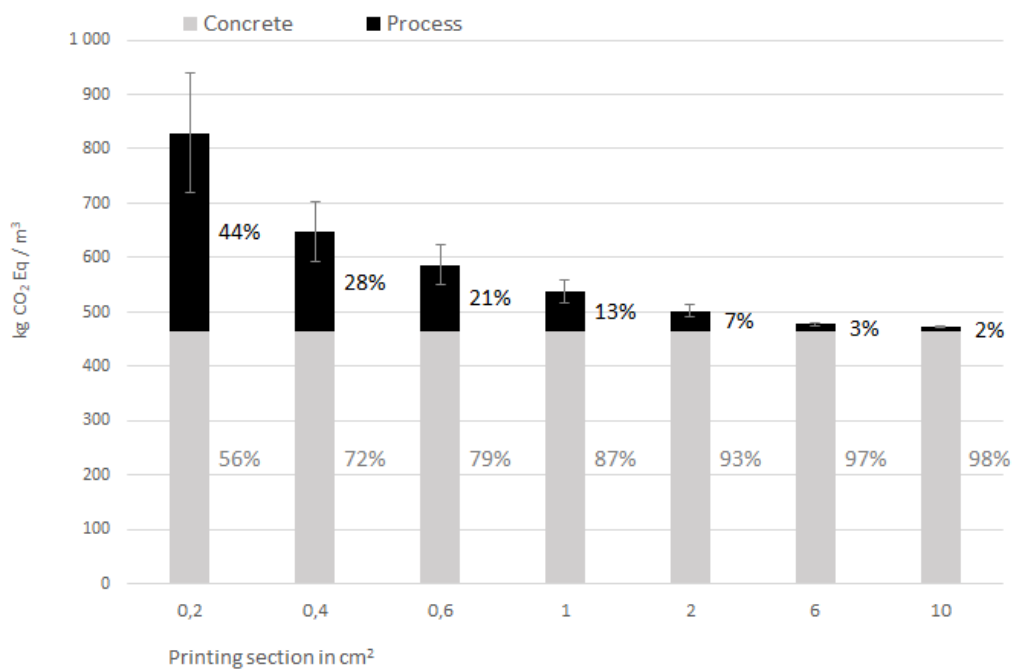


Figure 3.4. Variation of the Climate Change impact per cubic meter of printed concrete in function of the printing resolution, defined by the printing section area A . The whiskers correspond to the lower and upper bounds of the embodied process-related impact related to the life-span of the robotic printing cell.

3.1.2. Conclusions & Perspectives 3.1

The environmental analysis accomplished on the elementary level of the 3D Concrete Printing technology has provided the first synthesis of all the characterized impacts at the scale of one printed filament, outlining the following.

In the first place, a supplementary impact brought by the processing technology based on robotic printing represents around 13% in the Climate Change category. It should be considered as a significant contribution, as about ten times higher than the supplementary impact of conventional construction techniques (cf. Section 1.3).

Yet, this supplementary impact of 13% obtained with the world average electricity may vary significantly in function of the local type of electricity generation, which means that the same process will have different impacts in different geographical zones. Idem, for the life-span parameter of the robotic printing cell that may increase/decrease importantly the current results.

Regarding the parameters that can be controlled during the formal design and/or the setup of the printing process, this 13% of the process-related impact is also specific to a printing resolution and will vary importantly in function of the area of the printing section. Concretely, by increasing the printing section, the supplementary process-related impact decreases to almost insignificant part, see Figure 3.4.

Nevertheless, this relation does not imply that the object printed with a large section, almost free from the supplementary process-related impact will perform more optimal environmental impact, as a large printing section means a large material amount, which persists to dominate the Climate Change impact of the system.

In other words, if the *raison d'être* of 3D Printing in the construction sector is the principle of smart and rational material deposition, then the fine printing section may be an integral part of that approach. The optimal relation of the material-process partitioning of impact must be researched at the scale of the building system, detailing the compromise those two can make within the overall objective of the general efficiency improvement.

This question will be studied in the next section.

Additionally, as it was mentioned previously, the current power consumption of the printing process is largely related to the rheological properties of the material. In other words, the power consumption of the pumping & mixing process (in our case equal to 1.5 kW) may be greatly relevant to the liquid nature of the ultra-high performance printable concrete, that does not include any large aggregates and is processed in very small quantities. Therefore, the eventual modifications of the material mix (e.g. the decrease of the cement portion or the introduction of the large aggregates) may entail some important increase of the power consumption of the pumping & mixing process (which last 13,9 hours for a printing section of 1cm²). As a consequence, the reduction of the material-related impact may increase substantially the process-related impact.

This former point raises an auxiliary question of the general environmental relevance of materials used for 3D Printing. For example, the study of Alhumayani et al. [6] has shown that

the process-related impact of 3D Printing cob represents around 83% of the final impact, when considered *only* the electricity consumption of the robotic arm for the estimation of that process-related impact.

Thus, based on the analysis carried out in the present part, and considering all types of impacts characterized in the present study, it is possible to conclude that on the scale of one printed filament the environmental impact of earth- or clay-based material will ultimately come from the printing process.

Furthermore, due to the low mechanical strength of earth or clay (equal to 2-5 MPa on compression), little of material gains may be possible on the scale of a building system. Therefore, the 3D Printing may have more environmental relevance with high-performance concretes, possessing high volumic impact hand-by-hand with high mechanical strength (up to 120 MPa on compression), which at the scale of a construction element may provide a large range of possibilities for optimal and lightweight formal lay-out.

The following section will study the environmental performance of 3D Concrete Printed structure (building system) with high-performance concrete as well as its environmental relevance in two structural categories: masonry and reinforced concrete.

3.2.

Environmental Impact of 3D Concrete Printed Structure & Building System

In the previous section, the environmental evaluation has been done on an elementary level, providing the primal insights on the process-related impact of the 3D Concrete Printed element on the material scale. The present part provides a synthesis of all those parameters on a scale of building system in order to answer the following question: whether the environmental impact of the 3D Concrete Printed structure enabling some important material saving is lower than the current industrial solution fabricated conventionally?

In other terms, even with the current consideration of an important supplementary impact coming from the robotic printing process (cf. Section 3.1) in addition to the already highly impacting nature of printable concretes (cf. Section 2.3), the material savings potential inherent to that process and material remain quite promising nevertheless (cf. Figure 1.3). Thus, this upheld question of the efficiency trade-off between material savings and the supplementary burden of the process is studied in the present section with a case-study of a building system designed specifically for the 3D Concrete Printing technology enabling over 80% of material savings in terms of mass.

The analysis is organized as follows. In the first place, the environmental impact of the structure is evaluated, maintaining the focus on the contribution coming from the robotic printing process. Then, a series of sensitivity studies on the process-related contribution are effectuated and the overall environmental impact of the structure is compared to its conventional analogues in two structural categories: masonry and reinforced concrete. In closing, a general discussion on the sustainable potential of 3D Concrete Printed structures is carried out, concluding on the contribution of this work to the field and drawing the research perspectives.

3.2.1. Space-truss wall system

The design, fabrication as well as the *raison d'être* of the space-truss wall system has originally been described by R. Duballet et al. in [7], [8] and [9]. In brief, the structure has been specifically designed to fit the 3D Concrete Printing technology, taking a particular advantage of “*putting material exactly where it needed*” moto. Concretely, the system enables over 80% of materials saving in terms of mass, compared to its conventional masonry analogues, while largely assuring the structural and thermal requirements.

In the present study, the system is not considered as a specific structural solution based on a space-truss, but rather a generalization of topologically optimized structures produced with 3D Concrete Printing, enabling some important material savings due to the smart and rational material deposition. In other words, we are not searching to evaluate the environmental performance of the industrial validity of this specific solution, but rather to analyze a global environmental relevance of the approach.

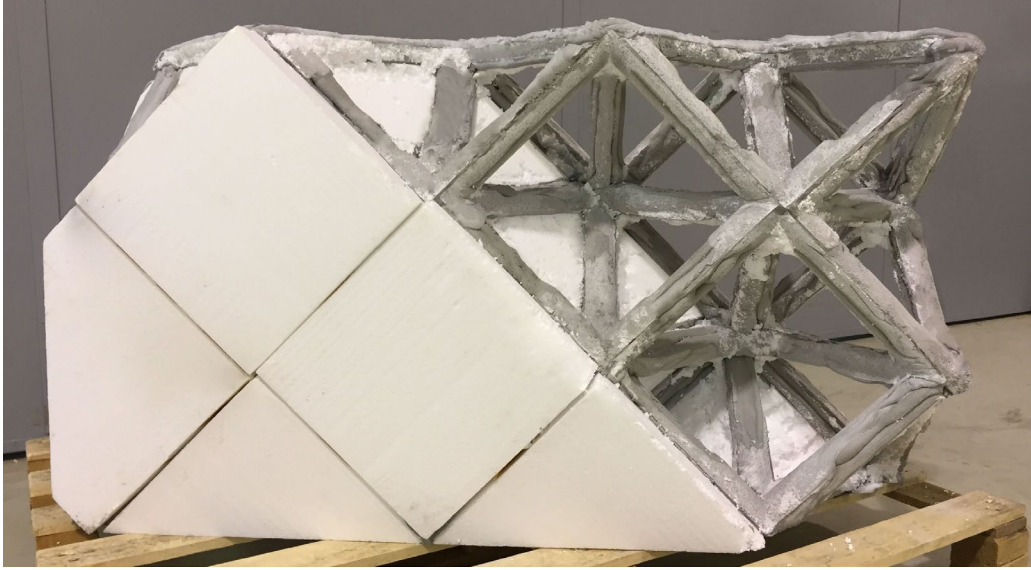


Figure 3.5. Space-Truss Masonry Wall prototype [7]



Figure 3.6. The curved version of the space-truss wall with continuous fiber reinforcement presented on the IASS 2019 symposium

The morphology of the wall-system is based on a principle of spatial tessellation, sub-dividing a given volume in polyhedra. The concrete is printed on the polyhedra edges, shaping in that way a space-truss. The final object performs the high load-bearing properties hand by hand with the material efficiency, as based on the truss behavior. By filling the polyhedra's volumes with a thermal-resistant material, e.g. polystyrene or cementitious foam, an insulating function can be obtained. Beyond the vertical wall applications, the system as such can be extrapolated to almost any flat or curved membrane, e.g. slab or roofing system. The present study will focus on one specific application of the space-truss system, i.e. load-bearing and insulating wall, suitable for the exterior walls of building envelopes.

A first prototype of the space-truss was made and presented at IASS 2018 [7], see Figure 3.5. A curved version of the space-truss including the continuous fiber reinforcement, that will be described in Section 3.2.6.2 was exhibited during IASS 2019 and shown on Figure 3.6.

The production sequence of the space-truss consists of the following steps. First, the insulating blocks are shaped and then progressively assembled in order to support the concrete extrusion. Once assembled, the blocks support and protect the curing concrete that progressively acquires the mechanical strength, getting ready to bear its own weight as well as the additional matter above. As follows, the blocks act as a support withdrawing the early age resistance requirement for the concrete.

For prototyping purposes, the insulating blocks were made of the robotically hot-wire cut polystyrene foam. Within the full-bodied industrial hypothesis of the flat version of the space-truss system, the blocks could be shaped by molding in three standard units: side block, corner block and inner block, see Figure 3.7. Additionally, the initial industrial hypothesis of the system considers the cementitious foam for the insulating blocks that possesses similar insulating properties with much higher mechanical strength. Both materials will be considered in the LCA study.

For the in-depth details on the design, calculation and fabrication as well as the *raison d'être* of the space-truss wall system, see R. Duballet et al. in [7], [8].

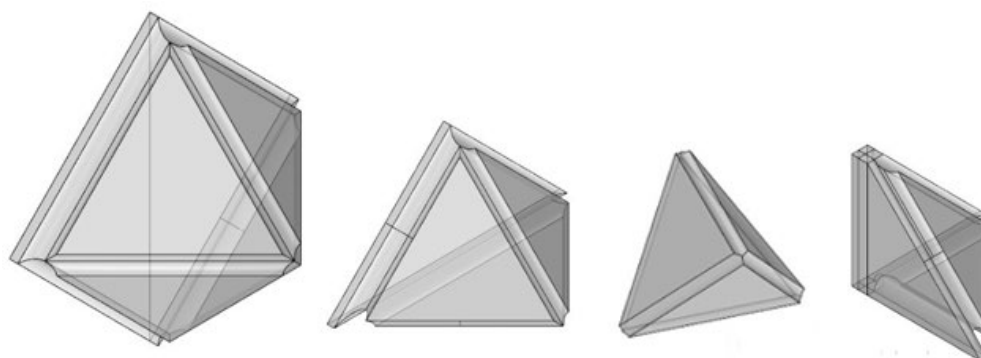


Figure 3.7. Insulating blocks geometry and internal space: Side block, Edge block, Inside block, Corner block; Reproduced from [8]

3.2.2. Normative framework

The normative acceptance of the 3DCP structures remains a hot topic in the field with no universal consensus established for the time of writing. The preliminary strategies applied by the pioneers of the practice have been overlooked in [8], proposing a normative acceptance puzzle for the space-truss wall system.

In brief, the building regulations in Europe are framed by the Eurocode, which regroups a set of standards for design and sizing of buildings and civil engineering structures, including foundations and earthquake resistance. Established by Technical Committee 250 of the European Committee for Standardization (CEN / TC 250), the Eurocode is split into 10 parts according to the construction technique. The Eurocode 2 bounds the normative framework for reinforced concrete structures and thus implies that the concrete structure must be reinforced. This is not currently the case for the concrete elements produced with the 3D Printing technology and thus a valid reinforcement method remains an important research question in the field. Multiple leads are currently studied in academia and practice comprising a variety of technological strategies [10], [11], [12]. In the present work, a solution of continuous fiber reinforcement will be studied in Section 3.2.4.2.

Hence, initially, the space-truss wall has no reinforcement and thus possesses a very low tensile strength and almost no ductility, which disables its validity for the Eurocode 2. The solution proposed hereby by the authors suggests rolling away from the natural implications coming from the structural material used, focusing rather on the morphology of the constructive system than on its material. In other terms, as fundamentally the constructive system constitutes a pack of blocks stuck together with concrete, it can be seen as reinterpretation of traditional breeze-blocks masonry and thus can be inscribed into the Eurocode 6. As follows, this normative framework will limit the potential applications of the system till the masonry structures, e.g. a multi-story shear wall or a single-house wall with insulation.

A comparison in terms of weight with other masonry wall systems currently available in the industry has been carried out in [7], showing that the space-truss system reaches the target performances in mechanics and thermic, while greatly reducing the surfacic weight (up to 80%).

The following section studies the environmental impact of the space-truss system by the means of a previously developed method in two structural categories: masonry and reinforced concrete perspective.

The following section describes the Life-Cycle Assessment setup.

3.2.3.

Environmental Life-Cycle Assessment of Space-Truss Wall

The boundaries of the LCA study are set to cradle-to-gate or A1-A3,A5, as the problematic of the study addresses mainly the construction phase (in prefabrication context). Regarding the end-of-life, the recycling scenario based on the current industrial practice will be discussed in Section 3.2.5.

The functional unit is set to the 1m^2 of the space-truss wall with the target performance for thermal resistance according to RT2020²⁸ and represents $6,6\text{ m}^2\text{K.W}^{-1}$ for masonry (Section 3.2.4.1) and $5,12\text{ m}^2\text{K.W}^{-1}$ for the reinforced concrete perspective (Section 3.2.4.2). The mechanical resistance in line with Eurocode 6 for the masonry (Section 3.2.4.1) and with Eurocode 2 for the reinforced concrete perspective (Section 3.2.4.2). Figure 3.8 depicts a diagram of the fabrication processes considered within the life-cycle study. The process of reference corresponds to the production phase of the functional unit, i.e. printing and assembly of 1m^2 of the space-truss wall. The calculation method of EN 15804 is used in order to have comparable results with the EPD files (fiches FDES) regrouped in the INIES database [3] for the comparison study of the space-truss performances with its conventional analogues, described in Section 3.2.6.

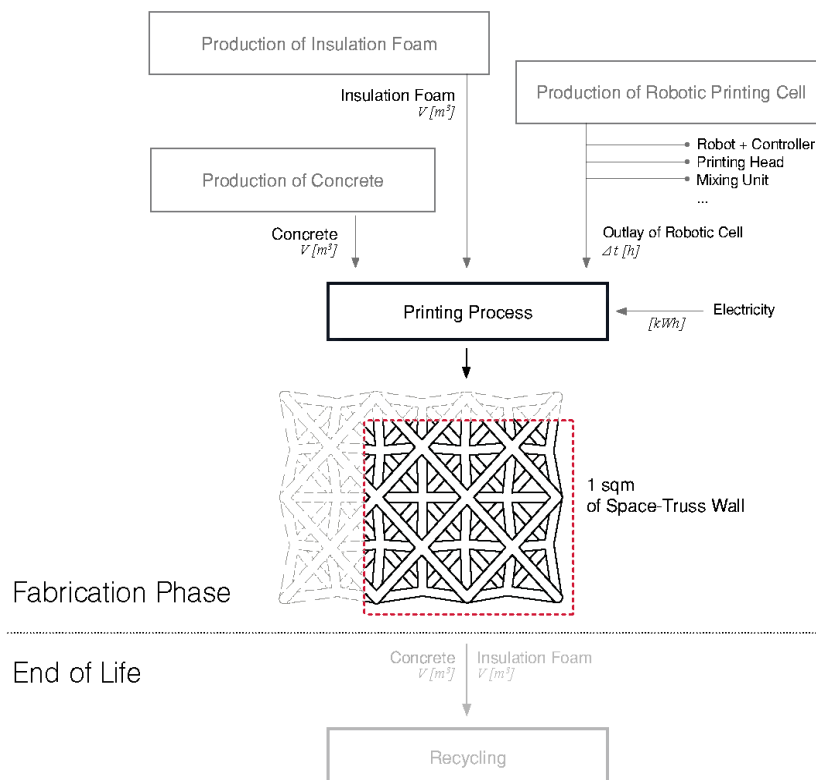


Figure 3.8. Flowchart of the Life-Cycle Model of the Space-Truss wall

²⁸ Règlementation Thermique (environnementale) 2020; <http://www.rt-2020.com/>

The FDES (*Fiche de déclaration environnementale et sanitaire*) is a standardized document, providing the results of environmental life-cycle assessment and health information of construction products, deployed in the french normative framework for sustainable construction development. The INIES database [3] regroups the available FDES sheets for construction products and will be used for the comparison part of this study, detailed in Section 3.2.4. Table 3.2 regroups the inventory for the present Life-Cycle Assessment study. The EcoInvent process for polystyrene foam corresponds to the polystyrene foam used for the prototyping.

Table 3.2. LCA Inventory for the fabrication of 1 sqm of space-truss wall

Inventory	Quantity	Inventory / Ecolnvent 3.2. Cut-Off Process
Concrete	60 kg	Table 2.2.
Robotic Printing Cell	30 min _ 6 pass per ray	Cf. Section 2.4; Annex 1.
Electricity	2 kWh	<i>market for electricity, medium voltage RoW</i>
Insulation foam	0.25 m ³	<i>market for polystyrene foam 45% recycled RoW</i>

The specificity of the topological lay-out of the space-truss imposes an even number of the printing passes per each ray and therefore depending on the sizing requirements, it can go up to 6 passes per ray.

As the initial structure was designed without integrated reinforcement, operating within the framework of masonry structures (cf. Section 3.2.2, Figure 3.5), the structural sizing of the wall was determined by the tensile resistance of the rays, rather than by the buckling factor of the entire wall, as it is usually the case for the vertical load-bearing elements [8]. As follows, considering the low tensile strength of the printed concrete, the ray diameter of the first prototype necessitated 6 printing passes per ray to deposit the needed amount of material [8].

Thus, for the primal synthesis, 6 passes per ray are considered. The sensitivity study on this parameter will be carried out in Section 3.2.3.2.

Similarly, the polystyrene foam will be considered in the present evaluation as a material solution for the insulating/supporting blocks, in order to keep the coherence with the initial fabrication set-up. The full-bodied industrial hypothesis including the cementitious foam for insulating blocks, optimized tool-path as well as the specificities of french industrial context, e.g. electricity mix, will be evaluated in Section 3.2.3.3.

Two electricity mixes are studied for the robotic printing processes: the world average mix and the french national mix. They will be compared in the sensitivity study detailed in Section 3.2.3.3. Figure 3.9 depicts the comparison of environmental impact of some national electricity mixes calculated with the EN 15804.

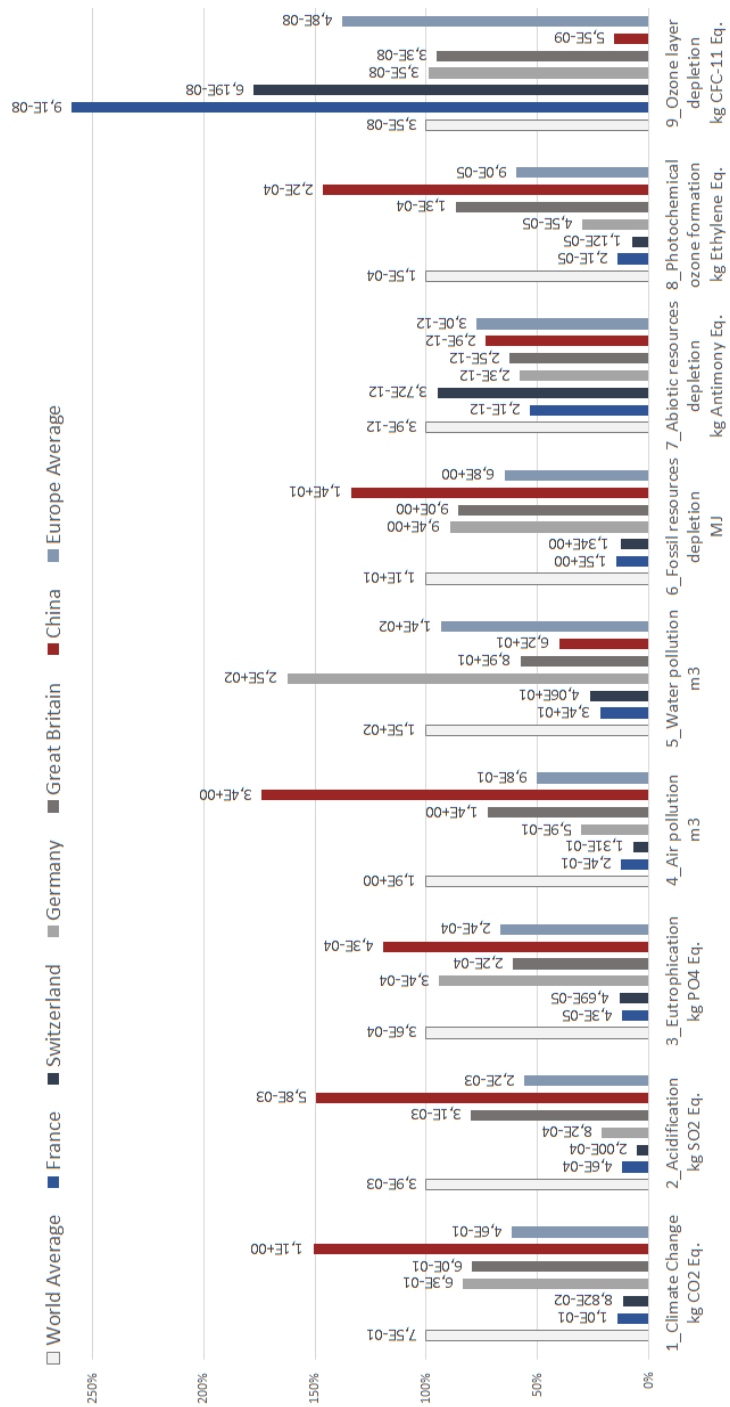


Figure 3.9. Environmental Impact per 1 kWh of energy produced in different countries. Market data based on 2012 year statistics from EcoInvent database 3.2 Cut-Off

3.2.3.1. Results

Figure 3.10. depicts the results of the environmental impact of the space-truss wall system for the initial fabrication set-up featuring the impact partitioning between its components.

The contribution of the robotic printing process represents around 12% of the Climate Change impact and is almost half as big as the one of concrete, representing around 35%. The process-related impact dominates within the Eutrophication indicator, overpassing the contribution coming from concrete and from polystyrene foam, as mainly influenced by the metal-related impacts. It is almost absent (less than 5%) within the indicator of Abiotic Resources Depletion, which quantifies the rarefaction of the mineral resources absent into the robotic hardware inventory.

The contribution of the polystyrene material solution for supporting and insulating blocks is impressively high, i.e. higher than the one of concrete- and process-related impacts within the majority of indicators. Concretely, it represents more than 50% of impact within the categories of Climate Change, Acidification, Air Pollution, Fossil Resources Depletion and Photochemical Ozone Formation, which means that the impact transfer and pollution shift in the life-cycle balance of the space-truss at the present stage isn't resulted from the robotic printing process (as it was the case at the material scale, cf. Section 3.1), but rather from the over-utilization of the polystyrene foam for the insulation purposes as well as for the printing support.

In other words, the impact reduction due to the optimal utilization of the structural material is getting cancelled by the introduction of the auxiliary supporting material. As follows, the contribution of the last dominates more than half of indicators, while the only major contribution of concrete dwells in the category of Abiotic Resources Depletion, quantifying the rarefaction of mineral resources.

The contribution of robotic construction processes is explicitly present within all environmental categories of impact in a non-negligible way. It overpasses the concrete's share of impact in the categories of Acidification, Eutrophication, Water Pollution and Photochemical Ozone Formation.

Therefore again, the impact transfer and the pollution shift phenomena occur in the environmental balance of the system, due to the deployment of the fabrication process initially intended to reduce the material quantity and its associated impact. The reduction potential of that process-related impact is studied in the next section within the sensitivity analysis on the process-related parameters.

3.2.3.2.

Sensitivity study on the printing process-related parameters

The purpose of this sensitivity study is to evaluate the improvement potential of the overall environmental impact of the space-truss coming from the optimization of its process-related impact. The process-related impact is defined by the fabrication time parameter Δt resulted from a series of rheological and formal requirements defining the printing toolpath. On the material scale, it was defined by the printing section A (cf. Section 3.1.2).

In the current case-study it will be also linked to the number of printing passes that robot performs on each ray of the space-truss. For reminder, due to the topological lay-out of the space-truss, the number of passes is constrained to an even number. Therefore, the minimum number of passes is equal to 2 passes per ray, representing the overall printing time of 10 minutes for 1m² of the wall. The maximum number of 6 passes per ray comes from the initial sizing hypothesis of the space-truss from the Eurocode 6 (cf. Section 3.2.2) and its printing time is equal to 30 minutes for 1m² of the wall. Table 3.3 regroups the variation of passes number per ray and its associated printing time.

Needless to say, that the environmental benefits are obvious within the shorter fabrication time, however the magnitude of those improvements remains unknown and therefore important to quantify in order to understand if and how much the toolpath parameter participates in the global environmental impact of the 3D Concrete Printed element.

Table 3.3. Inventory parameters variation for the for sensitivity study on process-related parameters

Inventory	Parameters	Details
Concrete	60 kg	Without changings
Robotic Printing Cell Electricity	30 minutes 2 kWh	6 pass per ray
	20 minutes 1.3 kWh	4 pass per ray
	10 minutes 0.8 kWh	2 pass per ray
Insulation foam	0.25 m ³	Without changings

Figure 3.11. depicts the results of the sensitivity study accomplished on the process-related parameters, consisting of the variation of the number of passes per ray, influencing the printing time Δt . The results show a decrease of around 5% within the majority of indicators of the process-related impact when optimizing the toolpath (curtailing it from 6 to 2 passes per ray).

In a way, the present analysis recalls the sensitivity study performed in Section 3.1.1 on the size of the printing section A , and interrogates the same question of the process-related parameters of material deposition. As both studies confirm the importance of the toolpath parameter and since the material deposition process can be as pricey as the material itself, therefore, it is not only the material quantity that would define an environmental impact of a 3D Concrete Printed element but also the way that material is deposited.

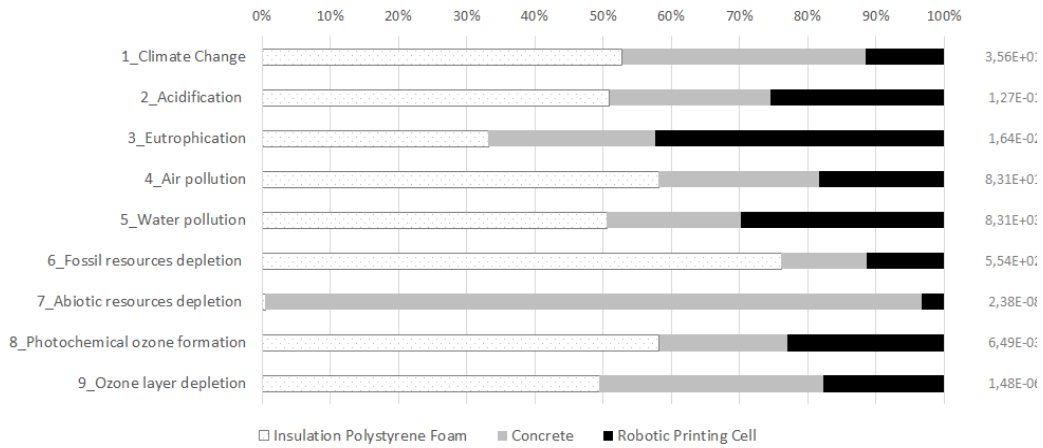


Figure 3.10. Environmental impact of Space-Truss masonry wall

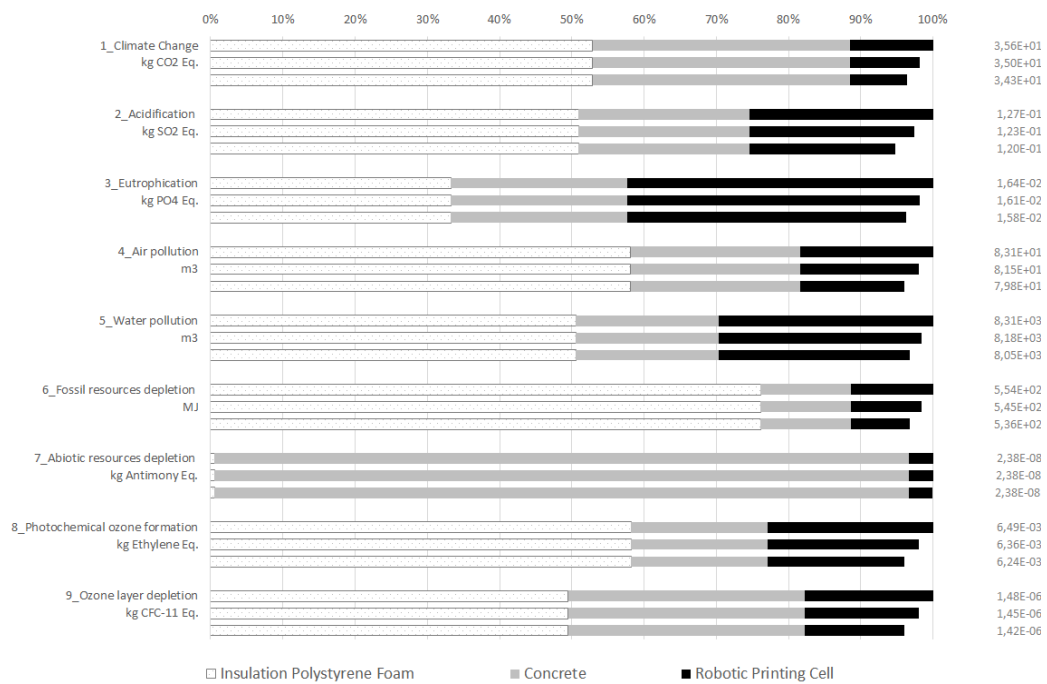


Figure 3.11. Sensitivity study on the process-related parameters of the Space-Truss masonry wall. The 1st line depicts the 6 passes per ray toolpath; The 2nd line depicts the 4 passes per ray toolpath; The 3rd line depicts the 2 passes per ray toolpath (cf. Table 3.3)

3.2.3.3. French Industrial Context

The french industrial scenario stands for the full-bodied optimized industrial scenario in french geographical zone. Practically, it means that all the printing process runs on the french electricity mix.

The french industrial context is simulated for the following reasons. In the first place, it is the original birthplace of the space-truss system, which means that some material and technology choices made by the authors were naturally influenced by the local industrial context. In the second place, the french electricity mix is on 70% composed of nuclear power, which despite its very controversial character in terms of radiation, waste and water pollution, remains nearly emission free in terms of greenhouse gases, shifting the overall environmental balance of the process-related impact, in particular its Climate Change contribution.

The full-bodied industrial scenario means that the mature industrial hypotheses are defined for the production sequences of space-truss and insulating blocks. Concretely, the present simulation is based on the most optimal toolpath for material deposition, i.e. 2 passes per ray representing 10 minutes of printing time for 1 m² of the space-truss wall.

Additionally, the material used for the supporting-insulating blocks is composed of the cementitious foam [13], sized for the same thermal resistance performances of 6,6 m²K.W⁻¹ (RT2020) with much higher mechanical performances [8], [13].

Table 3.4 regroups the inventory for the Life-Cycle Assessment study of the space-truss wall for french industrial scenario.

Table 3.4. LCA Inventory for the fabrication of 1 sqm of the Space-Truss wall in french industrial scenario

Inventory	Quantity	Inventory / EcolInvent 3.2. Cut-Off Process
Concrete	60 kg	Table 2.2.
Robotic Printing Cell	10 min _ 2 pass per ray	Cf. Section 2.4 and Annex 1.
Electricity	0.8 kWh	<i>market for electricity, medium voltage FR</i>
Insulation foam	100 kg	<i>cement mortar market for cement mortar FR</i>

Figure 3.13. regroups all the results of the life-cycle assessment of the space-truss wall including the sensitivity analysis and the french industrial scenario simulation. In general, even within the french industrial context, where the electricity mix is almost decarbonized, the contribution of the robotic printing cell remains considerable, i.e. around 8% in Climate Change, against 1-2% of conventional construction techniques (cf. Section 1.3). It however decreases on 5% compared to the world average electricity mix.

Regarding the rest of indicators, the part of the robotic construction processes gets generally more polluting when running on the french electricity, which can be explained by the prevailing of nuclear power generation (cf. Figure 3.9).

The situation is quite opposite for the part of impact related to the production of the insulation blocks based hereby on the cementitious foam, that decreases significantly within the majority of indicators. In general, comparing the absolute values of every studied scenario within the sensitivity study, some significant impact savings can be outlined within all environmental categories for the full-bodied french industrial scenario with a sole exception for the Abiotic Resources Depletion. This later stands for the rarefaction potential of minerals and rare earths, that are intensively used for the production of concrete for the minerals and for the robotic hardware for the rare earths.

In the next section a comparison study is carried out, between the space-truss wall produced within the full-bodied french industrial scenario and the existing masonry wall solutions currently available in the industry. Right after, in Section 3.2.4.2, the comparison is carried out for the reinforced concrete perspective with the hypothesis of continuous fiber reinforcement for the space-truss.

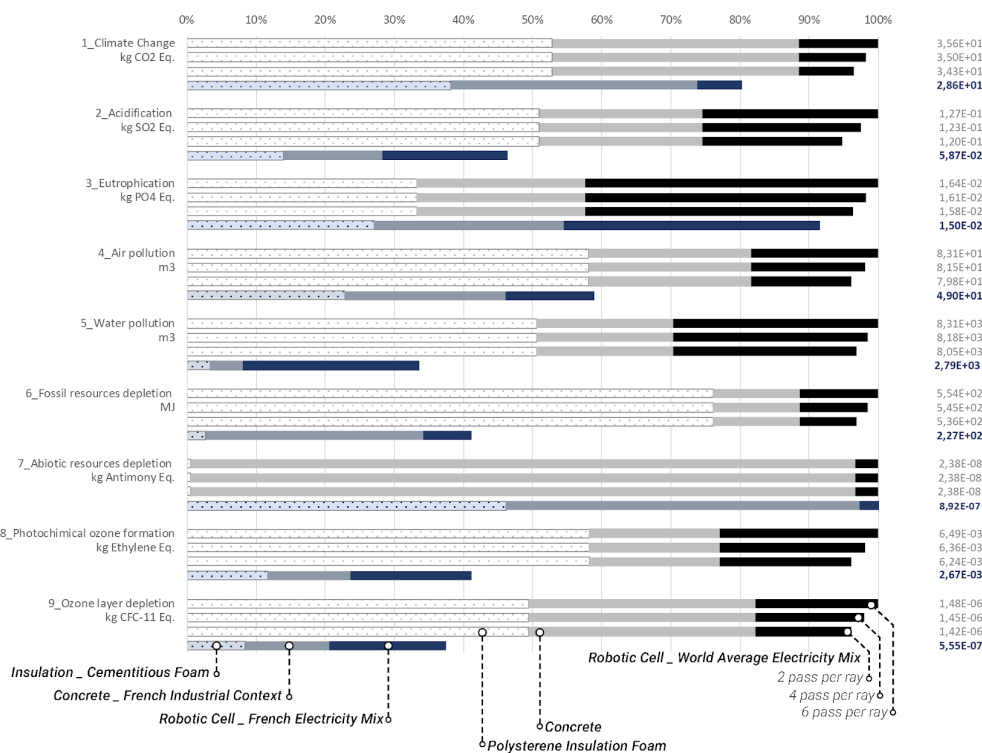


Figure 3.12. Synthesis of LCA Results & Sensitivity Analysis of the Space-Truss masonry wall

3.2.4. Comparison with conventional structural systems

In this section the space-truss wall system will be compared with traditional building systems on the basis of accomplished LCA study within two structural categories: masonry and reinforced concrete. The comparison study is performed on the basis of previously introduced EPD files (fiches FDES), available in INIES database [3] for the environmental and health reference for buildings, regulated by NF EN 15804+A1 standard.

3.2.4.1. Masonry

The present part compares the overall environmental impact of the full-bodied french industrial scenario of the space-truss masonry wall system with the existing solutions in industry. The compared systems are shown and referenced in Table 3.5.

Precisely, the comparison is carried out on the construction phase in the prefabrication context (A1-A3, A5) of 1m^2 of masonry wall with insulation. As the thermal transmission of the space-truss wall system has been sized according to the latest french thermic regulation RT2020, the insulation efficiency of conventional masonry systems is substantially lower than the one of the space-truss, i.e. $1\text{ m}^2\text{K.W}^{-1}$ versus $6,6\text{ m}^2\text{K.W}^{-1}$. Therefore, a supplementary 180mm of a glasswool insulation by exterior was added, providing additional thermal resistance of $5,6\text{ m}^2\text{K.W}^{-1}$ [14] and adjusting in that way the main target performances of all competing systems. Regarding the mechanical resistance, all compared systems are sized according to Eurocode 6.

Figure 3.13 depicts the comparison of environmental impacts of masonry wall systems, pointing out that the impact of the space-truss wall is comparable to the existing parpaing solutions, with no substantial progress. As a matter of fact, the space-truss system turns out to be more impactful in categories of Climate Change, Eutrophication and Water Pollution. The impacts are circa similar for the Acidification and Eutrophication indicator. However, in the rest of categories, i.e. Air Pollution, Abiotic Resource and Ozone Layer Depletion, Photochemical Ozone Formation, the space-truss wall system outperforms significantly its conventional analogues. This latter is mainly explained by the absence of the glasswool insulation, usually used in traditional constructive systems, replaced by the cementitious foam in the case of a space-truss, as it can be observed from the contribution partitioning of impact featured on Figure 3.12.

In general outline, the comparison study reveals a systematic occurrence of an impact transfer and pollution shift within different environmental categories when comparing one constructive system to another. Putting it differently, it is barely possible to tell in an absolute way which system performs the most optimal environmental impact. Still, focusing specifically on the Climate Change indicator, a general conclusion can be drawn, that despite a significant material saving performing by the space-truss, it does not bring any environmental advantages in terms of $\text{kg CO}_2\text{ Eq}$ reduction. Indeed, the structure utilizes less of construction materials (mineral ones in particular), however the impact related to the production and processing of those materials is importantly high. In essence, this former point proves that the initial hypothesis raised in Part I, that the material quantity is not a proper metric for the environmental optimization of the structures.

Table 3.5. Comparison of environmental impacts of masonry wall systems

	3D Concrete Printed Wall	Concrete Blocks Parpaing	Cellular Concrete Parpaing	Terracotta Parpaing
Impact category	Space-truss Wall	Kosmo R1 [15] + Insulation [14]	Xella [16] + Insulation [14]	Porotherm [17] + Insulation [14]
1_Climate Change kg CO ₂ Eq	2,86E+01	1,96E+01	3,23E+01	2,80E+01
2_Acidification kg SO ₂ Eq	5,87E-02	6,96E-02	8,51E-02	6,56E-02
3_Eutrophication kg PO ₄ ³⁻ Eq	1,50E-02	3,02E-02	1,55E-02	1,06E-02
4_Air Pollution _m ³	4,90E+01	1,84E+03	3,67E+03	2,82E+03
5_Water Pollution _m ³	2,79E+03	2,26E+01	6,20E+00	4,69E+00
6_Fossil resources depletion _MJ	2,27E+02	1,52E+02	2,58E+02	2,99E+02
7_Abiotic resources depletion kg Antimony Eq	8,92E-07	4,92E-06	4,20E-06	2,65E-05
8_Photochemical ozone formation kg Ethylene Eq	2,67E-03	7,35E-03	3,11E-02	1,18E-02
9_Ozone layer depletion kg CFC-11 Eq	5,55E-07	1,55E-06	2,15E-06	2,96E-06

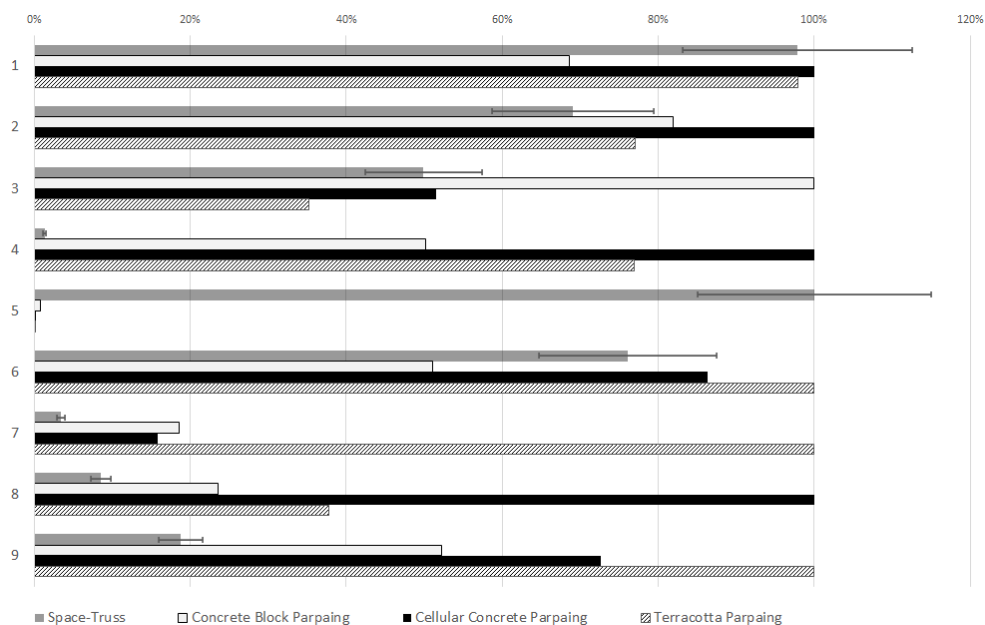


Figure 3.13. Comparison of environmental impacts of masonry wall systems. The whiskers represent the uncertainties related to the life-cycle modelling (inventory in particular).

3.2.4.2. Reinforced concrete

A reinforcement solution for the space-truss studied in the present section was developed by Ducoulombier et al [11]. It consists of an integration of a continuous fiber in the printing filament along the printing direction. As follows, since the fiber is placed unidirectionally in the printed filament, the output material is strongly anisotropic and significantly strengthened in the printing direction.

This strategy provides the printed concrete with an increased tensile strength (in the printing direction), roughly proportional to the embedded fiber volume ratio, and ensures the ductile behavior of the filament again in the printing direction.

The first structural tests on the fibered filaments have shown that for the fibers volume ratio of 1%, the material obtains a strain-hardening behavior with a yield stress of 10 MPa and a tensile strength of 14 MPa, when submitted to the tie stress aligned with printing direction, see Figure 3.14.

It is therefore a naturally fitting reinforcement solution for the space-truss constructive system, as based on the structural behavior combining compression with tension resistance. Hence, the structural model, initially designed and sized for the masonry constructive system, is generalized till the category of the reinforced concrete, with a morphological reorganization of the space-truss on the internal truss and the surrounding frame, reorganizing the redistribution of the internal forces, see Figure 3.15.

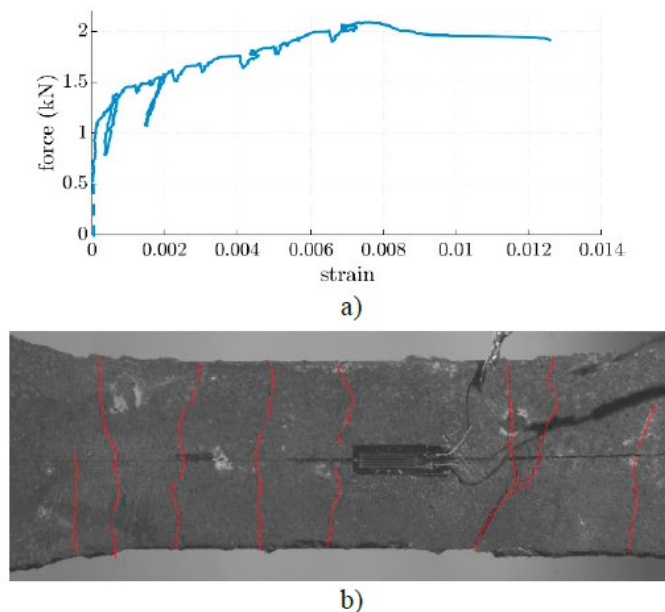


Figure 3.14. Direct tension test of anisotropic concrete: a) Force-strain graph depicting strain-hardening behaviour. Curve jumps are linked with cracking phenomena. b) Video capture of the test specimen at ultimate state showing multiple cracks highlighted in red;
Reproduced from [11]

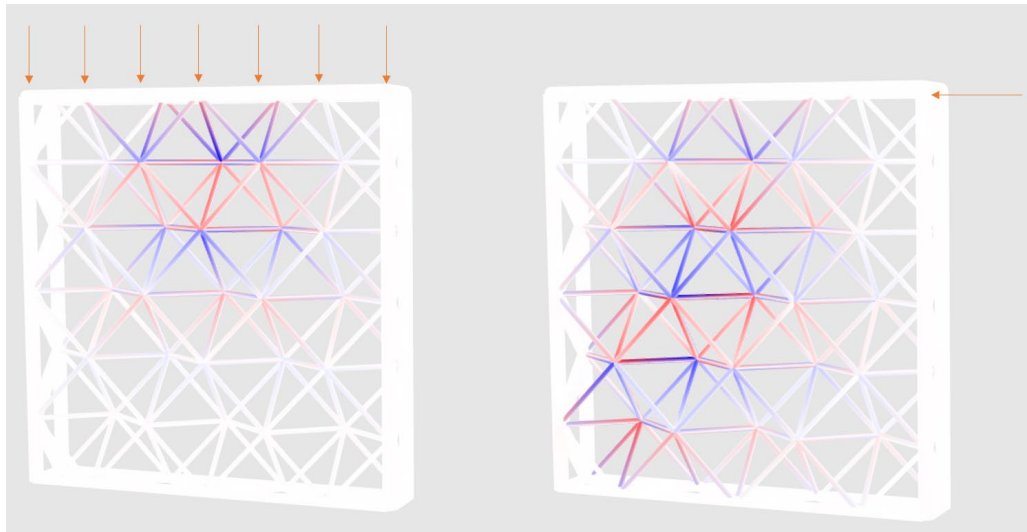


Figure 3.15. Fibered reinforced truss-wall structural concept for vertical (left) and shear (right) loading [18]

The pre-sizing carried out for the space-truss compute the vertical and in-plane shear loads applied of the magnitudes corresponding to the reinforced concrete wall sizing (cf. Eurocode 2) with clamped bottom supports, where the tensile strength in the bars does not exceed 9 MPa, and each member has a buckling factor of at least 300, see Figure 3.15.

Summing up, the introduction of the fiber reinforcement provides the local ductility in the bars and increases linearly the tensile strength of a printed filament. As follows, the overall load-bearing capacity of the space-truss increases significantly, which in its turn, implies an upgrade of a structural category from masonry (Eurocode 6) to reinforced concrete (Eurocode 2). The next section describes an environmental life-cycle assessment of the fiber-reinforced space-truss wall system and compares its overall environmental performance with the traditional reinforced concrete wall.

Life-Cycle Assessment of fiber reinforced Space-Truss

The general settings of the life-cycle study were described in Section 3.2.3. The functional unit of the study is set to the 1m^2 of the space-truss wall with the target performance for thermal resistance of $5,12\text{ m}^2\text{K.W}^{-1}$ (in line with RT2020) and mechanical resistance in line with Eurocode 2. Concretely, the wall dimensions set for the structural sizing were set to 3,3m height and 0,3m width. The vertical charges are 217kN; horizontal charges applied in the support plane are 6,75kN.

Table 3.5 depicts the inventory for the fabrication of 1m^2 of the space-truss wall integrating the continuous fiber reinforcement. The technological integration of the continuous fibers into the printing filament is designed to be low-tech and thus basically consists of hooking the fiber-coils on the printing nozzle and letting gravity do the rest.

Concretely, the process of material extrusion drags the fibers into the printing filament, unrolling the coils while the printing goes.

As a consequence, in terms of life-cycle inventory, only the glass fiber quantity is additionally introduced to the initial set-up, and the rest of components remain unchanged, maintaining the full-bodied french industrial scenario.

Table 3.6. Life Cycle Inventory for 1m² of fiber reinforced space-truss wall

Inventory	Parameters	Details
Concrete	0.054 m3	Table 2.2.
Fiber	1,4 kg	<i>glass fibre production glass fibre cut-off, RER</i>
Robotic Printing Cell	10 minutes 2 pass per ray	Cf. Section 2.4 and Annex 1
Electricity	0.8 kWh	<i>market for electricity, medium voltage FR</i>
Insulation foam	100kg	<i>cement mortar market for cement mortar FR</i>

Table 3.6 compares the results of the LCA study of the fiber-reinforced space-truss concrete wall with the conventional reinforced concrete wall with insulation. The LCA results of the conventional building system come from the EPD file [19] from INIES database [3].

Table 3.7. Comparison of environmental impact of reinforced concrete wall systems

	3D Concrete Printed Wall	Conventional Concrete Wall
Impact category	Fiber - reinforced Space-truss Wall	Pre-wall with integrated formwork and insulation [19]
1_Climat Change kg CO₂ Eq	4,42E+01	1,05E+02
2_Acidification kg SO₂ Eq	9,72E-02	2,82E-01
3_Eutrophication kg PO₄³⁻ Eq	2,17E-02	3,42E-02
4_Air Pollution m³	7,89E+01	6,96E+03
5_Water Pollution m³	3,99E+03	1,27E+01
6_Fossil resources depletion MJ	4,46E+02	8,61E+02
7_Abiotic resources depletion kg Antimony Eq	1,44E-06	3,45E-05
8_Photochemical ozone formation kg Ethylene Eq	4,22E-03	1,23E-01
9_Ozone layer depletion kg CFC-11 Eq	1,08E-06	4,52E-06

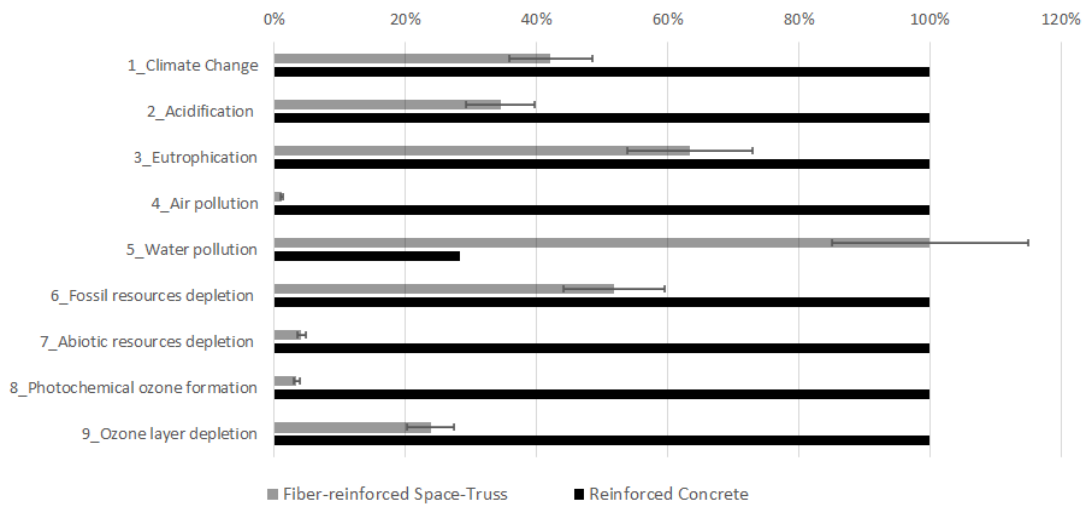


Figure 3.16. Comparison of environmental performance between fiber-reinforced space-truss and traditional reinforced concrete wall. The whiskers represent the uncertainties related to the life-cycle modelling (Inventory in particular).

Figure 3.16. depicts a relative comparison of the environmental impacts of both structural systems, normalized to the traditional reinforced concrete one. The results show that the fiber-reinforced space-truss wall-system outperforms substantially the traditional reinforced concrete wall in all environmental categories, with the sole exception of Water Pollution, where the impact of the space-truss is about 30 times higher. This latter derives from the process-related contribution of the robotic printing, in particular from the nuclear power it runs on within the french industrial context. Otherwise, the impact of the space-truss wall is more than two times lower in the categories of Climate Change, Acidification, Eutrophication, Fossil Resource and Ozone Layer Depletion. Furthermore, in such categories as Air Pollution, Abiotic Resources Depletion and Photochemical Ozone Formation, the impact of the space-truss wall stands for less than 5% of that of conventional reinforced concrete wall system.

In general outline, even if the Eurocode 2 comparison is accomplished with the pre-sized structural dimensions of the space-truss system, the magnitude of potential improvement within all environmental categories combined shows that it may be a promising solution for the environmental melioration of the concrete structures. More detailed further studies are needed to confirm this thesis.

3.2.5. Approach to the End-of-Life

The current normative framework for concrete recycling practice is overlooked in this section. The current recycling practice of concrete elements consist mainly in crushing them into the second-handed aggregate usually used in the road's construction. It is a highly laborious and energy-intensive process that usually ends up producing more of an environmental burden than the virgin extraction of gravel [20]. In this context, the absence of metal reinforcement or large aggregates can be seen as a certain recycling flair, as excludes all those laborious processes of sorting and separation of concrete from armature, implying that the structure can be simply and directly crushed.

An environmental evaluation of recycling is usually covered by the allocation principle in the LCA methodology [21] and is a very polemic topic amongst LCA practitioners [22]. The allocations deal with the partitioning of environmental impact/benefits between various co-products of a system. In the case of reuse or recycling, the allocations deal with the impact/benefits partitioning between the successive life-cycles of the system. In other words, in the case of recycling the structure from the first life-cycle acts as a resource deposit for the structure of the second life-cycle, implying the need of a redistribution of the impact coming from the first life-cycle to the second as well as of the benefits of the second life-cycle with the first. The allocations would hereby frame that redistribution.

The current industrial practice considers an incoming material for recycling as a scrap and thus attributes a zero value for its embodied impact. Therefore, it would be only the processes deployed to recycle that scrap into the new product that will compose the environmental burden of the recycled content. As follows, the first life-cycle keeps entirely the burden related to the primal material production and no burden for the end-of-life phase. The recycled content acquires zero burden from the virgin material processing but keeps an entire impact of the recycling processes. To sum up, no impact needs to be attributed to the end-of-life phase of the space-truss masonry wall, considering the recycling scenario.

3.2.6. Conclusions & Perspectives 3.2

The present analysis considers the space-truss system as a structural concept enabling the material saving using 3D Concrete Printing rather than a specific industrial solution. Therefore, a general conclusion can be drawn hereby that the environmental profile of 3D Printed concrete structures is strongly determined by the process-related impact, representing around 10% of the overall impact. Thus, it is not only the material quantity that would define an environmental impact of 3D Concrete Printed structures but also the way that material is deposited.

As a masonry concept, the space-truss does not bring any tremendous progress from environmental standpoint compared to traditional thermo-mechanical systems. The space-truss only performs advantageously in the category of Abiotic Resources Depletion, as it consumes very little of mineral materials. Nevertheless, within the Climate Change indicator, the space-truss system does not reach an optimal performance, despite its great material savings. From the sensitivity study it can be understood that it is in part related to the process-related burden coming from the robotic printing technology. As follows, as far as 3D Concrete Printed structures are concerned, it is not only the material quantity that would define its environmental impact, but also the way that material is deposited. In other words, the material quantity is not a proper metric for the environmental optimization of structures, 3D Concrete Printed structure in particular.

An important impact reduction potential can be outlined within the reinforced concrete perspective, studied with a continuous fiber reinforcement hypothesis for the space-truss. This latter brings a great impact decrease in all environmental categories compared to the traditional reinforced concrete wall. However, regarding the impact related to the fiber reinforcement itself, its contribution to the Climate Change category represents around 10% of that of concrete with only 1% of volume ratio of the embedded glass fiber. Thus, with an increase of the containment ratio of embedded fiber, the impact of reinforcement can rapidly exceed the one of concrete. Anew, the optimal relation of those two from the environmental standpoint may pertain to further investigations, using the characterization data provided in the present work. As in the case of masonry, the decrease of environmental impact of the reinforced space-truss system is not proportional to its structural mass and remains highly influenced by the robotic construction processes. As follows, once again, the material quantity is shown to be a wrong metric for environmental optimization of the 3D Concrete Printed structures.

The present results have been obtained with assumptions on the robotic printing process specific to the french industrial scenario, in particular to its highly decarbonized electricity mix, with one of the lowest Climate Change impact in Europe, see Figure 2.9 and Figure 3.9. The sensitivity study has demonstrated the importance of this parameter within the overall environmental impact of the final structure. As follows, even with a hypothesis of world average electricity mix that would double the contribution of robotic construction processes in the Climate Change category, the space-truss would still perform beneficially within the reinforced concrete perspective. However, it is doubtful that it will do so as a masonry concept.

Finally, regarding the material design, it has been mentioned before that the reduction of the cement quota in the material mix would always bring some substantial environmental improvements to any concrete element (cf. Section 1.3 and Section 2.3). However, as it was

outlined in the conclusion of the filament-based analysis, the modification in the material mix may entail a changing in its processing requirements, in particular the power consumption of pumping & mixing process (constituting half of the operational process-related impact). In other words, a less liquid material mix may cause a higher power consumption for its processing and as a consequence a higher process-related impact. As follows, a straightforward solution of the material replacement with a less impacting low-carbon alternative, may involve the increase of the process-related impact, which means that no absolute conclusion can be drawn at the present stage regarding the optimal relation of material-process impact partitioning at the scale of 3D Concrete Printed building system.

Nevertheless, this former point as well as a global environmental optimization of 3D Concrete Printed building systems can now be investigated using the impact model proposed in this work and described in Part II.

Industrial relevance of the Space-Truss Wall system

In closing, let us take a closer look at the industrial relevance of the space-truss wall solution from an environmental standpoint.

First of all, the accomplished LCA study has allowed us to delimit the environmental interest for the space-truss system applications, pointing out its irrelevance within masonry framework and its strong competitiveness within reinforced concrete perspective.

This conclusion has been drawn uniquely from the comparison of mechanical and thermal performances of the systems, when in reality, the design and sizing of the current industrial solutions comprises a much wider range of performances.

For example, the sizing of the vertical load-bearing elements, e.g. walls and columns, is usually defined by the buckling and therefore by the stiffness of the structure, rather than by its compression strength. Thus, it is basically the main reason why the ultra-high-performance concretes have not replaced the conventional C25/30 concretes, as despite the substantial difference in their compression strength, 100-120 MPa versus 25-30 MPa, their Young modula are quasi similar. As follows, even when using the ultra-high-performance concrete in a vertical load-bearing concrete wall, its buckling stiffness will thus be ensured by the inner rebars. According to the current regulations for the sizing of the reinforced-concrete structure, the rebars need to be covered by an additional exterior layer of concrete sized to protect the metal rebars from the oxidation and rustiness.

Thus, there is a systematic non-structural use of concrete in reinforced-concrete structures for the rebars protection, which will not be a case in the fiber-reinforced space-truss wall. Furthermore, the overall stiffness of the wall, based on the space-truss behavior, will be significantly higher than the one of conventional solution.

Furthermore, considering the great reduction of the surfacic weight of the space-truss compared to its conventional reinforced-concrete analogue, 135 versus 309 kg.m⁻², it may have an indirect positive impact on the sizing of surrounding structures, when embedded in a multi-story building for instance, as it was previously stated in [7].

Finally, the currently absent data on the durability and fire-resistance of printable concretes may also bring some important additional elements for the further evaluation of environmental and industrial relevance of the 3D Concrete Printed structures. Similarly, the acoustic performance can be integrated into further studies.

The further analysis on a building scale including the additional performance data may pertain to the further investigations.

Bibliography of Part III

- [1] « EN 15804:2012 Sustainability of construction works - Environmental product declarations - Core rules for the product category of construction products ».
- [2] « ecoinvent ». <https://www.ecoinvent.org/> (consulté le oct. 19, 2020).
- [3] « Construction products (FDES) – INIES ». <https://www.inies.fr/construction-products/> (consulté le avr. 20, 2020).
- [4] I. Agustí-Juan et G. Habert, « Environmental design guidelines for digital fabrication », *Journal of Cleaner Production*, vol. 142, p. 2780-2791, janv. 2017, doi: 10.1016/j.jclepro.2016.10.190.
- [5] I. Agustí-Juan, F. Müller, N. Hack, T. Wangler, et G. Habert, « Potential benefits of digital fabrication for complex structures: Environmental assessment of a robotically fabricated concrete wall », *Journal of Cleaner Production*, vol. 154, p. 330-340, juin 2017, doi: 10.1016/j.jclepro.2017.04.002.
- [6] H. Alhumayani, M. Goma, V. Soebarto, et W. Jabi, « Environmental assessment of large-scale 3D printing in construction: A comparative study between cob and concrete », *Journal of Cleaner Production*, vol. 270, p. 122463, oct. 2020, doi: 10.1016/j.jclepro.2020.122463.
- [7] R. Duballet, O. Baverel, et J. Dirrenberger, « Space Truss Masonry Walls With Robotic Mortar Extrusion », *Structures*, vol. 18, p. 41-47, avr. 2019, doi: 10.1016/j.istruc.2018.11.003.
- [8] R. Duballet, « Building systems in robotic extrusion of cementitious materials », Université Paris Est, Paris, France, 2019.
- [9] R. Duballet, O. Baverel, et J. Dirrenberger, « Classification of building systems for concrete 3D printing », *Automation in Construction*, vol. 83, p. 247-258, nov. 2017, doi: 10.1016/j.autcon.2017.08.018.
- [10] F. P. Bos, Z. Y. Ahmed, E. R. Jutinov, et T. A. M. Salet, « Experimental Exploration of Metal Cable as Reinforcement in 3D Printed Concrete », *Materials*, vol. 10, n° 11, p. 1314, nov. 2017, doi: 10.3390/ma10111314.
- [11] N. Ducoulombier, L. Demont, C. Chateau, M. Bornert, et J.-F. Caron, « Additive Manufacturing of Anisotropic Concrete: a Flow-Based Pultrusion of Continuous Fibers in a Cementitious Matrix. », *Procedia Manufacturing*, vol. 47, p. 1070-1077, janv. 2020, doi: 10.1016/j.promfg.2020.04.117.
- [12] D. Asprone, C. Menna, F. P. Bos, T. A. M. Salet, J. Mata-Falcón, et W. Kaufmann, « Rethinking reinforcement for digital fabrication with concrete », *Cement and Concrete Research*, vol. 112, p. 111-121, oct. 2018, doi: 10.1016/j.cemconres.2018.05.020.
- [13] Lafarge, « Airium. L'isolation autrement. La mousse minérale isolante ». <https://www.airium.fr>
- [14] S.-G. ISOVER, « FDES_GR32 Kraft / Laine de verre 180 mm R=5.6 K.m2 / W ». Inies database, déc. 2015.
- [15] ALKERN, « FDES_Block Kosmo R1 ». Inies database, oct. 2019.
- [16] Xella, « FDES_Mur en maçonnerie de blocs Ytong COMPACT ». Inies database, déc. 2019.
- [17] Wienerberger BORO THERM, « FDES_Briques Porotherm de type A ». Inies database, sept. 2018.
- [18] K. Kuzmenko, R. Duballet, N. Ducoulombier, N. Roussel, et A. Feraille, « On Environmental Performance of 3D Concrete Printed Structures. A Case-study of Space-Truss Wall System », In progress.
- [19] CERIB, « FDES_Mur a coffrage et isolation intègres (avec béton de remplissage, CEM III/A et isolant PSE) ». Inies database, août 2019. [En ligne]. Disponible sur: N°7-415:2019
- [20] F. de Larrard et H. Colina, *Concrete Recycling: Research and Practice*, 1st Edition. CRC Press, 2019.
- [21] O. Jolliet, M. Saadé-Sbeih, S. Shaked, A. Jolliet, et P. Crettaz, *Environmental Life Cycle Assessment*, 1st Edition. CRC Press, 2016.

- [22] K. Kuzmenko, C. Roux, A. Feraille, et O. Baverel, « Assessing environmental impact of digital fabrication and reuse of constructive systems », *Structures*, juin 2020, doi: 10.1016/j.istruc.2020.05.035.

Part IV
Conclusions & Perspectives

4.1. Conclusion

The ongoing development of 3D Concrete Printing technology is currently associated with the boons of the mass-customization industry, with the potential of productivity, time and cost optimization, as well as with the sustainable potential of the practice, leaning on a largely discussed capacity of the smart and rational material deposition offered by additive manufacturing. This latter vision for the environmental performance of the practice has been investigated in the present work by the means of the Life-Cycle Assessment method.

Amongst the variety of the technological set-ups available today in the field, a specific 3D Concrete Printing technology has been studied in the present work, referred to as an extrusion-based printing built upon a 6-axis robotic arm. A particular focus on the impact coming from the robotic printing process has been carried out along the whole study.

A model of environmental impact of 3D Concrete Printing has been proposed and the impact characterization has been carried out. Concretely, the impact related to the robotic construction processes has been divided in two categories: embodied and operational. The embodied impact is related to the production of the robotic hardware and to the rest of printing cells components and was evaluated by the means of the LCA model assembled using the EcoInvent database. The operational impact is related to the power demand of the printing process and was characterized with an experimental measurement.

Within the present hypothesis for the life-cycle assessment study, both impacts are of the similar magnitude when normalized to the duration of working.

Focusing on the operational impact, the experimental measurements of the power demand of the printing process have demonstrated an equal contribution share between the robotic arm and the material pumping & mixing process. Therefore, the operational process-related impact is not only defined by the quantity of mechanical energy needed to transport the mass of the robotic arm, but also, and probably dominantly, by the energy associated with the pumping & mixing process extended through the whole printing duration.

Concretely, considering the printing section of 1cm^2 and the printing speed of 200 mm/s the time needed to deposit one cubic meter of concrete would equal to 13,9 hours, which means 13,9 hours of continuous pumping & mixing. As follows, it is not only the technological set-up of the printing cell that would define the process-related impact but also, and probably majorly, the material type used within that process.

In other words, the power consumption of the pumping & mixing process is directly linked to the rheological properties of the processed material, such as yield-stress, viscosity, etc. Therefore, the low power consumption measured for this position ($1,5\text{ kW}$) can be explained by the particularly liquid nature of the printable concrete used in the studied system, with the yield stress $\sim 100\text{ Pa}$. The impact of the operational phase may thus increase significantly if the system functions with the less liquid materials (for example the materials containing lower cement portion and higher share of aggregates, idem for clay- and earth-based materials). The investigation of the evolution of the process-related impact in function of material rheology may pertain to further research.

In the meantime, the research of the optimal relation between material- and process-related impacts can be carried out using the impact model described in Part II.

The model of environmental impact proposed in this work has been applied on two case-studies in order to provide the synthesis of all characterized impacts on the scale of material and on the scale of a building system. The following outcomes have been outlined.

In the first place, at the scale of one printed filament, the supplementary process-related impact represents around 13% in the Climate Change category and is directly linked to the printing resolution. The process-related process will be strongly defined by the life-span of industrial equipment and by the type of the operational power. In other terms, exactly like in the case of an electric car, the same technology will not have the same impact in different geographic areas. Typically, most present simulation have been accomplished with the world average electricity mix, however, considering that the planet's construction site of the future might be the African continent (cf. Figure 1.1) where the coal-fired power is prevailing²⁹, the impact of the 3D Printing process may rise at least twofold therein.

Scaling up the analysis to the building system, case-studied hereby with the space-truss wall system, this supplementary process-related impact can potentially get compensated by the material savings resulting from the smart and rational material placement. The impact reduction has been obtained with a series of sensitivity studies on the process-related impact, using the previously characterized data of its environmental impact. In other words, the environmentally efficient character of the structure has been mainly obtained due to the optimization of its process-related impact and therefore, as far as the 3D Concrete Printed structures are concerned, it is not only the material quantity that will define their environmental performance, but also the way that material is deposited. Furthermore, the material quantity is proven to be a wrong metric for the environmental optimization of the 3D Concrete Printed structures.

The results of the LCA study performed in the present work allow to calculate the environmental impact of any 3D Concrete Printed object. Furthermore, the coefficients of material and process-related impacts, characterized in Part II, allow the further integration of environmental data into design and optimization studies.

²⁹ <https://www.iea.org/countries/south-africa>

4.2. Perspectives

4.2.1. Towards an Industrial Deployment of 3D Concrete Printing Technology

As it was mentioned in the beginning of this manuscript (cf. Section 1.2.2), the practice of additive manufacturing with cementitious materials has emerged in academic circles with the work of Pegna [14] (broadly recognized as a founder of the practice) and followed with the development of various printing techniques and applications. Initially, Pegna seems to avoid the metaphor of the “printer” [15] and mainly builds-up his vision for this technology on its free-form potential, intrinsic in his opinion to the formwork abolishment.

Furthermore, he describes his invention as a “*new approach to a masonry*”, instead of going for the generalization of concrete structures, which naturally implies itself by the material analogy. Indeed, the conceptual relevance of the 3D Concrete Printing within the masonry theoretical framework has been outlined by a series of academic works [16], [17] following Pegna's research. The formal analogy between 3D Printing and masonry is depicted on Figure 4.1, and their normative coherence has been described in Section 3.2.2.

The current technological obstacle preventing the practice to operate within the category of reinforced concrete addresses mainly the reinforcement integration into the 3D Printed concrete. Thus, considering the current active development of the various technological solutions for that question (cf. Section 3.2.2 and Section 3.2.4.1), the problem may be solved in the following years. Ultimately, both solutions will settle their structural and normative validity and thus some additional arguments may enter the debate on the application adequacy.

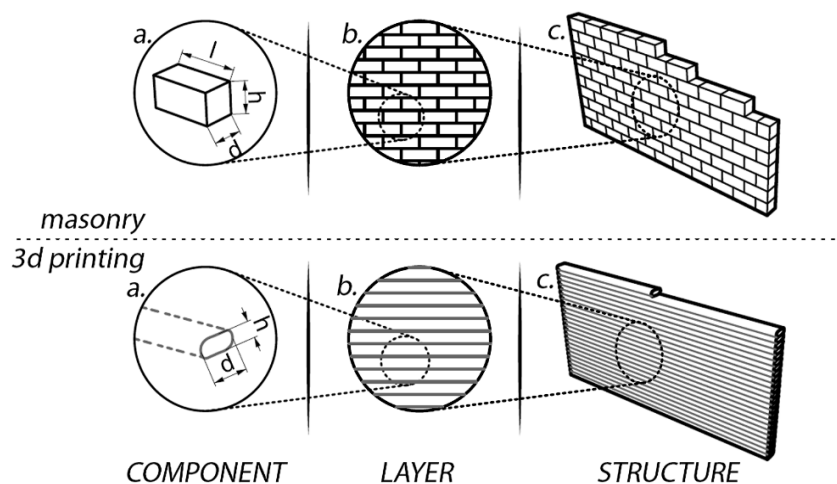


Figure 4.1. Masonry wall vs. 3d printed wall at the three different scales.
Reproduced from [17]

The present work has provided insights into the environmental relevance of both solutions, pointing out a limited interest of the masonry framework and strong potential of the reinforced concrete perspective (cf. Section 3.2.6)

To sum up, besides the conceptual difference addressing the structural category (masonry or concrete), the intrinsic distinction of both solutions implies two different normative frameworks (Eurocode 6 or Eurocode 2), reinforcement consideration, levels of mechanical resistance and ultimately two different industrial adoptions of the technology in the sector.

Thus, zooming onto the ongoing industrial adoption of the 3D Concrete Printing, since *circa* 2014, a series of construction companies have announced their technological integration (XtreeE³⁰, CyBe³¹, Bruil³², Cobod³³, Total Kustom³⁴, ApisCor³⁵, WinSun³⁶) and in the following years, many announcements were made on the matter of productivity, time and cost optimization.

In fact, for a long time, the industrial adoption of 3D Concrete Printing technology has been closely associated with an amelioration of industrial efficiency of construction process (i.e. productivity, time and cost), in large part ignoring the morphological improvements potential. In the end, not only little evidence of the productivity increase have been collected from those claims, but also, that supposedly more optimized production consisted mainly of the printing close to conventional building and elements, with no particular or notable progress.

Towards 2019, it seems that a consensus has been achieved (at least in academia), agreeing that this technology will mainly be of interest if it can enable some superior performances in building elements [15], [18], [19], [20]. The relevance of this approach has been partly confirmed by the first environmental study in the field [19], reinforcing in that way a sustainable vision for this technology that was, before that work, mainly based on material savings potential.

The present work has shown that the material quantity will not be a sufficient metric for the environmental optimization of the 3D Concrete Printed elements; the model of environmental impact developed in the present work can be used to address that question.

In closing, regarding the industrial context in which the 3D Concrete Printing technology is deployed, it is possible to suggest that the prefabrication framework may allow the most adequate integration of the previously listed objectives. In other words, the current on-site printing techniques (CyBe, Cobod, ApisCor, WinSun), has broadly demonstrated their capacity to produce close to conventional, barely more efficient, and definitely less sustainable houses in eventually faster way. Thus, either by intention or rather as a consequence of the on-site set-up, it does not seem possible to go towards the principle of smart and rational material placement when operating with a large-scale gantry limited to the orthogonal trajectory. As follows, despite the limited printing area of the robotic printing cells based on 6-axis robotic arms (the

³⁰ <https://www.xtreee.eu/>

³¹ <https://cybe.eu/>

³² <https://www.bruil.nl/3dprinten>

³³ <http://cobod.com/>

³⁴ <http://www.totalkustom.com/>

³⁵ <https://www.apis-cor.com/>

³⁶ <http://www.winsun3d.com/En/About/>

biggest robot available in the ABB catalog provides a printing area of 25m²), being placed into the prefabrication context, they can provide much larger potential for the morphological amelioration of the building elements, by taking advantage of 6 degrees of liberty for material placement. Furthermore, the industrial sequence based on numerical controlled machine as 6-axis robotic arm, may finally happen the postmodern dream of mass-customization construction, i.e. the serial production of non-standard elements (cf. Section 1.1.2).

The current market of the prefabricated concrete elements in France represents almost the third part of the global national concrete market. In detail, by the year of 2019, the annual french market of prefabricated structural components for building and civil engineering was estimated to be around 1,75 billion euros³⁷, when the total national market for the ready-mix concrete was around 4,2 billion euros³⁸, both having performed the growth of 200% since the 2000s. In parallel, the national french market for the prefabricated buildings have performed a total growth of 400% since the 2000s and currently represents around 185 million euros³⁹. Thus, considering the ongoing growth of the prefabrication concrete market hand by hand with the growing interest for the 3D Concrete Printing technology, the potential merge of those two may perform a substantial efficiency improvement in the sector. Concretely, drawing upon the conclusions of Part III, the impact reduction potential of the optimized 3D Concrete Printed elements is almost twofold in the Climate Change category for the reinforced concrete perspective.

As follows, scaling up those gains to the industry-wide scale, the impact reduction can be expected proportionally. However, the efficiency gains in industries are never proportional, as in the industry-wide scale the gains-related technology tends to increase the overall consumption instead of decreasing it, provoking in that way a so-called Jevons paradox, largely known as the *rebound effect*.

The following section provides a brief theoretical overview of these notions, putting the 3D Concrete Printing technology into this historical perspective of the controversial nature of industrial efficiency.

4.2.2. Jevons Paradox

The present discussion emerges from the physical measurement of the power consumption of the robotic printing cell, in particular of the low values those measurements have provided compared to the initial analytical assumptions (cf. Section 2.4.2). In fact, the robots consume very little of power. Concretely, a 5-tonnes thing travels 10 kilometers to deposit one cubic meter of material and consumes an equivalent of a home Hoover to do so⁴⁰, which means that the energy consumption of a home 3D Concrete Printing plant is comparable to the one of an average Parisian household⁴¹. Hence, this counterintuitive result raises some important

³⁷<https://www.nationmaster.com/nmx/timeseries/france-sold-production-of-prefabricated-structural-components-for-building-or-civil-engineering-of-cement-concrete-or-artificial-stone>

³⁸<https://www.nationmaster.com/nmx/timeseries/france-sold-production-of-ready-mixed-concrete>

³⁹ <https://www.nationmaster.com/nmx/timeseries/france-sold-production-of-prefabricated-buildings-of-concrete>

⁴⁰ An average power consumption of a home Hoover is 3-4 kW.

⁴¹ An average cost for the EDF subscription for 50 m² condo in Paris is 80 euros/month. The cost of one kWh in France = 0,17 euros, thus by paying 80 euros per month an average energy consumption may be around 470 kWh (80 / 0,17 = 470,588); XtreeE prints 8 h/day, 4 days/week which equals to 4kW*8h*4j*4 = 512 kWh/month.

questions on the general state of things of the broad deployment of construction automation. Putting it differently, an impending conclusion drawing itself naturally down, at the present stage, is that within the material-savings approach enabled by robotic printing, the environmental improvement potential for the concrete industry is at least twofold.

Concretely, if the impact reduction represents at least 50% at the scale of a building system, then it is possible to assume the industry-wide improvements would be of the same order.

However, if the former conclusion was true, then the automobile industry would already achieve a close to zero impact instead of progressively increasing it year after year [1]. Indeed, along technological advancements, the fuel consumption of a car engine has been constantly decreasing, whereas the overall fuel consumption on the industry-wide scale is *au contraire* constantly increasing. The phenomenon is only partly relevant to the general rise of the car number worldwide, explained by the growth of affordability of market size. Otherwise, observing a single car fuel consumption per one traveled kilometer versus the overall distance traveled by that car during its life-time, both act in inverse proportion when an efficiency gain occurs for the first. As follows, a car that consumes less fuel per kilometer, intrinsically will travel more kilometers over its life-time, repealing in that way the first-placed environmental gains.

Idem for the lightning devices [2], computers and the current (for the time of writing) polemic on the 5G internet deployment in France, where again, by dividing by 4 the energy consumption per unit of transmitted information [3], the overall information flow per device as well as industry-wide is expected to rise tenfold [4].

In other words, there is a kind of inverse relation between the unit piece efficiency increase and the overall situation at the industry-wide scale, that systematically cancels the expected resource use decrease.

Back to 1886, in the beginning of the industrial era, the british economist William Stanley Jevons was first to suggest the possibility of a fall out of that kind of paradox. Concretely, in his book *The Coal Question* [5], Jevons put forward a theoretical assumption that by optimizing the use of a given resource, coal in his case, it will not necessarily imply the decrease of the general use of that resource:

“It is wholly a confusion of ideas to suppose that the economical use of fuel is equivalent to a diminished consumption. The very contrary is the truth... Every improvement of the engine, when effected, does but accelerate anew the consumption of coal “ (Jevons, 1886; pp. 140, 152–53). [6]

The Jevons’ inference is inductive and based on a historical correlation between an increase of the coal consumption and the technological advancements of industries, that is only in minor part justified by the population growth.

“In round numbers, the population has about quadrupled since the beginning of the nineteenth century, but the consumption of coal has increased sixteen-fold, and more” (Jevons, 1886, pp. 196) [1]

In summary, Jevons was arguing that an increase of efficiency will inevitably bring to an increase of consumption, producing a so-called *backfire* largely known today as the *rebound effect*.

The rebound effect is thus an offspring term for the Jevons paradox taking place specifically within the energy efficiency actions at the macro level. It was independently re-discovered by two economists, Leonard Brookes and Daniel Khazoom, working on the energy demand models after the first oil crisis. Thus, after the years of ignorance of Jevons announcement of the efficiency paradox, Brookes developed a series of coherent arguments in its favor alongside with a fierce critic of the energy-efficiency politics of the state (Brookes 1978, 1984, 1990a/b, 2000, 2004) [7]. His work has immediately restored the polemics on the subject matter and received some furious critiques [8], [9], [10], to which Brookes delivered a complete set of solid come-backs [11], [12].

The debate was in part concluded with a work of another british economist Harry Saunders providing the following statement that he named *the Khazoom-Brooks postulate*, where “*with fixed real energy prices, energy-efficiency gains will increase energy consumption above what it would be without these gains*” (Saunders, 1992) [7]. Essentially, Saunders shows that the Jevons Paradox is inexorable for all industrial efficiency-improvements occurring within the economic framework based on the neoclassical growth theory [13].

In other words, Saunders basically outlines the fact that if an industry seeks some resource-efficiency optimizations hand by hand with the productivity increase, the backfire is inevitable.

In the end, as no other industry can be cited as an example of the non-occurring of the Jevons Paradox, then there is no empirical grounding to suppose that it will not be the case for the concrete construction embracing the 3D Printing technology.

4.2.3. Rebound effect of 3D Concrete Printing Technology

In the previous section, we have outlooked the potential industrial deployment of 3D Concrete Printing technology, describing the current directions as well as our opinion on those directions, based on the outcomes of the present work. Yet, our position being clear, the fine printing of more efficient building elements with the performances comparable to reinforced concrete, produced in prefabrication context, does not seem to dominate the current practice development. Nevertheless, let us imagine the best scenario for the industrial adoption of the 3D Concrete Printing technology and draw the industry-wide picture of its environmental profile based on the results of the present work.

In our opinion, the best scenario would consist in the generalization of the optimized construction elements (similar to those analyzed in this work, see Section 3.2). As follows, the concrete poured worldwide in *gargantuesque* quantities finally gets deposited in a smart and rational way by the hint of robotic additive manufacturing reducing at least twofold the worldwide intensity use of concrete for construction purposes.

For reminder, the current statistics of the yearly concrete consumption represents roughly 35 billion tonnes (cf. Section 1.3). Thus, considering the current population growth and the

associated need in terms of new construction, the intensity use of concrete may remain the same or even increase in the next 40 years.

Furthermore, according to Van Damme, the current intensity of the concrete use worldwide is in a big part due to the infrastructure network, rather than to the building sector. Concretely, *“a medium size country like France, for instance, with a mainland area of 550,000 km² (roughly, a pentagon with 600 km long sides) has built more than 1 million km of two lane roads and close to 20,000 km of four- or six-lane freeways or national highways, almost exclusively with asphalt pavement. More than 260,000 bridges have been built to avoid crossings. The operating railway network has a total length approaching 30,000 km. Half of it is electrified and 2600 km are devoted to high speed lines operating at more than 300 km/hr. More than 1000 km of road and rail tunnels have been dug. The waste- and rainwater network, made essentially of large diameter concrete pipes, has an estimated length of 250,000 km whereas the fresh water network is about four times longer. Fifty-eight nuclear reactors (approximately one per million inhabitants) deliver about 75% of the total electric power”*.

Thus again, considering the current population growth and the associated future need for infrastructures along with the maintenance and renovation needs of existing ones, the intensity use of concrete may remain of the same order.

In terms of environmental impact, the main environmental impact category of concrete material is the Climate Change. In other words, the concrete industry rather pollutes the atmosphere, than oceans or soils. The Climate Change impact of concrete is defined by the cement portion in the mix-design and therefore currently represents around 300 kg CO₂ Eq per cubic meter of conventional C25/30 concrete and around 500 kg CO₂ Eq per cubic meter for printable concretes (cf. Section 2.3). The current impact coming from conventional construction techniques is around 2% in the Climate Change category and rises up to 10-15% with the introduction of robotic printing. This latter however promises some substantial material savings within the construction elements, which means that the overall environmental gains may remain positive, again from the Climate Change perspective (cf. Section 3.2.6).

All considered, let us now include into discussion the associated arguments on the deployment of construction automation, in particular those of the productivity increase along with time and cost optimization. In practical terms, these latter mean more intense and rapid production of constructive elements at lower price. As follows, even if those constructive elements hold henceforth a twice lower environmental impact but get produced in twofold quantity, then at the industry-wide scale the overall impact would remain the same as before those efficiency gains, when normalized to the unit of time. In other terms, by producing two or three times more elements, the impact of which is twice or thrice lower, the overall hourly or yearly impact of the automated concrete construction industry may remain unchanged if not increased.

Now let us zoom closely on those 10-15% of supplementary impact in the Climate Change category related to the robotic printing of one cubic meter of concrete. From the contribution analysis, depicted on Figure 3.3., it can be understood that half of that impact is related to the production of robotic hardware, however the other half is entirely related to the operational energy demand of that process. From experimental measurements, it can be precisely stated that in order to deposit one cubic meter of concrete with a flowrate of 7,2E-2 m³/h, the amount of

energy needed is equal to 55,6 kWh. Therefore again, that seemingly harmless augmentation of the amount of energy needed for the production of a unitary piece, that can be compensated by the material savings in terms of kg CO₂ Eq, may have a completely different outcome at the industry-wide level.

In concrete terms, even if the automation of the concrete deposition will indeed divide the yearly use of concrete by two, i.e. from 35 billion tonnes to 17, the overall energy amount needed to deposit those 17 billion tonnes would be approximately 389,2 billion kWh per year⁴². Except, considering the phenomenon of the Jevons paradox, that decrease of the yearly consumption intensity to 17 billion tonnes is very doubtful, due to the rebound effect, and therefore the real consumption of the concrete construction may remain at least 35 billion tonnes per year with the energy amount associated to its automated processing of around 778,4 billion kWh per year.

In order to give an order of magnitude of that number, based on IEA⁴³ statistics [21], the yearly energy consumption of France is around 470 billion kWh, the one of Switzerland is around 63 billion kWh and the one of Denmark is 32 billion kWh. Therefore, even with the hypothesis of a totally decarbonized electricity mix of the future, the need in terms of supplementary infrastructure for the electricity production presents to be tremendous and may represent an equivalent to the current industrial park of France and Italy combined. Furthermore, within the present industrial set-up and considering the pollution associated with the world average electricity mix, those 778,4 billion kWh would represent around 583,8 billion kg CO₂ Eq yearly.

This previous and with no doubt too coarse conclusion at the present stage, however, addresses only the concrete material and does not include all the impact related to the processing of additional materials currently under development for the 3D Printing, e.g. clay- and earth-based. It was mentioned in Conclusion 3.1. that at the scale of one printed filament the overall environmental impact may be dominated by the robotic construction process, due to the very low embodied impact of those materials. Furthermore, the 3D Printing of those materials will barely perform the mechanical strength comparable to the reinforced concrete structures, which means that they would probably be inscribed into the masonry framework, shown to have a very limited environmental interest (cf. Conclusion 3.2). As follows, at the industry-wide scale, the automation of those construction techniques may represent some important quantities of energy consumption, as it was demonstrated on the case of concrete, while no particular interest has been found for the automation of earth- or clay-based construction processed, in the first place.

In order to study properly the industry-wide implications of the global deployment of 3D Concrete Printing technology, further research is needed within the methodological framework of the Consequential Life-Cycle Assessment. This latter deals with the potential consequences of the technical changes and the global environmental implications of the industrial modifications. Therefore, the general environmental profile of the 3D Concrete Printing technology remains to be studied at the industry-wide level with the consequential method. The inventory provided in the present work (cf. Annex 1 and Annex 2) can be used for those studies.

⁴² The volumic mass density of concrete is 2400kg/m³, thus 17 billion tonnes of concrete are equal to around 7 billion cubic meters of concrete. Considering 55,6 kWh/m³ characterized in Section 2.4.2.1, the energy amount needed to deposit 17 billion of tons of concrete would represent 389,2 billion kWh.

⁴³ <https://www.iea.org/>

Apart from the consequences related to the increase of the energy demand coming from the robotic printing process, there is also the production of the robotic hardware itself, the impact of which is blatantly present in all environmental categories, see Figure 3.3. As it was mentioned in the conclusion 3.1, the evoked pollution shift needs to be normalized to the global impact of other industries in order to understand its magnitude.

Nevertheless, considering the previous argumentation on the effects and paradoxes occurring when scaling up to the industry-wide level and thus imagining the quantity of robotic hardware needed to be produced in order to ensure that industrial shift towards the construction automation, then its impact may rapidly become comparable to the one of the automobile industries for example. Again, this hypothesis should be studied within the framework of the consequential LCA and can be grounded on the inventory provided in the present work (cf. Annex 1).

4.2.4. Sustainable potential of construction automation

Apart from the architectural vision of the construction automation usually associated with the non-standard production for its complex and parametric forms, the present work has provided some insights into the sustainable profile of construction automation with a case-study of 3D Concrete Printing technology.

A primal conclusion of this work outlines the importance of environmental impact coming from the digital construction process that prompts the impact transfer and the pollution shift into the environmental balance of a concrete element. Thus, despite being focused on the singular construction technique, this conclusion can be generalized to any construction material processed with digital fabrication, e.g. timber, steel as well as clay, earth and stone. In other words, the burden related to the production of robotic hardware and to the operational energy will inevitably provoke the modifications of environmental profile of the final element, and therefore these former must be taken into account when addressing the environmental performance of those elements. In other words, exactly as in the case of 3D Concrete Printed structures the material quantity may not be a proper metric for environmental optimization of structural systems produced with automated construction processes.

Still, in general outline, the construction automation does provide an efficiency increase, from industrial as well as from environmental standpoint and does present itself as a very promising strategy for the environmental improvement of constructive systems and individual buildings. Yet, the generalized deployment of construction automation may have a powerful backfire coming from the rebound effect always occurring in industries improving their efficiency (cf. Section 4.3).

This later, being situated long way out of the scope of the individual exercise usually presented in front of an architect and/or an engineer may fairly be considered as a political problem rather than an architectural one. Therefore, if the present study has been accomplished within the boundaries of a single element and has provided some data for design and production-oriented exercise, the consequential LCA studies carried out on the industry-wide scale may provide the figures about the global sustainable development of the practice.

As it is usually the case in science, the things are complicated and largely relative when regarded in in-depth details, and a persistent non-obviousness of an absolutely legitimate environmental strategy is a perfect illustration of this point. In the meantime, some answers can be provided with the relevant studies, sticking to what a very smart man said once, that *'things are better when we do them right'*.⁴⁴

⁴⁴ Kai-Uwe Bletzinger, key-note speech at Design Modeling Symposium, Berlin 2019

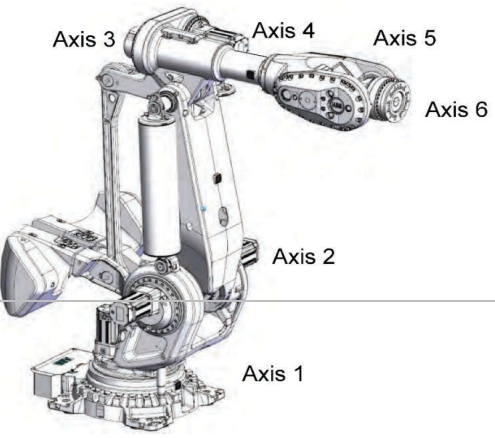
Bibliography of Conclusion & Perspectives

- [1] V. V. Munyon, W. M. Bowen, et J. Holcombe, « Vehicle fuel economy and vehicle miles traveled: An empirical investigation of Jevon's Paradox », *Energy Research & Social Science*, vol. 38, p. 19-27, avr. 2018, doi: 10.1016/j.erss.2018.01.007.
- [2] R. Fouquet et P. J. G. Pearson, « Seven Centuries of Energy Services: The Price and Use of Light in the United Kingdom (1300-2000) », *Energy Journal*, vol. 27, n° 1, p. 139-177, janv. 2006, doi: 10.5547/ISSN0195-6574-EJ-Vol27-No1-8.
- [3] Orange, « 5G et efficacité énergétique : de nouveaux mécanismes pour progresser », *Hello Future*, févr. 10, 2020. <https://hellofuture.orange.com/fr/la-5g-lefficacite-energetique-by-design/> (consulté le oct. 26, 2020).
- [4] ARCEP, « Marché des communications électroniques en France - Année 2019 - Résultats provisoires », ISSN n°2258-3106, juin 2020. Consulté le: oct. 26, 2020. [En ligne]. Disponible sur: <https://www.arcep.fr/cartes-et-donnees/nos-publications-chiffrees/observatoire-des-marches-des-communications-electroniques-en-france/marche-des-communications-electroniques-en-france-annee-2019-resultats-provisoires.html>
- [5] W. S. Jevons, *The Coal Question: An Inquiry Concerning the Progress of the Nation, and the Probable Exhaustion of our Coal Mines*, 2nd Edition. London: MacMillan, 1886.
- [6] B. Alcott, « Jevons' paradox », *Ecological Economics*, vol. 54, n° 1, p. 9-21, juill. 2005, doi: 10.1016/j.ecolecon.2005.03.020.
- [7] S. Sorrell, « Jevons' Paradox revisited: The evidence for backfire from improved energy efficiency », *Energy Policy*, vol. 37, n° 4, p. 1456-1469, avr. 2009, doi: 10.1016/j.enpol.2008.12.003.
- [8] M. Grubb, « Communication Energy efficiency and economic fallacies », *Energy Policy*, vol. 18, n° 8, p. 783-785, oct. 1990, doi: 10.1016/0301-4215(90)90031-X.
- [9] M. Grubb, « Reply to Brookes », *Energy Policy*, vol. 20, n° 5, p. 392-393, mai 1992, doi: 10.1016/0301-4215(92)90060-F.
- [10] D. Toke, « Increasing energy supply not inevitable », *Energy Policy*, vol. 18, n° 7, p. 671-673, sept. 1990, doi: 10.1016/0301-4215(90)90085-I.
- [11] L. G. Brookes, « Energy efficiency and economic fallacies: a reply », *Energy Policy*, vol. 20, n° 5, p. 390-392, mai 1992, doi: 10.1016/0301-4215(92)90059-B.
- [12] L. G. Brookes, « Energy efficiency fallacies: the debate concluded », *Energy Policy*, vol. 21, n° 4, p. 346-347, avr. 1993, doi: 10.1016/0301-4215(93)90274-J.
- [13] H. D. Saunders, « The Khazzoom-Brookes Postulate and Neoclassical Growth », *Energy Journal*, vol. 13, n° 4, p. 131-148, sept. 1992, doi: 10.5547/ISSN0195-6574-EJ-Vol13-No4-7.
- [14] J. Pegna, « Exploratory investigation of solid freeform construction », *Automation in Construction*, vol. 5, n° 5, p. 427-437, févr. 1997, doi: 10.1016/S0926-5805(96)00166-5.
- [15] R. Duballet, « Building systems in robotic extrusion of cementitious materials », Université Paris Est, Paris, France, 2019.
- [16] R. Duballet, O. Baverel, et J. Dirrenberger, « Space Truss Masonry Walls With Robotic Mortar Extrusion », *Structures*, vol. 18, p. 41-47, avr. 2019, doi: 10.1016/j.istruc.2018.11.003.
- [17] P. Carneau, R. Mesnil, N. Roussel, et O. Baverel, « Additive manufacturing of cantilever - From masonry to concrete 3D printing », *Automation in Construction*, vol. 116, p. 103184, août 2020, doi: 10.1016/j.autcon.2020.103184.
- [18] C. Gosselin, R. Duballet, Ph. Roux, N. Gaudillière, J. Dirrenberger, et Ph. Morel, « Large-scale 3D printing of ultra-high performance concrete – a new processing route for architects and builders », *Materials & Design*, vol. 100, p. 102-109, juin 2016, doi: 10.1016/j.matdes.2016.03.097.
- [19] I. Agustí-Juan et G. Habert, « Environmental design guidelines for digital fabrication », *Journal of Cleaner*

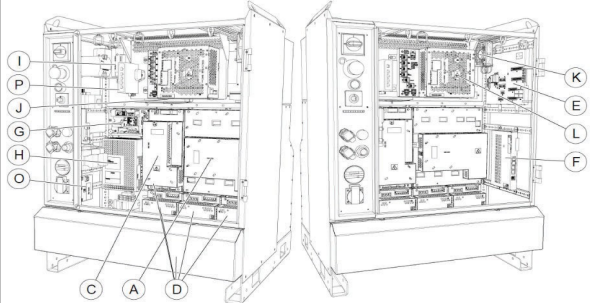
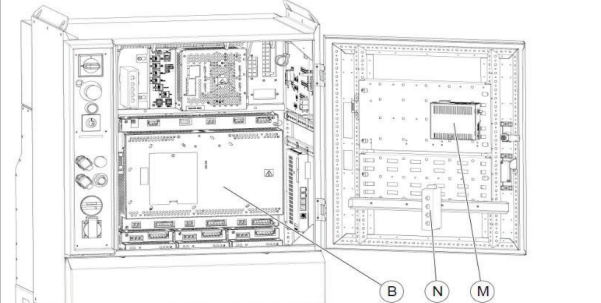
Production, vol. 142, p. 2780-2791, janv. 2017, doi: 10.1016/j.jclepro.2016.10.190.

- [20] A. Perrot, D. Rangeard, V. N. Nerella, et V. Mechtcherine, « Extrusion of cement-based materials - an overview », *RILEM Technical Letters*, vol. 3, p. 91-97, 2018, doi: 10.21809/rilemtechlett.2018.75.
- [21] « World energy balances and statistics – Data services », *IEA*. <https://www.iea.org/subscribe-to-data-services/world-energy-balances-and-statistics> (consulté le janv. 19, 2021).

Annex 1
Life-Cycle Inventory
of the Robotic Printing Cell

Component	Element / Spare Part	Source / Reference	Details	Corresponding Process in Ecolnvent 3.2 CutOff
		// Product Specification	Weight _kg	
Robot	https://new.abb.com/products/3HAC020536_024/irb_8700			
Robotic Arm _ ABB IRB 8700 :	ABB 2016 "Product manual, spare parts ; IRB 8700 - 550/4.20 ; IRB 8700 - 800/3.50 ; IRC5" Document ID: 3HAC052854-001, Revision: A		4575	
	Robot's Body:		2531,92	<i>market for steel, low-alloyed, hot rolled steel, low-alloyed, hot rolled cut-off, U</i>
	Upper Arm & Excluding Wrist	3HAC048079-006	409,00	
	Wrist	3HAC048653-006	380,00	
	Lower Arm & Parallel Arm			
	Lower arm	3HAC048081-005	331,00	
	Spherical roller bearing	3HAC12441-3	4,86	
	Parallel arm	3HAC049074-003	253,00	
	Spherical roller bearing	3HAC12441-4	3,06	
	Parallel Bar	3HAC048077-003	59,00	
	Balancing Device	3HAC048239-003	195,00	
	Frame	3HAC048537-005	554,00	
	Base	3HAC048072-006	259,00	
	Cross roller bearing	3HAC048069-003	71,00	
	Mechanical stop pin	3HAC048180-001	13,00	
	Contre-Poids; Base et autres		1295,31	
	Motors (6 Servo-Motors)	EPD _ AC Low voltage cast iron motor, type M3BP 315 _ cf.ABB	156,7	Servo-Motor - FR
		Values per 1 kg of Servo-Motor	0,4191	<i>steel, low-alloyed steel production, electric, low-alloyed - RER</i>
			0,0609	<i>steel, low-alloyed, hot rolled market for steel, low-alloyed, hot rolled - GLO</i>
			0,4155	<i>cast iron market for cast iron - GLO</i>
			0,0147	<i>aluminium, cast alloy market for aluminium, cast alloy - GLO</i>
	0,0430		<i>copper market for copper - GLO</i>	
	0,0000		<i>metal working, average for copper product manufacturing market for metal working, average for copper product manufacturing - GLO</i>	
	0,0011		<i>tube insulation, elastomere market for tube insulation, elastomere - GLO</i>	
	0,0358		<i>Resin timber board</i>	
	0,0043		<i>epoxy resin insulator, Al2O3 market for epoxy resin insulator, Al2O3 - GLO</i>	
	0,0057		<i>electrostatic paint market for electrostatic paint - GLO</i>	
		156,7		
Axis 1,2,3,5 _ Rotating AC motor (including PINION)	3HAC058949-003	28,6 x 4		
Axis 4 _ Rotating AC motor (including PINION)	3HAC058950-003	28,5		
Axis 6 _ Rotating AC motor (including PINION)	3HAC058951-003	13,8		

	Gear Boxes (6 Gear Boxes)		591,07	<i>market for steel, low-alloyed, hot rolled steel, low-alloyed, hot rolled cut-off, U</i>
	Axis 1 _ Reduction gear RV 700CS	3HAC048963-002	147,8	
	Axis 2,3 _ Reduction gear RV 900N incl in-put gear	3HAC048392-003	157 x 2	
	Cover	3HAC048177-006	7,6	
	Hub with pinion	3HAC049795-003	2,12	
	Axis 4,5 _ ReductionGearRV-500N-236.36	3HAC043073-003	56 x 2	
	Motor flange	3HAC048254-006	5,7	
	Hub with pinion	3HAC049906-003	1,85	
	Electrical Parts			
	Ethernet cable, Upper arm	3HAC054803-001	0,48 / 5m	<i>market for cable, data cable in infrastructure cable, data cable in infrastructure cut-off, U</i>
	Cable harness	3HAC050792-001	16 / 8m	<i>market for cable, three-conductor cable cable, three-conductor cable cut-off, U</i>
	SMB unit			
	SMB	3HAC043904-001 RMU102	0,18	<i>market for aluminium alloy, metal matrix composite aluminium alloy, metal matrix composite cut-off, U</i>
	Bracket	3HAC044073-001 RMU102	0,28	<i>market for electronics, for control units electronics, for control units cut-off, U</i>
	Brake release unit		0,25	
	Brake release unit	3HAC046642-001 BRK001	0,2	<i>market for steel, low-alloyed, hot rolled steel, low-alloyed, hot rolled cut-off, U</i>
	Bracket	3HAC049785-001		
	Other parts			
	A Gasket	3HAC044074-001	0,2	<i>market for tube insulation, elastomere tube insulation, elastomere cut-off, U</i>
	B Cover	3HAC044076-001		<i>market for aluminium alloy, metal matrix composite aluminium alloy, metal matrix composite cut-off, U</i>
	C Push button guard	3HAC6499-1		
	D Button guard plate	3HAC026331-001	0,1	<i>market for aluminium alloy, metal matrix composite aluminium alloy, metal matrix composite cut-off, U</i>
	E Battery holder	3HAC044161-001	0,05	<i>market for aluminium alloy, metal matrix composite aluminium alloy, metal matrix composite cut-off, U</i>
	F Battery pack	3HAC044075-001 RMU		<i>market for battery cell, Li-ion battery cell, Li-ion cut-off, U</i>
	G Rubber cloth	3HAC044200-001	0,15	
	H Cover	3HAC044205-001		<i>market for aluminium alloy, metal matrix composite aluminium alloy, metal matrix composite cut-off, U</i>
	Teach Pendant			
	GTPU3 avec câble de 10 m	3HAC028357-001	1 Unit	<i>market for electronics, for control units electronics, for control units cut-off, U</i>

Control Cabinet _ IRC5		ABB "Manuel du produit IRC5 / Design 14" ; ID du document: 3HAC047136- 004 ; Révision: G	150 x 2 Units		
Pièces du système du contrôleur:	Variateur principal MDU-430A (pour les petit robots)/ Drive Unit	A _ 3HAC035301-001	7,82		
	Variateur principal MDU-790A (pour les gros robots) / DRIVE UNIT	B _ 3HAC029818-001	13,96	<i>market for electronic component, active, unspecified electronic component, active, unspecified cut-off, U</i>	
	Redresseur supplémentaire ARU-430A (pour les petits robots avec variateur supplémentaire)	C _ 3HAC035381-001	4,78		
	Variateur supplémentaire, ARU-790A	D _ 3HAC030923-001	2,36		
	Carte du panneau	E _ 3HAC024488-001	0,34	<i>market for integrated circuit, logic type integrated circuit, logic type cut-off, U</i>	
	Carte d'axes	F _ 3HAC029157-001	0,58		
	Carte d'alimentation électrique	G _ 3HAC026254-001	0,42	<i>market for integrated circuit, logic type integrated circuit, logic type cut-off, U</i>	
	Alimentation électrique du système	H _ 3HAC026253-001	2,46		
	Alimentation d'E/S client	I _ 3HAC14178-1	0,46	<i>market for power supply unit, for desktop computer power supply unit, for desktop computer cut-off, U</i>	
	Retenue d'énergie de secours (UltraCap)	J _ 3HAC026585-001	0,62		
	Retenue d'énergie de secours	J _ 3HAC025562-001	0,62	<i>market for capacitor, auxiliaries and energy use market for capacitor, auxiliaries and energy use cut-off, U</i>	
Ventilateur	K _ 3HAC025466-001	0,25			
Boîtier Remote Service	M _ 3HAC043053-001	0,43	<i>market for fan, for power supply unit, desktop computer fan, for power supply unit, desktop computer cut-off, U</i>		
Commutateur Ethernet	N _ 3HAC034884-001	0,416			
Carte d'interface des contacteurs	O _ 3HAC13389-2	0,14	<i>market for electronic component, active, unspecified electronic component, active, unspecified cut-off, U</i>		
Commutateur Eth. DSQC1007 (MultiMove)	P _ 3HAC045976-001	0,36			
Interrupteur à came 3 positions Std // CAM SWITCH	3HAC052287-002		<i>market for integrated circuit, logic type integrated circuit, logic type cut-off, U</i>		
Interrupteur à came 3 positions étendu // CAM SWITCH	3HAC052287-004				
Interrupteur à came 2 positions Std // CAM SWITCH	3HAC052287-001				
Interrupteur à came 2 positions étendu // CAM SWITCH	3HAC052287-003				
Boîtier			127,454		
			100	<i>market for steel, low-alloyed, hot rolled steel, low-alloyed, hot rolled cut-off, U</i>	
			13	<i>market for glass fibre reinforced plastic, polyamide, injection moulded glass fibre reinforced plastic, polyamide, injection moulded cut-off, U</i>	
			10	<i>market for epoxy resin insulator, SiO2 epoxy resin insulator, SiO2 cut-off, U</i>	
			1	<i>market for polycarbonate polycarbonate cut-off, U</i>	
			3	<i>market for electrostatic paint electrostatic paint cut-off, U</i>	

Printing Head			180	
Pompe de dosage	Moteur_ Rockwell _ AC Servomotor	VPL-B1152C-PJ12AA	8	electric motor, for electric scooter market for electric motor, for electric scooter - GLO
	Details en Inox		10	steel, chromium steel 18/8 market for steel, chromium steel 18/8 - GLO
	Pompe		5	market for pump, 40W pump, 40W cut-off, U
Carters				
Chassis				
Outillage fixation				
Entrée béton				
Mélangeur dynamique	Moteur	VPL-B1152C-PJ12AA	8	electric motor, for electric scooter market for electric motor, for electric scooter - GLO
	Details en Inox		10	steel, chromium steel 18/8 market for steel, chromium steel 18/8 - GLO
	Pompe		5	market for pump, 40W pump, 40W cut-off, U
Adjuvantation	Details en Inox		15	steel, chromium steel 18/8 market for steel, chromium steel 18/8 - GLO
	Composant electronique		1	electronic component, active, unspecified market for electronic component, active, unspecified - GLO
	Pompe		3	market for pump, 40W pump, 40W cut-off, U
			16	TOTAL
			5	
Climatisation			2	fan, for power supply unit, desktop computer market for fan, for power supply unit, desktop computer - GLO
Cablage / Isolation			1	tube insulation, elastomere market for tube insulation, elastomere - GLO
			1	epoxy resin insulator, Al2O3 market for epoxy resin insulator, Al2O3 - CLO
			1	epoxy resin insulator, SiO2 market for epoxy resin insulator, SiO2 - GLO
			5m	cable, data cable in infrastructure market for cable, data cable in infrastructure
			3 kg	cable, unspecified market for cable, unspecified
			5m	cable, three-conductor cable market for cable, three-conductor cable

Concrete Preparation Unit				
Conteneur			1200	<i>market for steel, low-alloyed, hot rolled steel, low-alloyed, hot rolled cut-off, U</i>
			2216	<i>market for steel, low-alloyed, hot rolled steel, low-alloyed, hot rolled cut-off, U</i>
Motors			384,2	
	Malaxeur :	moteur interne, 117.430 kg, 230/400V, 18.2A/10.5A, 5.5kW	117,5	<i>electric motor, vehicle market for electric motor, vehicle - GLO</i>
		moteur externe, pareil	117,5	<i>electric motor, vehicle market for electric motor, vehicle - GLO</i>
	Agitateur :	moteur, 30.153 kg, 400/690V, 1.02/0.59A, 0.37kW	30,2	<i>electric motor, vehicle market for electric motor, vehicle - GLO</i>
	Pompe de gavage	moteur 80kg (estimé), 400V, 16A, 3kW	80	<i>electric motor, vehicle market for electric motor, vehicle - GLO</i>
	Pompe de gavage d'adjuvant	moteur 3kg, 12V, 8A; 0,1 kW	3	<i>electric motor, vehicle market for electric motor, vehicle - GLO</i>
	Balance de dosage :	- Pompe vidange moteur, 21kg, 230/400V, 2.1A, 0.75kW - Pompe adjuvant moteur 15kg (estimé), 400V, 1.2A, 0.73kW	21	<i>market for pump, 40W pump, 40W cut-off, U</i>
			15	<i>market for pump, 40W pump, 40W cut-off, U</i>
Command Station			1 Unit	<i>market for computer, desktop, without screen computer, desktop, without screen cut-off, U</i>
				<i>market for hard disk drive, for desktop computer hard disk drive, for desktop computer cut-off, U</i>
				<i>market for pointing device, optical mouse, with cable market for pointing device, optical mouse, with cable cut-off, U</i>
				<i>market for liquid crystal display, unmounted market for liquid crystal display, unmounted cut-off, U</i>
Ventilation			1 Unit	<i>market for ventilation system, decentralized, 6 x 120 m3/h, steel ducts ventilation system, decentralized, 6 x 120 m3/h, steel ducts cut-off, U</i>
Building Hall	25 sqm (Printing zone) x 2,4 (efficiency coefficient for industrial buildings)		60 sqm	<i>market for building, hall building, hall cut-off, U</i>

Annex 2
Power Measurements
Experimental Protocol & Technical Details

Power Measurements

The power measurements accomplished on the components constituting the robotic printing cell represent an important part of the present work, as basically define the operational impact of the robotic construction processes.

The theoretical framework and the outcomes of the measurements are described in the Section 2.2.1. The present part unfolds the practical aspects of the measurement procedure, including the design and wiring of power measurement devices, electric connections and the processing of the measured data. To drop into the topic, the following part will provide a brief review on the theoretical aspects of the electricity power consumption.

1. Electric Power

The electric power is the rate of the flow of electric energy transferred by an electric circuit at a given point per the unit of time. The electric power consumption rate of the device is thus a necessary measure to calculate its final energy consumption for a given operation. The energy E is the function of the power consumption P over the running time Δt and equal to the line integral of the power along the time axis.

$$E = \int_{t_0}^{t_0+\Delta t} P \Delta t$$

Since the power consumption of electrical devices is usually an approximately constant value, then the energy equation can be simplified to a simple multiplication of the power consumption P over the global running time Δt .

$$E = P \Delta t$$

Three types of power are distinguished for electrical devices. The first one, the real active power P sold in watts or more frequently in kilowatts [kW], stands for the real amount of power used to accomplish a given work. The second one, the apparent power S measured in volt-amperes or kilovolt-amperes [kVA], describe the total amount of electricity consumed by the device. Finally, the reactive power Q [kVAR] is a vectorial difference between the apparent power S and the real power P , describing thus a non-used power or the power loss of the device. As follows, the power factor, describing the efficiency of the device, can be defined by the relation of the real power P to the apparent power S .

$$\text{Power Factor} = P/S$$

The relation between those three can be illustrated by the so-called power triangle depicted on Figure A.1. The mathematical relation between those three can thus be described by the Pythagorean theorem, see equation below.

$$S^2 = P^2 + Q^2$$

$$P = \sqrt{S^2 - Q^2}$$

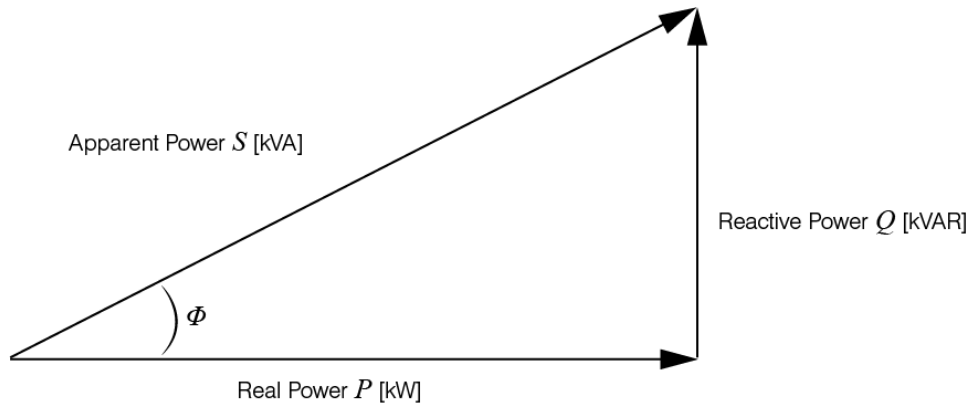


Figure A.1. The Power Triangle describing the relation between different types of power

Hence, within the present study, it is not the real power P that we are interested in but rather the apparent power S , as this latter would describe the global electricity amount consumed by the device including the power losses related to its efficiency. The scalar difference between both power types can be explicitly observed on Figure A.2.

Furthermore, for the devices performing mechanical work, e.g. motors, generators and torque engines, the real power consumption P can occasionally appear as a negative value, see Figure A.3. and A.5. It is explained by the fact that some engines performing mechanical work, for example torque movement performed by the concrete mixer during the pumping & mixing processes, see Figure A.3, can periodically develop an inertial motion, which means that in that instance no electricity consumption occurs to accomplish the mixer's spindle rotation. As follows, at this moment of the inertial motion, the real power value is negative, when the apparent power is *au contraire* higher than average, as the electric current is still supplied into the system and therefore stocks within.

Figures A.2, A.3, A.4 and A.5 depicts respectively the power consumption of the robotic arm, Pumping & Mixing process, the printing head and the hairdryer, systematically used for the referential measurement, featuring both curves of the real power in kW and the apparent power in kVA.

To sum up, the real power will not be a proper unit to measure the power consumption of the components as it does not describe the global amount of electricity consumed by the construction process. It is thus the apparent power that is observed in the present study.

The following section describes the power measurement devices, installed in the robotic printing cell.

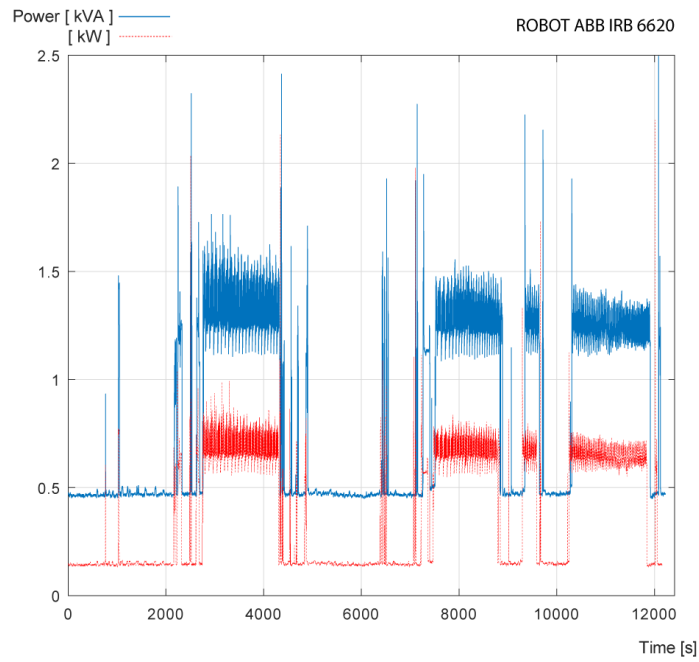


Figure A.2. Power consumption of Robotic Arm ABB IRB 6620 featuring the apparent power [kVA] and the real power [kW].

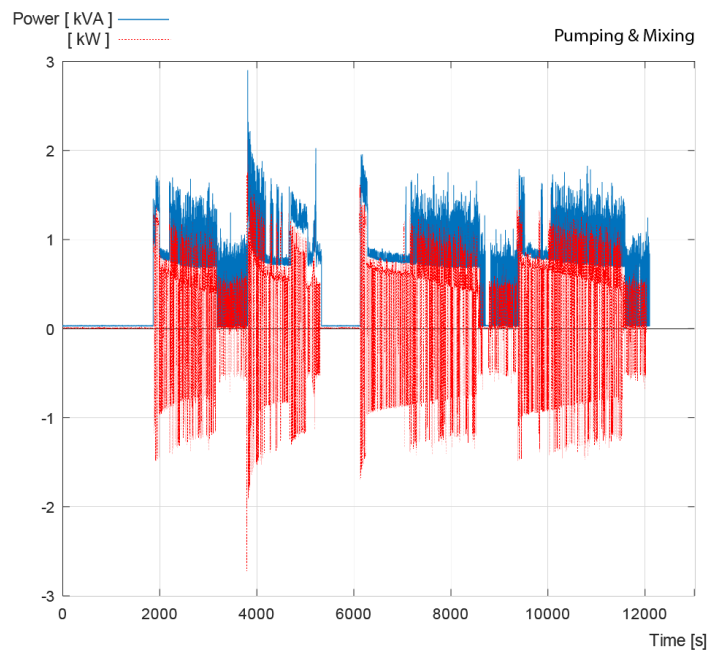


Figure A.3. Power consumption of Pumping & Mixing process featuring the apparent power in [kVA] and the real power in [kW].

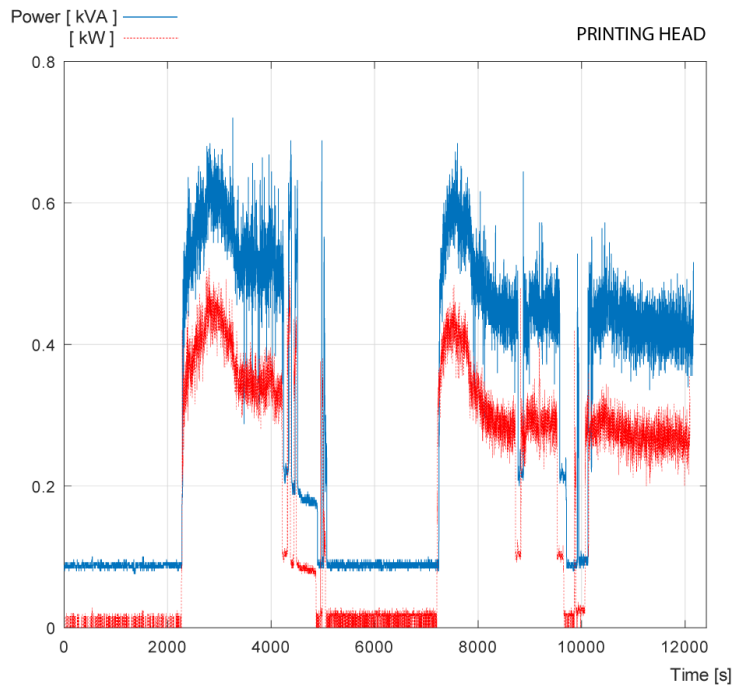


Figure A.4. Power consumption of the Printing Head featuring the apparent power in [kVA] and the real power in [kW].

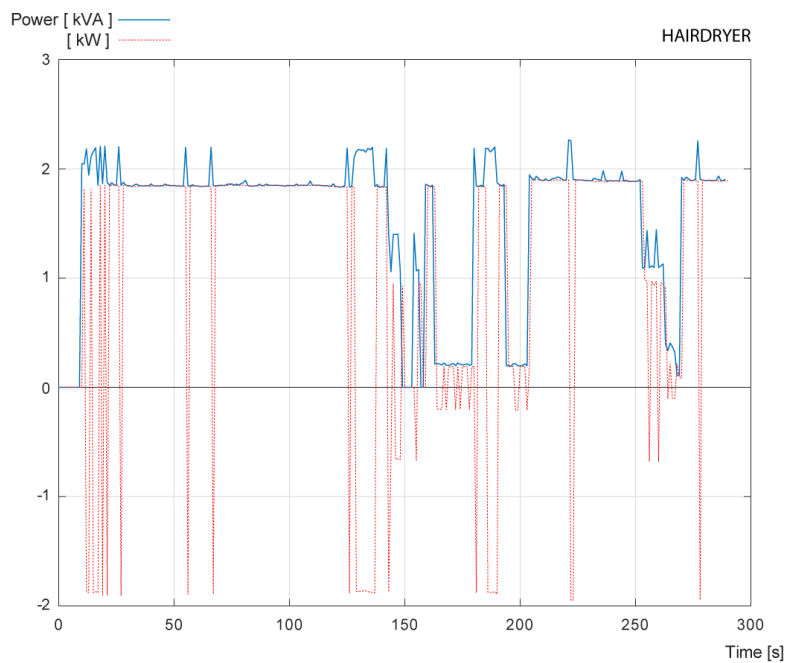


Figure A5. Power consumption of Hairdryer featuring the apparent power in [kVA] and the real power in [kW].

2. Power Measurement Devices

As it was outlined in the previous section the type of power observed in the present study of the apparent power measured in kVA, which is a product of the voltage and of the electric current intensity of the electric system. The voltage of electrical systems is usually constant and thus it would be mainly the variation of the electric current intensity that will increase/decrease in function of the power demand of a given process. As follows, the power measurement devices represent basically an ampere-meter with an integrated power meter, through which every component of the robotic printing cell is plugged to the source power outlet. The measured data are then transmitted to the command station computer.

Precisely, four power measurement devices have been installed onto the following components of the robotic printing cell:

1. *Concrete Preparation Mixer* for the primal concrete preparation;
2. *Pump*, performing continuous concrete *Pumping & Mixing*
3. *Robot*
4. *Printing Head*

Figure A.6. depicts the location of the power measurement devices within the printing cell and their connection to the measured positions and to the command station computer.

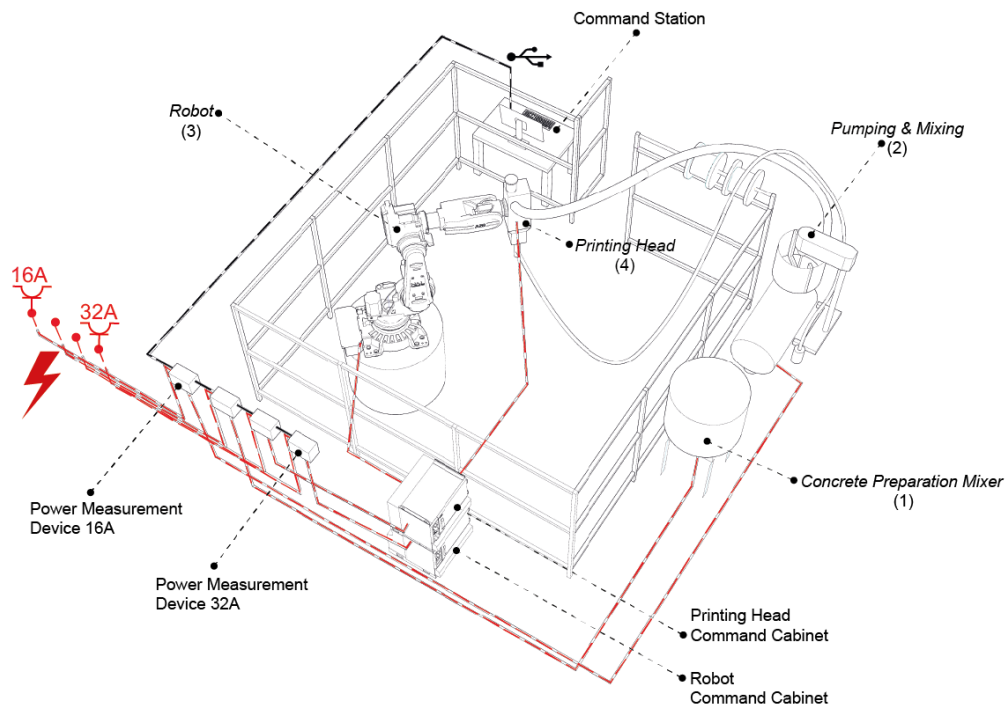


Figure A.6. Lay-out of the Robotic Printing Cell featuring the Power Measurement Devices.

The power measurement devices were designed and fabricated by the technical team of Navier Laboratory, in particular by Eden Berro. The device is embedded into a box containing the power meter plugged after the current transformers. As the device repeats the outlet connection of the component it measures, its embedded meter and current transformers are scaled accordingly to the outlet amperage as well as of the power demand of the component, in order to have a high precision of the measurements. Figure A.7 depicts the power measurement device for a concrete mixer plugged in to the 32A outlet.

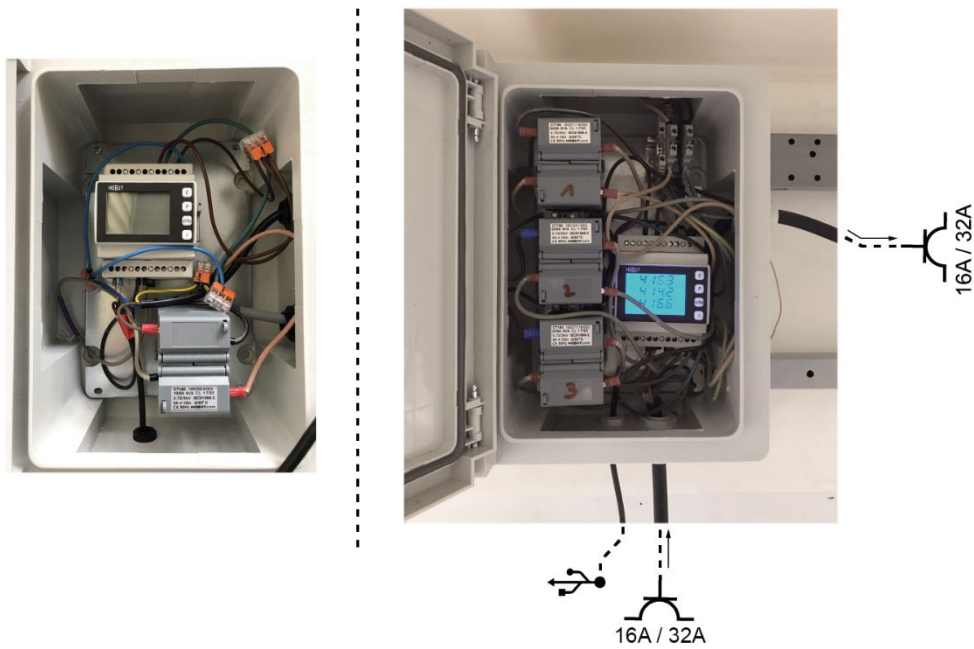


Figure A.7. Photo of Power Measurement Devices for single-phase outlet (left) and for the triple-phase outlet (right)

Figure A.8 and A.9 depict the wiring principle of the embedded power meter including the current transformers for single-phase and triple-phase outlets.

The current transformer is placed on every phase wire of the power cable before the power meter and as its title indicates transforms the electric current till the value bearable by the power meter. Concretely, the bearable electric current intensity of the meter is around 5A and the amperage of the outlets can go up to 16A, 32A and 63A. The transformer's capacity is thus chosen accordingly and depending on the measured component performs the transformation factor equal to 2 (10/5A), to 4 (20/5A) and to 10 (50/5A). Consequently, as the power consumption unit is kVA, which is the product of the volts and amperes, and as the measured amperes arrive with the transformation factor, then the final kVA will also possess the same factor. This later has not been identified from the beginning of the experiment and in fact, for a long time, the measurements were proceeded without the factor correction.

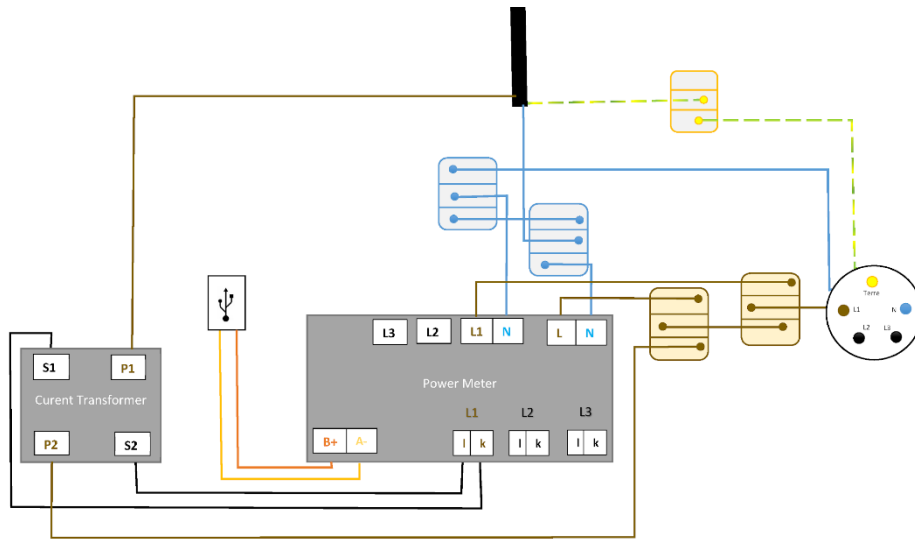


Figure A.8. Wiring diagram of the Power Measurement Device for the single-phase component
Image © Eden Berro

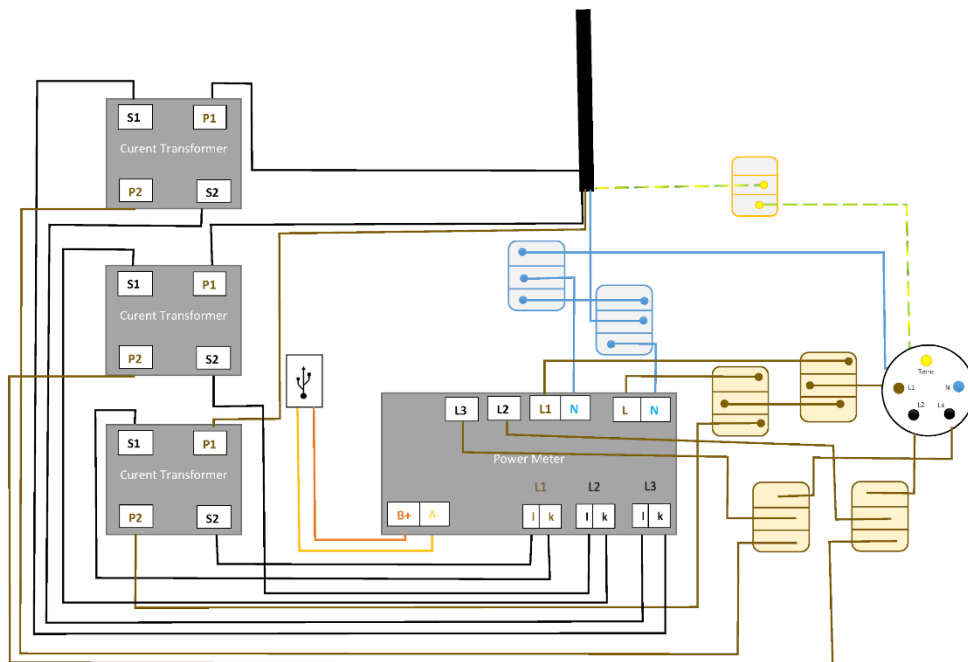


Figure A.9. Wiring diagram of the Power Measurement Device for the triple-phase component
Image © Eden Berro

The factor was properly identified in a collaboration with Nicolas Ducoulombier during the measurements accomplished on the XtreeE site. As a matter of fact, without taking into account the factor introduced by the current transformer, the magnitude of the power consumption of the whole printing cell is comparable to a hairdryer or a small kitchen appliance. This latter was thus used as an etalon measure in order to establish a physical reference of the energy amount needed to perform a certain work and to then verify the accuracy of the values displayed by the fabricated devices. As follows, one litre of the cold water was boiled with a small kettle and then, using the thermal capacity of the water and considering the time that one litre took to get boiled, the total energy amount for the operation was calculated. In the end, the power consumption of the kettle displayed by the power measurement device was 4 times lower than the one of the analytical calculation. Further, by repeating the boiling water experiment with different power measurement devices, the factor 2 and 10 was discovered. In the end, the factor was linked to the capacity of the embedded current transformer, see figure below.

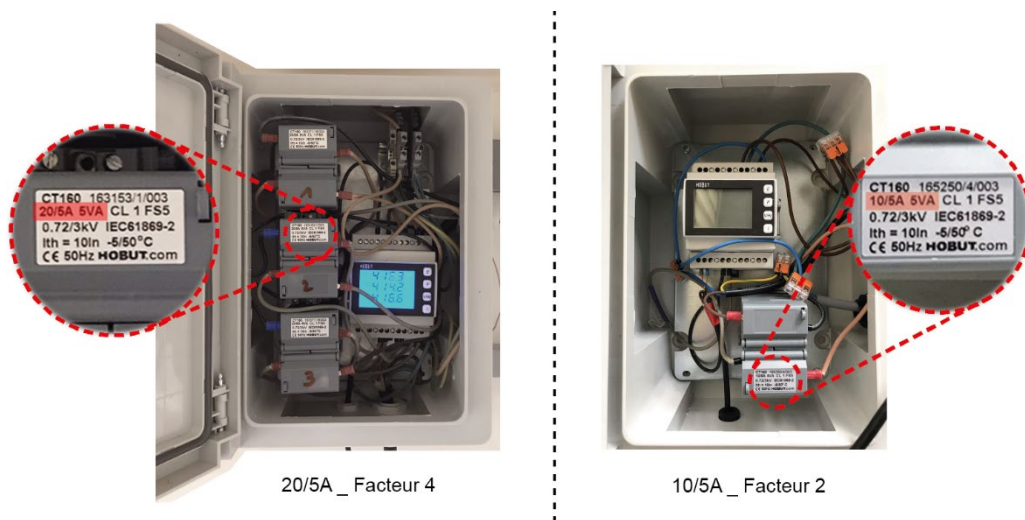


Figure A.10. The factor of the measurements related to the capacity of the current transformer: Factor 4 of triple-phase power measurement device (left); Factor 2 of single-phase power measurement device (right)

3. Data Processing

Every power measurement device is equipped by the USB output, through which the measured data can be continuously sent to the computer, see Figure A.7. Then using the software of power-meter's manufacturer *HOBUT - Multiview*⁴⁵, the direct on-screen monitoring of the measurements can be carried out hand by hand with the logging of the measured data into the text file for the further treatment. Table A.1. depicts an extract of the logged data for the power consumption measurements of the robotic arm. No factor correction is effectuated on this stage.

⁴⁵ <https://www.hobut.co.uk/>

Table A.1. Extract of the power measurement data for the robotic arm

Oct 22 2020 11:19:39	V L1-2 412.724	V L2-3 413.216	V L3-1 415.585	V1 238.624	V2 237.543	V3
239.914	I 1 0.527	I 2 0.553	I 3 0.336	kW Sum 0.181	kVA Sum 0.338	kVAR Sum -0.010
Oct 22 2020 11:19:40	V L1-2 412.416	V L2-3 412.919	V L3-1 415.253	V 1 238.435	V 2 237.684	V3
239.545	I 1 0.502	I 2 0.526	I 3 0.296	kW Sum 0.164	kVA Sum 0.315	kVAR Sum -0.010
Oct 22 2020 11:19:41	V L1-2 412.335	V L2-3 412.850	V L3-1 415.176	V 1 238.318	V 2 237.245	V3
239.528	I 1 0.472	I 2 0.493	I 3 0.234	kW Sum 0.144	kVA Sum 0.286	kVAR Sum -0.013
Oct 22 2020 11:19:42	V L1-2 411.838	V L2-3 412.437	V L3-1 414.805	V 1 238.152	V 2 237.168	V3
239.277	I 1 0.479	I 2 0.502	I 3 0.244	kW Sum 0.147	kVA Sum 0.291	kVAR Sum -0.013
Oct 22 2020 11:19:43	V L1-2 411.638	V L2-3 412.259	V L3-1 414.649	V 1 238.239	V 2 237.232	V3
239.261	I 1 0.435	I 2 0.459	I 3 0.164	kW Sum 0.116	kVA Sum 0.252	kVAR Sum -0.015
Oct 22 2020 11:19:44	V L1-2 411.452	V L2-3 412.078	V L3-1 414.512	V 1 238.090	V 2 237.063	V3
239.239	I 1 0.487	I 2 0.505	I 3 0.240	kW Sum 0.146	kVA Sum 0.293	kVAR Sum -0.013
Oct 22 2020 11:19:45	V L1-2 411.365	V L2-3 412.005	V L3-1 414.399	V 1 238.037	V 2 237.050	V3
239.091	I 1 0.596	I 2 0.619	I 3 0.545	kW Sum 0.205	kVA Sum 0.419	kVAR Sum -0.011

The further treatment of the logged data was accomplished within the *MATLAB*⁴⁶ software. Concretely, an automated routine was set up for the processing of the logged data, automating the files reading and the extraction of the researched information. Additionally, the correction of the current transformation factor was set within the plotting code.

Figure A.12 depicts the final power consumption measurements of the robotic printing cell components including the correction of the current transformation factor.

In closing, besides the LCA study purposes, the power measurements of the concrete mixing unit can be used as a rheometer. Concretely, the curve of the concrete preparation depicts exactly the behaviour of the fresh cement paste within the mixer and therefore the asymptote of that curve stands for the mixture stabilization value as well as the viscosity/yield stress reference of a given material mix. These rheological properties of the material mix may thus directly influence the power consumption of the whole system, and furthermore, as it was pointed out in the previous conclusions, may significantly influence the global environmental impact of the printing process. Thus paradoxically, it may not be the type of the printing system that will define the impact of the construction process by printing but rather the rheological properties of the processed material. The detailed investigation of this former hypothesis will pertain to further investigations.

⁴⁶ <https://mathworks.com/>

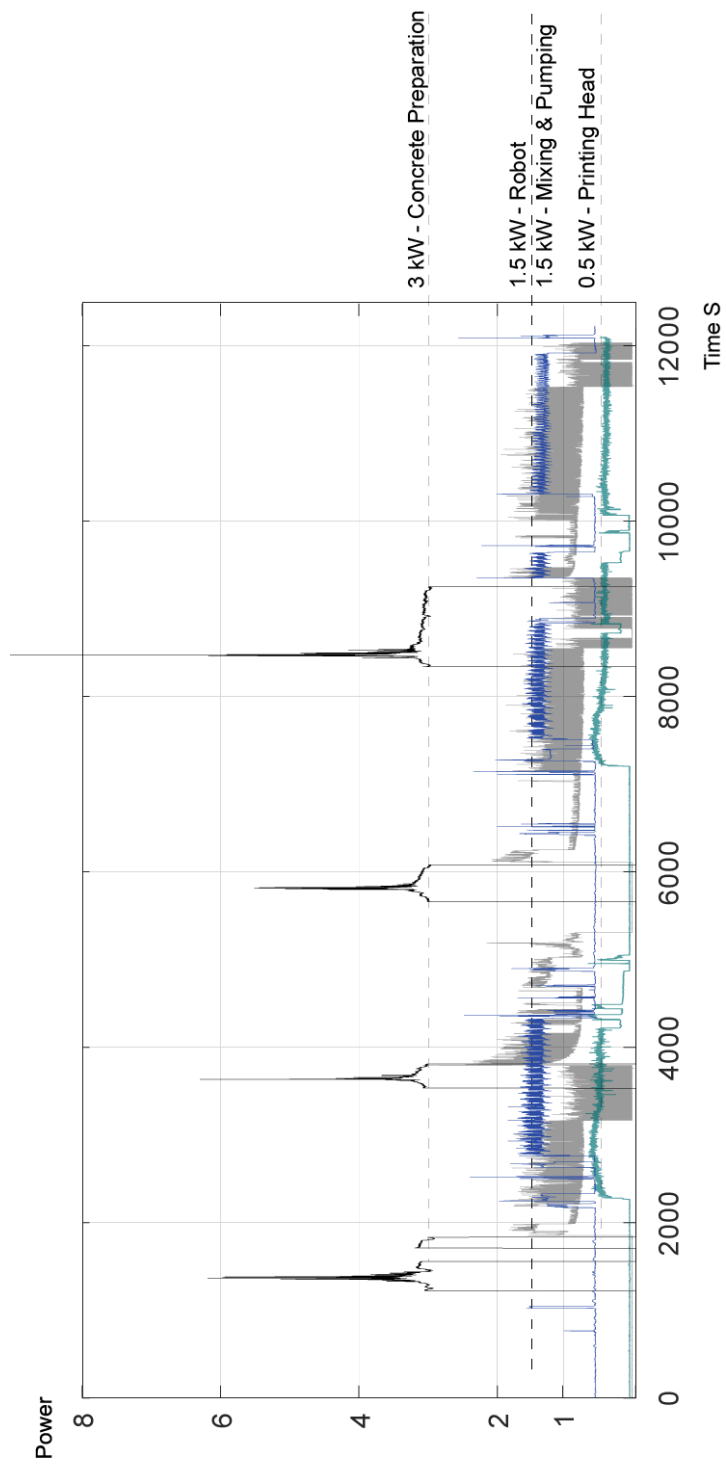


Figure A.12. Final Power Consumption Measurements of Robotic Printing Cell components including the Current Transformation Factor Correction

